JOURNAL OF THE

Electrochemical

Society

PRIME PERFORMANCE

The consistent experience records of major chlor-alkali producers everywhere provide ample evidence of the prime importance of GLC ANODES in electrolytic cell operations.

Journal of the Electrochemical Society

MAY 1955　　　　　　　　　　**VOL. 102 · NO. 5**

CONTENTS

Editorial

Technical Papers

Technical Note

Current Affairs

AN ADVENTURE

in SILICON

One example of junction technology at Bell Laboratories. Here a junction is produced on the surface of silicon by bombardment with alpha particles. Bombardment enhances silicon's performance at very high frequencies.
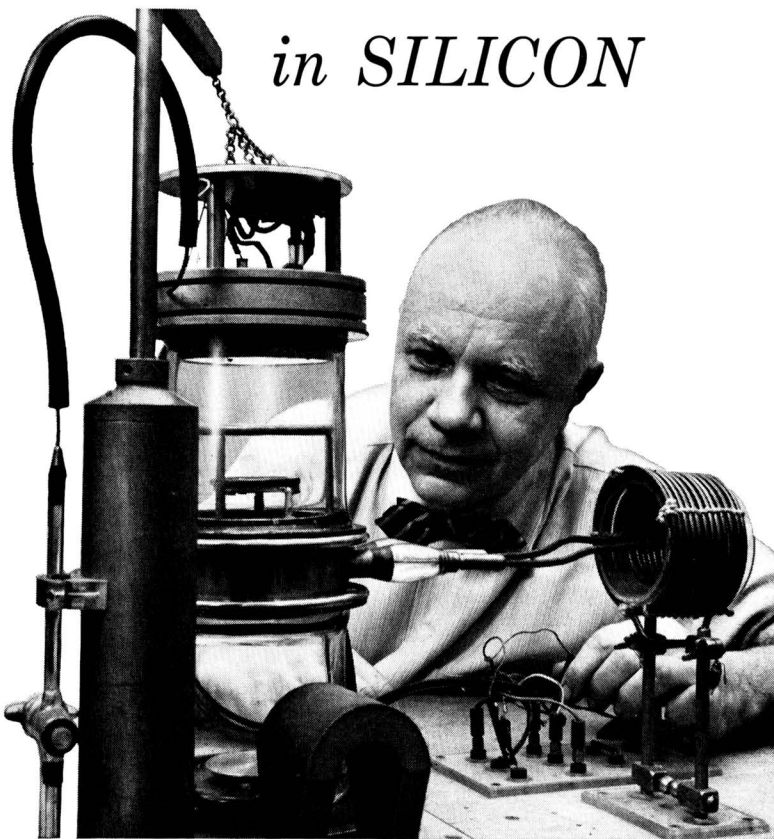
One day in the 'thirties a revolutionary adventure began for Bell scientists. They were testing an experimental silicon crystal they had grown to make microwave detectors.

Intriguingly, they found that one end of the crystal conducted by means of positive charges, the other end with negative. Positive and negative regions met in a mysterious barrier, or junction, that rectified, and was sensitive to light. It was something entirely new ... with challenging possibilities.

The scientists went on to develop a theory of junction phenomena. They showed that two junctions placed back-to-back make an amplifier. They devised ways to make reproducible junctions. Thus, junction technology came into being, and the 20th Century had a new horizon in electronics.

This technology has already produced at Bell Telephone Laboratories the versatile junction transistor (useful in amplifiers and switches); the silicon alloy diode (surpassingly efficient in electronic switching for computers); and the Bell Solar Battery which turns sunshine directly into useful amounts of electric current.

This is one of many adventures in science which make up the day-to-day work at Bell Laboratories... aimed at keeping America's telephone service the world's best.

Bell Telephone Laboratories

Improving telephone service for America provides careers for creative men in scientific and technical fields

Editorial

The Future of Electrochemistry

*I*N THE EARLY 1800's, Michael Faraday and Sir Humphrey Davy carefully formulated the basic elements of electrochemical theory. Not until 50 years later were further important details filled in through energetic research carried on in the scientific laboratories of Ostwald, Nernst, LeBlanc, and other classical investigators of Continental Europe. This was followed by an upsurge of electrochemical applications, and by the phenomenal development of the electrochemical industry. It was during the latter period that our Society was founded by a group of active young electrochemists who met in Philadelphia in 1902.

There has been steady growth since then both of the electrochemical industry and of the Society. Unfortunately, the same cannot be said for the growth of scientific research of the kind that early nourished both the Society and industry. For this reason, substantially new ideas in electrochemistry over the past 25 years or more have been conspicuously scarce. It now appears, in fact, as if the source-spring of basic information, so much talked about today in terms of fears of the well going dry in all branches of science, became murky decades ago in scientific areas close to home. This situation has prevailed for so long that a few pessimists believe the subject of electrochemistry is exhausted, and that all possible electrochemical phenomena have been discovered and are now commonplace. They would have us believe that radically new ideas are apropos to newer fields of activity, but should not be expected in a subject that matured before the year 1900.

Looking back, what are some of the factors that led to this pessimism and which discouraged continued scientific exploration in electrochemistry? There were, of course, particularly at the beginning of the century, trends of emphasis on the newly developing science of physical chemistry and the new field of chemical engineering, both of which appropriated part of the stage belonging to electrochemistry. This factor siphoned off some of the available men and money. Another important factor, hardly realized at the time, was the Chinese wall of high secrecy surrounding early electrochemical industry and the concurrent policy of isolationism. Despite brilliant engineering achievements within the industry, this wall, like its brick counterpart in Asia, served more effectively to keep ideas out than it did to keep them in. Even today it is not entirely appreciated that the black atmosphere of secrecy seldom produces healthy surroundings for creative effort upon which growth, if not survival, depends. A third factor can probably be laid to lack of proper leadership developing from the universities. This was no one's fault in particular; it occurred partially as a natural consequence of electrochemistry losing contact with enthusiastic support for fundamental research, and the accompanying inevitable loss of bright young men in competition with other fields of scientific or engineering activity.

Of the many needs that might have deflected early electrochemical trends, the most urgent was the need for maps of new territories to conquer, and this remains our primary need today. New—thoroughgoing different—ideas, of the kind which once served as the lifeblood of the present industry, are needed in large dose to support a modern electrochemical industry 10 to 25 years hence. It is not likely that any other prescription can so effectively stave off hardening of the arteries in the over-all industry that employs many of us today. For example, can anyone familiar with the subject adequately appraise the impact on electrochemical industry of basic research which ultimately resulted in improved current efficiency for aluminum production from

Editorial (*continued*)

80 to 99%, or which provided a light-weight storage battery having a thousand times the capacity of present batteries, or which produced an electrolytic cell economically converting salt water to fresh, or which resulted in a fuel cell that rendered steam-dynamo power generation obsolete? These are research goals that are far from visionary.

Tomorrow, far off though it seems, continually demands intelligent attention and planning today. Electrochemistry marks no exception, and there are several ways in which both industry and the Society should help plan a sound future. Much might be said in this regard about the increasing need for industry to support long-range scientific research, to establish fellowships and professorships, and to support the Society both financially and by adequate recognition of employees who contribute effectively to the Society's program. But this is a long story in itself, the Society's responsibilities being those that deserve emphasis at this time. These responsibilities include the following:

1. To encourage the continued growth and strength of the Theoretical Division. Doing so is vital to industry, and to every member of the Society whatever his Division affiliation. The impact of the Theoretical Division on the general health of the Society is tremendous.

2. To continuously assure that the JOURNAL maintains a high standard of technical reporting, and that nothing is allowed to compromise or detract from its scientific integrity. The JOURNAL is the Society's calling card to industry, to new members, to students who wonder whether they should become electrochemists, and to the general public who believe that "by their fruits ye shall know them."

3. To improve effective liaison between scientist and engineer, maintaining the individuality of both, but recognizing that one complements the other.

4. To continue and to improve facilities for the mutually advantageous interaction between men of industry, of government, and of the universities, and to outline and facilitate the broad education of scientists and engineers competent to handle academic, governmental, or industrial responsibilities at any level.

I am optimistic that with our present alert membership and our selfless devoted officers of Sections, Divisions, and of the National Society, these objectives do not lag, and will find still further expression in a Society growing in vision, this year and in the years to come. Along these lines, the Theoretical Division is now one of our most active groups; vitally important symposia are being organized by several Divisions overlapping theory and practice and attended by scientists and engineers; industry has responded magnanimously to our invitation to become sustaining members; and truly basic research in electrochemistry is currently being supported by the Office of Naval Research, by Army Ordnance, and by other organizations. Much more, of course, needs to be done but the difficult first steps have already been taken.

I am proud to be elected to high office in this Society, and I appreciate the confidence of my fellow members that this election implies. The office requires the best of my ability, and I shall aim my efforts so as not to fall short of the mark. I solicit the essential help and advice of each and every one of you in formulating a stronger Society which serves more effectively both its members and industry, and which always flexibly adapts itself to a mature position of responsibility and leadership in a changing world that has seen only a small portion of what electrochemistry can offer. —HERBERT H. UHLIG

Why Big Savings Result When You Electro-tin Copper Wire with B&A Tin Fluoborate

The use of a Baker & Adamson Tin Fluoborate bath in electro-tinning copper wire results in a uniform, easily-controlled tin coating. Tin consumption is reduced more than two-thirds as compared with hot-dipped coatings.

Moreover, copper wire with a fluoborate-plated tin coating of 100 millionths of an inch may be readily drawn through dies for burnishing or for reduction in gage. For example, a plated No. 20 wire can be reduced to a No. 34 wire—a type of processing impractical with hot-dipped wire because of the structure of the coating and its non-uniformity.

The electroplated wire comes from the fluoborate bath with a fine grain coating that has a white matte color, excellent solderability, and good shelf life. The fluoborate bath has no fumes, requires no ventilation, and operation is fast and simple compared with alkaline baths. For full information, write for Baker & Adamson Technical Bulletin TC-43441, or call your nearest B&A office. *No royalties need be paid to use this process!*

10 Basic Advantages of B&A Fluoborate Baths

1. No mixing or dissolving needed—supplied in concentrated form
2. Easier bath preparation
3. Stability of bath composition
4. Ease of control
5. Practically 100% anode and cathode efficiencies
6. High conductivity
7. Good covering power
8. Fine-grained deposits of good color
9. Fast, high-speed operation
10. Readily adaptable for lead-tin alloy deposits

As with Tin Fluoborate in the electro-tinning operation described, other B&A Metal Fluoborates offer additional special advantages in particular operations. Profit by using them!

REAGENTS

B/A

STANDARD OF PURITY

FINE CHEMICALS

BAKER & ADAMSON PRODUCTS
GENERAL CHEMICAL DIVISION
Allied Chemical & Dye Corporation
40 Rector Street, New York 6, N. Y.

Free! Data sheets giving full information on lead and tin fluoborates plus Bulletin TC-43441 on electro-tinning of copper wire. Write today!

Name_____

Company_____

Address_____

City_____ Zone_____ State_____ JE-5

BAKER & ADAMSON® *Fine Chemicals*

GENERAL CHEMICAL DIVISION
ALLIED CHEMICAL & DYE CORPORATION
40 Rector Street, New York 6, N. Y.

GC
Allied Chemical

announcing
GALVOMAG
Dow's new high potential anode cuts cost of corrosion protection
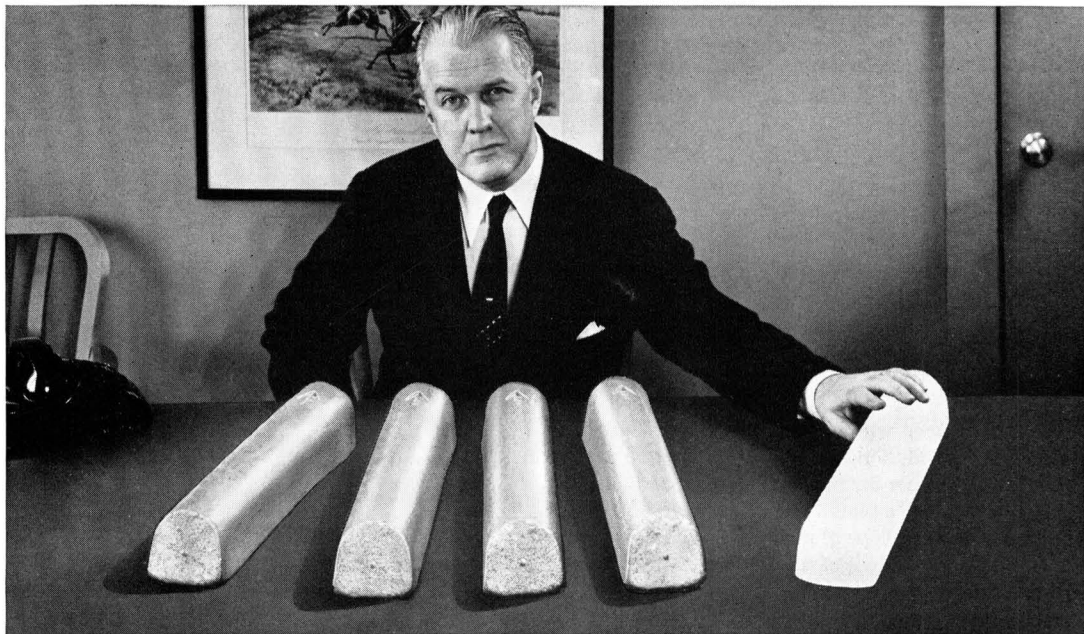
4 new GALVOMAG anodes do the job of 5 conventional anodes ... to reduce your original investment and installation cost, too

Let's take a new look at cathodic protection. Dow's new high potential anode, called GALVOMAG*, has 25% more current output than conventional anodes.

To put it another way—4 anodes now do the work of 5. It's easy to see why your installation costs in time and labor will go down in proportion.

In addition, economical protection in high resistivity soils can now be achieved. GALVOMAG's greater current output extends its use into ranges previously impractical for magnesium anodes.

Your Dow anode distributor is ready with all the facts and figures on GALVOMAG. Call him today. THE DOW CHEMICAL COMPANY, Midland, Michigan.   *Trademark

DISTRIBUTORS: ANTI-CORROSION MFG. CO., Atlanta, Georgia • CATHODIC PROTECTION SERVICE, Houston, Texas • CORROSION SERVICES INCORPORATED, Tulsa, Oklahoma ELECTRO-RUSTPROOFING CORP., Belleville, N.J. • ROYSTON LABORATORIES, INC., Blawnox, Pa. • STUART STEEL PROTECTION CORP., Kenilworth, N.J. • THE VANODE CO., Pasadena, California.

you can depend on DOW MAGNESIUM ANODES   **DOW**
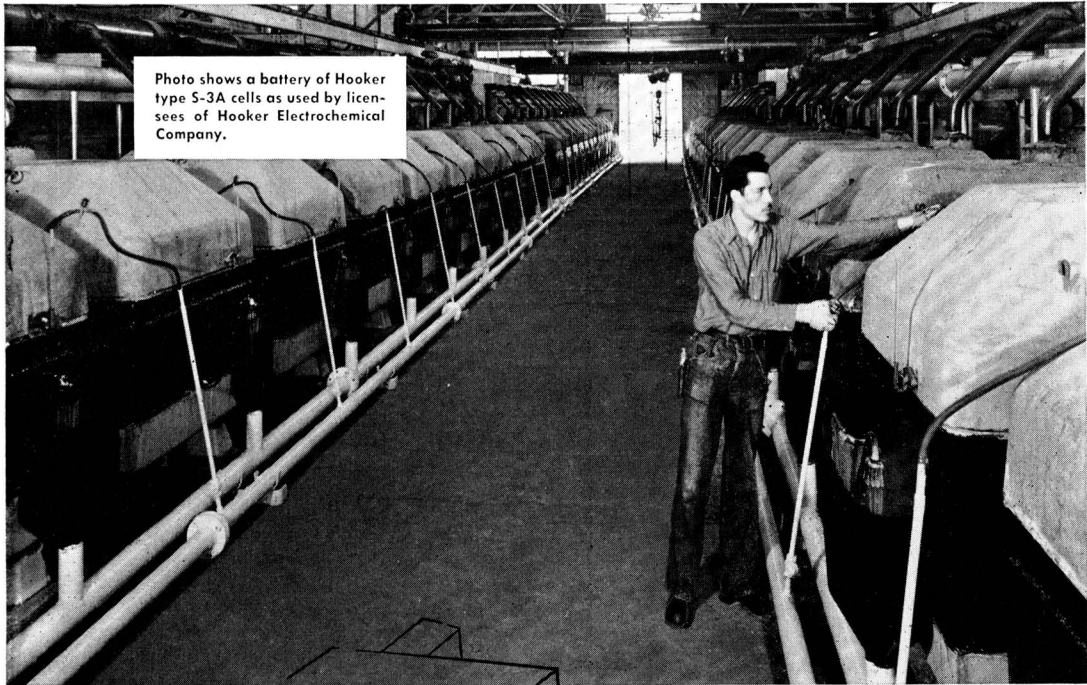
Photo shows a battery of Hooker type S-3A cells as used by licensees of Hooker Electrochemical Company.

THIS *is* ANODE PROGRESS

Today's graphite anodes last longer —
deliver more for the money . . . thanks
to a special Stackpole treatment that
minimizes deterioration, assures the
economy of low-voltage operation.
Write for Catalog 40A . . . or send
details of your carbon-graphite
requirements for recommendation by
Stackpole carbon-graphite specialists.

STACKPOLE CARBON COMPANY
St. Marys, Pa.

OTHER STACKPOLE PRODUCTS:

Brushes for all rotating electrical equipment (earth surface or high altitude) •
Electrical Contacts • Graphite Nozzles • Carbon Bearings • Seal Rings • Friction Segments •
Power Tube Anodes • Molds and Dies • Carbon Voltage Regulator Discs • Dash Pot Plungers •
Ground Rods • Carbon Rods for Salt Bath Rectification . . . and many more.

FUTURE MEETINGS OF
The Electrochemical Society

Pittsburgh, October 9, 10, 11, 12, and 13, 1955

Headquarters at the William Penn Hotel

Sessions will be scheduled on

**Batteries, Corrosion, Electrodeposition,
Electro-Organics, and Electrothermics and Metallurgy**

★ ★ ★

San Francisco, April 29 and 30, and May 1, 2, and 3, 1956

Headquarters at the Mark-Hopkins Hotel

Sessions probably will be scheduled on

**Electric Insulation, Electronics, Electrothermics
and Metallurgy, Industrial Electrolytics,
and Theoretical Electrochemistry**

★ ★ ★

Cleveland, October 28, 29, 30, and 31, and November 1, 1956

Headquarters at the Statler Hotel

★ ★ ★

Washington, D. C., May 12, 13, 14, 15, and 16, 1957

Headquarters at the Statler Hotel

★ ★ ★

Buffalo, October 6, 7, 8, 9, and 10, 1957

★ ★ ★

Papers are now being accepted for the meeting to be held in Pittsburgh. Triplicate copies of each abstract (not exceeding 75 words in length) are due at the Secretary's office, 216 West 102nd Street, New York 25, N. Y., *not later than June 15, 1955.* Complete manuscripts should be sent in triplicate to the Managing Editor of the JOURNAL at the same address.

Triplicate copies of abstracts of papers for the San Francisco Meeting must reach the Secretary's office not later than January 2, 1956.

The Crystallization of Anodic Tantalum Oxide Films in the Presence of a Strong Electric Field[1]

D. A. Vermilyea

Research Laboratory, General Electric Company, Schenectady, New York

ABSTRACT

Crystallization of amorphous anodic oxide films on tantalum may be accomplished by holding at temperatures in the neighborhood of room temperature provided a strong electric field is present in the film. This results in crystalline areas consisting of pie-shaped polycrystalline segments surrounded by coiled-up cylinders of the replaced amorphous phase. Factors affecting the nucleation and growth of these areas are discussed, and a mechanism of growth is proposed. The nucleation of the areas is not understood at present.

INTRODUCTION

There are at least two processes by which an amorphous anodic tantalum oxide film may be crystallized. It may be done simply by heating at 800°C (1). Recent experiments by Hillig (2) have shown that crystallization proceeds rapidly at temperatures as low as 650°C. This *thermal crystallization* apparently proceeds by the nucleation of a crystal and its growth into the amorphous phase.

The second process by which such films may be crystallized consists of holding them at temperatures from 0° to 100°C while a strong electric field is applied across the film. This paper presents the results of a study of crystallization by the second process, which will be referred to as *field crystallization*.

EXPERIMENTAL

The constant voltage power supply and constant temperature bath used in these experiments have been described previously (1). Measurements of amorphous and crystalline film thickness were made by comparison with the optical step gauge described in the previous paper (1). The growth of crystals was observed with a microscope using polarized light, and some electron micrographs were made using nitrocellulose replicas shadowed at 10° with chromium. Time-lapse motion picture studies were also made of some of the growing crystals.

THE PROCESS

Before discussing in detail the factors affecting the nucleation and growth of crystals in field crystallization, an example will be given to describe the over-all process. Consider an amorphous film being formed at 110 v in 2% HNO_3 at 99°C. Up to about 400 sec there is no crystallization, but the amorphous film grows in thickness and the current flowing

through the cell decreases as shown in Fig. 1. At about 350 sec the current starts to decrease less rapidly and, at the same time, examination with a microscope reveals a few very small crystals in the amorphous film. As time goes on these crystals grow, more crystals appear, and the current stops decreasing and begins to increase. Eventually the growing crystals impinge, the current reaches a maximum and then decreases again, and finally the entire oxide film has become crystalline. An electron diffraction pattern taken from a completely crystallized film by Alessandrini[2] showed that the crystals formed were Ta_2O_5.

NATURE OF THE CRYSTALS AND MECHANISM OF THEIR GROWTH

Fig. 2 and 3 show crystals formed on specimens held 2350 and 5500 sec under the conditions for which Fig. 1 was obtained. The individual crystals are irregular polygons with as few as 5 and as many as 11 sides, the average number being between 6 and 8. These polygons will be referred to as "crystalline areas" since they are not single crystals but consist of many smaller crystals as discussed below. On the top surfaces of the crystalline areas are a number of fine lines parallel to the sides and irregularly spaced. There is a broad out-of-focus region which looks like a cylinder outside of each side of the areas. These cylinders are above the plane of focus and frequently become detached as may be seen at a few places in Fig. 2. If the specimen is rubbed between the fingers this material in the cylinders is removed leaving only the crystalline areas as shown in Fig. 4. At the same time the appearance of the specimen to the naked eye changes from gray and dull to colored and shiny. It is believed that the presence of the material outside the crystals and raised above the surface

[2] Miss E. I. Alessandrini is associated with the General Electric Company, Schenectady, New York.
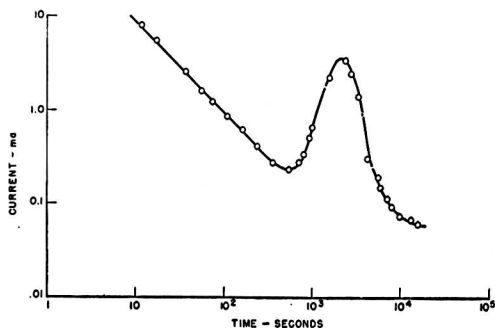
FIG. 1. Behavior of cell current during crystallization

simply diffuses light reflected from the surface causing a dull gray appearance.

The rolled-up material outside the crystalline areas is apparently the amorphous film which is pushed back and rolled up as the area grows. In other words, crystallization does not occur by consumption of the amorphous phase but by the replacement of it. The behavior of the cell current during crystallization provides support for the belief that an entirely new crystalline film is formed. For the run shown in Fig. 1 the total number of coulombs passed between 350 sec (when crystallization started) and 4500 sec (when the entire film was crystalline) was 6.4. If Ta_2O_5 of normal density was the product, this electrical energy would produce 4900 Å of oxide film on the 6.6 cm^2 specimen. The thickness of the crystalline film was estimated by comparison with the optical step gauge to be about 4200 Å. This estimate of thickness assumes that the refractive indexes of the amorphous and crystalline films are the same. While this may not be exactly true, a

FIG. 3. Crystalline areas formed in 5500 sec. 500× before reduction for publication. Unetched.

comparison of the refractive index determined for the amorphous films with that for crystals of Ta_2O_5 shows that the two are probably within 10% of each other [see reference (1)]. At any rate, it appears that more than enough coulombs have passed through the cell to completely replace the amorphous film with a crystalline one of the observed thickness.

When the crystalline areas are examined using polarized light, it is found that they are not single crystals but that each one consists of several pie-shaped segments. Fig. 5, of the same area illustrated in Fig. 3, shows that there is one segment for each

FIG. 2. Crystalline areas formed in 2350 sec. 500× before reduction for publication. Unetched.
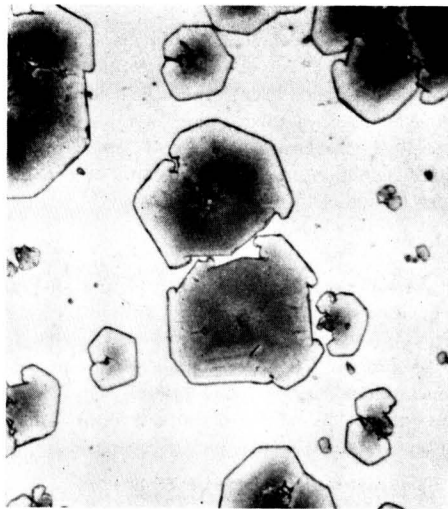
FIG. 4. Specimen after light rubbing to remove amorphous oxide. 500× before reduction for publication. Unetched.
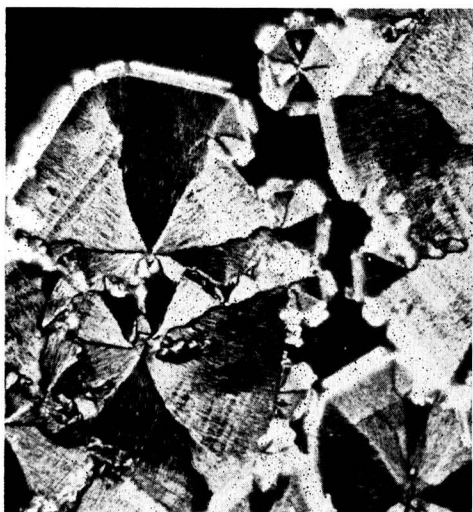
F𝐈G. 5. Same area as Fig. 3, polarized light. 500× before reduction for publication.

side of the crystal. Each of the segments is itself apparently not a single crystal, but is composed of smaller crystallites which appear to be elongated in the radial direction. The boundaries of the pie-shaped segments are generally jagged and uneven and not straight. Also, as impingement has occurred, or as interfaces have become stopped in their growth for other reasons, new small crystals have started at the stopped face and grown outward in all directions.

The electron microscope has been of great help in revealing the nature of the fine details of the crystalline films. The first observed indication of crystallization is a cracking of the amorphous oxide as shown in Fig. 6. From these cracked regions there next develops a crystalline area consisting of one or two segments as shown in Fig. 7. The impression of "flow lines" in the segments is obtained from subsequent figures. Cracks appear in the amorphous film at the intersections of the faces of the crystals. Fig. 8 shows larger crystalline areas which are beginning to assume a nearly equi-axial shape. The crystals usually start on one side of some region in the amorphous oxide and grow around it, although areas have been observed which were approximately equi-axial initially.

Only one of the crystalline areas shown in Fig. 6–8 exhibits any of the fine lines parallel to the crystal sides which were visible in Fig. 2 and 3. Fig. 9, taken of areas on a specimen which had an almost completely crystalline film, shows many such lines and also shows the manner in which the crystals have grown together. The fine lines apparently are produced more frequently after the crystals have become larger. The boundary between the segments of

the area becomes very jagged, with changes of direction occurring at positions where the fine lines meet the boundary. In Fig. 6–8, on the other hand, the boundaries are much less jagged and either straight or gently curved.

Observations on the nature of the crystalline areas suggest that growth occurs in the following manner. A nucleus forms beneath the amorphous film and starts to grow, producing a crack in the amorphous film. As the nucleus thickens, it pushes the amorphous film up off the metal, extending the original cracks, and producing more cracks. As the amorphous film is pushed off the metal the crystalline area grows radially, following the receding amorphous film. It is apparently often easier to strip back the amorphous film on one side of the nucleus than on the other, so that one or two wedge-shaped segments grow out first on one side of the nucleus and later others grow from these and, finally, completely surround the nucleus with crystalline material.

The number of segments in a crystalline area produced by such a process would be controlled by the number of cracks formed in the amorphous film, which might in turn depend on the surface condition of the metal, the presence of inclusions in the metal, and other factors which govern adherence of the
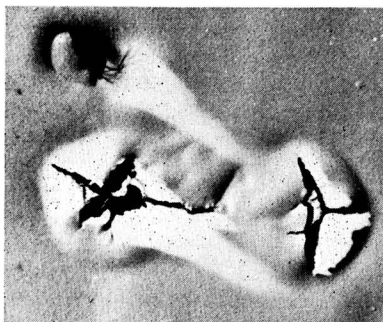
F𝐈G. 6. Start of crystallization. 15,000×
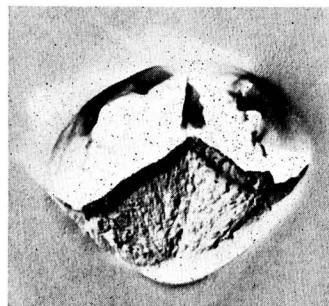
F𝐈G. 7. Crystalline area with 2 segments. 15,000×
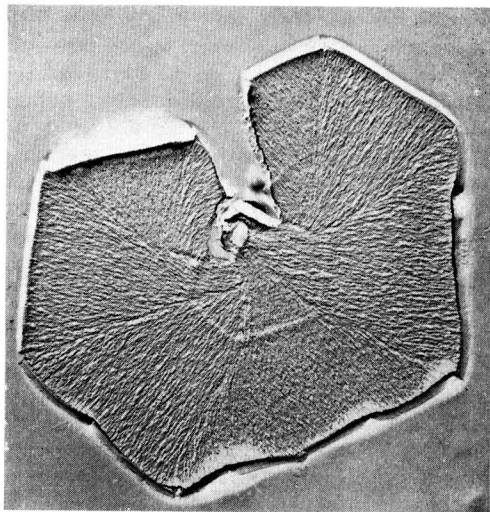
FIG. 8. Crystalline area nearly equi-axial. 5000×

oxide to the metal. It would be expected, therefore, that the number of segments would not be the same in all crystalline areas, in agreement with the experimental findings.

Each segment appears to consist of very small crystals elongated in the radial direction. Apparently when the amorphous film is pushed back many small crystals nucleate and grow, following the receding amorphous film. If there is a preferred growth direction, then those small crystals which are favorably oriented will grow most rapidly and crowd out the others. Each segment should thus consist not of a single crystal but of a number of small crystals with nearly the same orientation elongated in the radial direction, as observed. Such a preferred growth direction would result in the same orientation for most of the small crystals in each parallel segment of any crystalline area in the specimen. Fig. 5 shows that all parallel segments have the same appearance under polarized light, indicating that they have the same orientation. The growth of these small crystals with a long axis perpendicular to the advancing interface explains the appearance of flow lines in Fig. 6 through 8.

The forces acting on the amorphous film at the advancing crystal interface are those exerted by the crystal tending to push the film upward and the adhesion of the film to the metal. These forces tend to bend the amorphous film at its point of departure from the metal. Since the ions are mobile in the film due to the high electric field, presumably they move under the influence of the mechanical stresses in such a way that the stresses are relieved. In other words, the amorphous film becomes permanently curved. As the crystal grows, producing more curved

amorphous film, a cylinder of rolled up amorphous film is formed at the advancing interface, as shown in Fig. 2 and 3.

Crystalline areas growing by the mechanism suggested should show erratic growth rates, varying from place to place on the specimen as the ease of stripping the amorphous film varied. Time-lapse motion pictures have shown that the individual faces of the crystalline areas grow rapidly at some times and apparently stop at others. The fine lines visible in Fig. 2 and 3 are probably places where the crystal grew very slowly, or stopped altogether. The jagged boundaries between segments result when one segment stops or slows down while the other, growing more rapidly, attempts to grow around the stopped segment.

The rate of radial growth varies from place to place on the specimen, as might be expected on the basis of the proposed mechanism. Fig. 10 shows curves of diameter vs. time for crystalline areas growing simultaneously on one specimen. Not only are the growth rates different for the two areas, but they are not constant. This behavior is typical of radial growth and, while the growth rate usually decreases with time, in a few instances it has increased with time.

If the electric field is removed, growth ceases since no thickening of the crystals occurs and hence no further stripping of the amorphous film. If the field is reduced, the radial growth rate is decreased because the rate of thickening decreases, while increasing the field increases the radial growth rate. For a given formation voltage radial growth is also more rapid at high temperatures, as might be ex-

FIG. 9. Intersections of crystalline areas on a specimen almost completely crystallized. 5000×.

pected because the rate of thickening is greater at higher temperatures.

The rate of growth depends on the nature of the solution in which the film is formed as seen by Fig. 11. Fig. 12 shows that the number of crystals formed at a given time is about the same in both solutions. Average growth rates, however, were 1.13×10^{-6} cm/sec for H_2SO_4 and 2×10^{-6} cm/sec for KCl, so that the crystallization was completed sooner in KCl. Growth rates as low as 3.3×10^{-8} cm/sec have been measured for solutions of $Na_2B_4O_7$ at 99°C.

The difference in radial growth rates of crystalline areas formed in different solutions is believed to be the result of a difference in the rate of growth of the crystals in thickness. The thickness of the crystalline
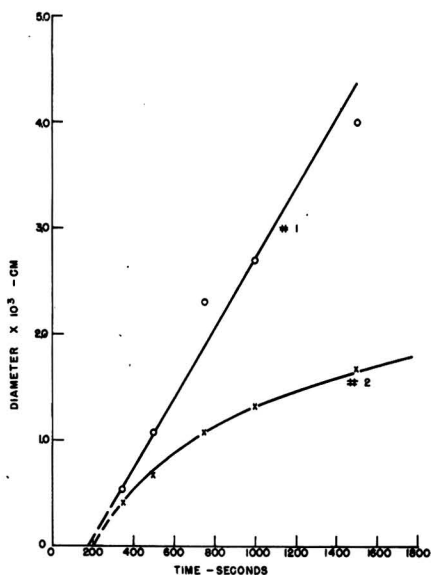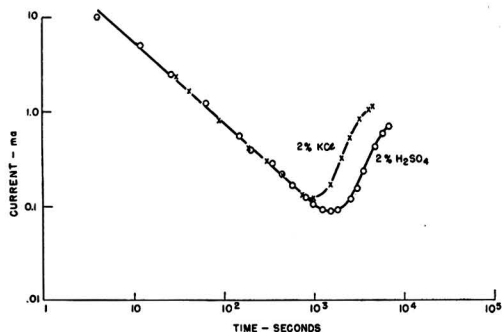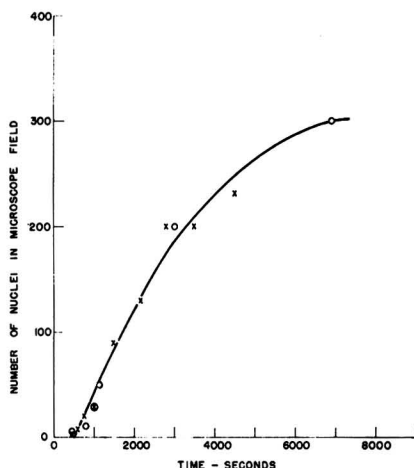
FIG. 12. Nucleation frequency in two solutions; O = 2% H_2SO_4; x = 2% KCl.

areas formed in 66,000 sec at 99°C, 100 v, was 4650 Å in 2% KCl, 4500 Å in 2% H_2SO_4, and 3900 Å in 2% $Na_2B_4O_7$. If radial growth occurs only as the crystals thicken and push back the amorphous film, these differences in thickness growth rate can explain qualitatively the difference in radial growth rate. Quantitative comparisons would require a greater knowledge of the stripping process and of the change in growth rate of the crystals with time.

The reason why the rate of thickness growth of the crystals depends on the solution in which they are formed is not known. The effect of solution composition is apparently associated with the oxide-electrolyte interface, however, because the rate of crystal growth changes immediately upon changing the electrolyte. For example, Fig. 13 shows a current-time curve for a specimen which was formed in 2% HNO_3 to 300 sec and in 2% $Na_2B_4O_7$ thereafter. When the electrolyte was changed, the growth of the crystals was drastically reduced and, since most of the current passing through the cell is used to form new crystalline material, the current fell to about 20% of its value in 2% HNO_3.

One further experiment supports the hypothesis that radial growth occurs only as the amorphous film is pushed back. If an amorphous film is formed in a solution containing a small amount of HF, the resulting film may be very easily stripped from the metal. When such a film is formed at 100 v in 2% HNO_3 at 99°C, no crystals of the type described in this paper are formed. Instead, at about 400 sec (the time at which crystals form in normal Ta_2O_5 films not easily stripped) there appear regions in the film where the amorphous film has been stripped away over a considerable area and is no longer in contact

FIG. 10. Growth of crystalline areas being formed simultaneously on the same specimen.

FIG. 11. Cell current in two electrolytic solutions each at 99°C with formation voltage of 100 v.
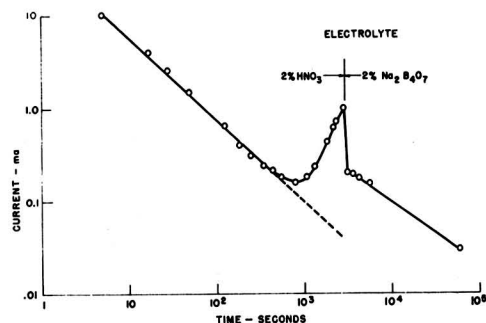
FIG. 13. Effect of changing solution composition on the progress of crystallization.
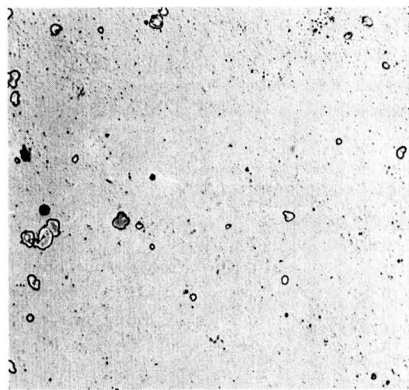
FIG. 14. Areas where amorphous film was stripped from the metal on a specimen with an easily stripped film. 100×. Unetched.

with the metal. Fig. 14 shows some of these areas. These regions are not crystalline, although very small crystals may be seen inside the areas. Presumably a crystal nucleates as usual but, instead of cracking, the amorphous film simply lifts the film off the specimen for a considerable distance. No further growth of the crystal, now buried beneath the stripped area, can occur.

Field crystallization thus produces crystalline areas composed of multicrystalline pie-shaped segments. These areas grow laterally by pushing the amorphous film aside, producing a coiled cylinder of amorphous film outside of each advancing side of the area. The remainder of this paper is concerned with the results of a study of the factors which affect the nucleation of these areas.

NUCLEATION OF CRYSTALLINE AREAS

The amount of time which elapses between the application of the voltage and the appearance of the first crystals has been found to be influenced by the temperature, the applied voltage, and the condition of the metal surface.

The effect of the metal surface.—The effect of surface condition of the tantalum sheet was investigated using as-rolled sheet, electropolished sheet, chemically polished sheet, and chemically polished sheet etched 30 sec in HF. These different surface treatments caused the nucleation time to vary between 150 and 600 sec, the shortest time being observed for as-rolled sheet and the longest for electropolished sheet. In addition, variations in the lot of tantalum used with one surface treatment caused the nucleation time to vary from 150 to 400 sec.

These observations indicate that inclusions or impurities present in the metal may play an important role in the nucleation process, and further support for this idea is found in the fact that, when time-lapse motion pictures are run in reverse, spots, presumably inclusions, are observed at places where the crystals disappeared. Since the surface treatment also influences nucleation, it is very important when evaluating the influence of other factors on crystallization to make certain that the material used is from the same lot and is prepared in the same manner. In the remainder of this work specimens from the same lot of material were chemically polished and then etched 30 sec in HF, since this treatment gave the most reproducible results.

Effect of formation voltage.—The influence of formation voltage on the nucleation rate was determined by holding specimens at 99°C in 2 % HNO_3 at various voltages and examining them periodically to determine whether any crystals had formed. Data obtained are given in Table I and plotted in Fig. 15 and 16. It may be seen that the time to start crystals is greater at lower voltages and that the field at the start of nucleation is less the lower the forming voltage. A lower forming voltage necessarily means a smaller film thickness.

Effect of temperature.—The effect of temperature on the time of nucleation was determined by holding specimens at 100 v in 2 % HNO_3 at various temperatures. Results are given in Table II. As the temperature decreases, nucleation time increases, the field in the amorphous film at nucleation increases, and

TABLE I. *Field crystallization in 2% HNO_3 at 99°C*

Formation voltage	Nucleation time, sec	Thickness of amorphous film, Å	Electric field, v/Å
41	4800	909	0.0452
61	2270	1305	0.0467
81	800	1640	0.0495
100	400	1960	0.0512
131	100	2435	0.0538
141	48	2574	0.0548
161	20	2830	0.0569
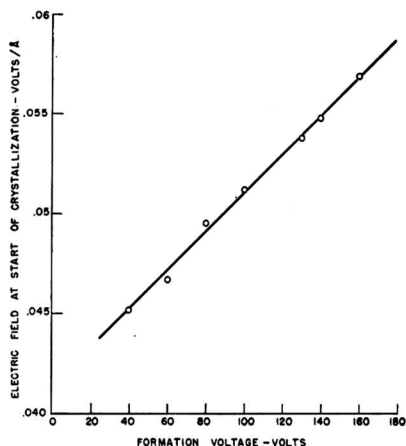
FIG. 15. Effect of formation voltage on the electric field at the start of crystallization.
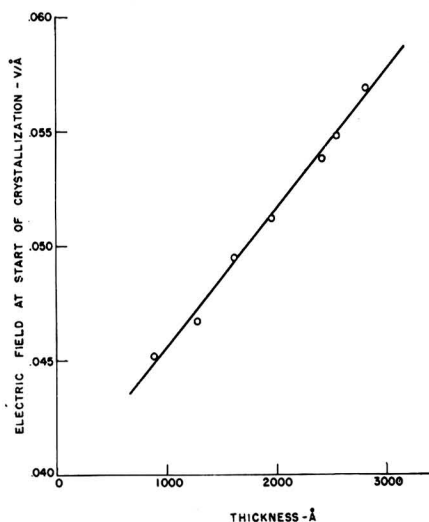
FIG. 16. Effect of thickness on the electric field at the start of crystallization.

the rate of amorphous film growth at nucleation decreases.

Effects of history, rate of amorphous film growth, and electrical breakdown.—Experiments in which the history of a film was varied indicate that at a particular voltage and temperature there is a critical thickness below which nucleation does not occur. For example, at 100 v, 99°C, nucleation was observed on holding for 400 sec, at which time the film thickness was 1960 Å. When a film was formed rapidly at a low temperature to a thickness greater than 1960 Å and subsequently etched in HF to below that thickness, nucleation occurred at 1960 Å when the film was subsequently held at 100 v, 99°C. In another

TABLE II. *Effect of temperature on nucleation, 100 v*

Temp, °C	Nucleation time, sec	Electric field in amorphous film, v/Å	Thickness, Å	Rate of growth of amorphous film, Å/sec
19	500×10^2	0.0554	1805	0.94×10^{-3}
29	250	0.0547	1830	1.95
40	150	0.0537	1866	3.5
49.5	70	0.0533	1875	7.78
60	40	0.0527	1900	14.5
73	20	0.0518	1930	30.9
86	10	0.0513	1950	66.0
99	4	0.0509	1965	166.0

experiment a film was formed for 300 sec at 100 v, 99°C, and the film was then corroded in HF to the starting thickness. The process was repeated four times, making a total of 1200 sec; no nuclei were observed. When the specimen was then held 100 sec longer at 100 v, nuclei appeared, and the film thickness was 1960 Å. Nucleation of crystals occurs at the same thickness regardless of the number of interruptions for the purpose of observing the film and of the temperature and rate of formation to the starting conditions.

If an amorphous film is formed at a low temperature to a thickness greater than the critical thickness but so great that on subsequent application of the test voltage the growth rate of the amorphous film is very low, crystal formation is greatly retarded. For example, at 100 v and 99°C nuclei are normally observed at 1960 Å, and growth of the amorphous film is extremely slow at thicknesses greater than 2300 Å. A film formed to 2525 Å at room temperature and then held at 100 v and 99°C showed no crystals after 3350 sec. It was calculated from other data that the rate of amorphous film growth would be 2.3×10^{-4} Å/sec. When the specimen was etched in HF to 2105 Å, however, where the rate of growth should have been about 0.02 Å/sec, nuclei were observed after holding at 100 v for an additional 750 sec. These experiments suggest that some ion movement in the amorphous film may be necessary for nucleus formation.

Crystals of Ta_2O_5 powder in contact with the outer surface of the oxide film do not hasten crystal formation. This fact supports the idea that nuclei are formed at the oxide-metal interface. Only one phenomenon is known which is a direct cause of crystal formation. When a film which has been formed under conditions which produce electrical breakdown is subsequently held under conditions where crystallization is possible, the regions where breakdown has occurred are found to be nucleation sites. The question arises whether all crystals start from electrical breakdowns in the film. If such were the case, it would be expected that nucleation would

occur at the greatest applied field strength, that is, as soon as voltage was applied. Also, it would be expected that, if the film thickness were reduced by a factor of two, the field necessary to cause breakdown would be increased tremendously, but in fact the field necessary for nucleation is smaller as shown in Fig. 16. These facts seem to make electrical breakdown unattractive as an explanation of the origin of crystal nuclei.

At the present time no satisfactory interpretation of the effects of voltage and temperature on nucleation has been discovered. Fig. 15 and 16, along with the evidence that at any temperature there is a voltage dependent critical thickness below which nucleation will not occur, suggest an influence of the electric field on the nucleation of crystals under those conditions. On the other hand, since the rate of growth of the amorphous film at any temperature is determined by the field, it may be that a critical growth rate is required for nucleation, and that the critical rate depends on the film thickness.

In either case it is surprising that at one temperature there should be such a marked variation of nucleation time with the thickness of the amorphous film. Further work will be directed toward an understanding of the mechanism of nucleation under these conditions.

DISCUSSION

It is interesting to inquire why the initial low temperature film which forms on tantalum, and on other metals such as aluminum, is amorphous rather than crystalline. When one of the films which has been partly or completely crystallized by field crystallization is anodized further the new film formed on top of the crystalline film is also crystalline. The maximum growth rate for which this observation has been made was only about 100 Å/sec, however, which is low compared to the rate of forming the first few layers of oxide when a clean specimen is exposed to air. It may be that at extremely rapid rates the molecules which are forming the new oxide do not have time to arrange themselves in the lattice structure of the crystalline phase.

It is also interesting that the field required to cause appreciable ionic movement at a given temperature is only about half as great for the crystalline as for the amorphous film. This fact and the fact that the thickness growth rate is a function of the solution composition indicate that interesting results might be obtained from a study of the kinetics of growth of the crystalline film.

CONCLUSIONS

1. Amorphous tantalum oxide films crystallize at temperatures between 0° and 100°C provided a strong electric field is present in the film. The result of such crystallization is crystalline areas consisting of pie-shaped polycrystalline segments surrounded by coiled-up cylinders of the replaced amorphous film. In each segment the individual crystallites have a preferred growth direction perpendicular to the edge of the segment.

2. The crystalline areas grow by pushing back the amorphous film, and this only occurs when the crystals thicken. Any reduction in the rate of thickness growth of the crystals, such as is produced by lower temperature or lower field, decreases the radial growth rate as well. The rate of growth of the crystals is also slightly different in different solutions.

3. Nucleation of the crystals occurs only below a critical electric field strength in the amorphous film. This critical field depends on the temperature of formation, the surface condition and impurity content of the metal, and the thickness of the amorphous film, but does not depend on the history of the film. At fields far below the critical field nucleation is greatly retarded. Nucleation apparently occurs at the oxide-metal interface.

4. Once a crystalline film has been formed subsequent growth in thickness is always crystalline.

5. The thickness of a crystalline film formed at a given voltage and temperature is about twice as great as that of an amorphous film formed under the same conditions.

Any discussion of this paper will appear in a Discussion Section to be published in the December 1955 JOURNAL.

REFERENCES

1. D. A. VERMILYEA, *Acta Met.*, **1**, 282 (1953).
2. W. B. HILLIG, Private communication.
3. D. A. VERMILYEA, *Acta Met.*, In press.

Results of Some Marine-Atmosphere Corrosion Tests on Magnesium-Lithium Alloys[1]

P. D. Frost, F. W. Fink, H. A. Pray, and J. H. Jackson

Battelle Memorial Institute, Columbus, Ohio

ABSTRACT

Magnesium-lithium binary alloys which contain just enough lithium (about 11 wt %) to produce a single-phase, body-centered cubic structure have shown surprisingly good resistance to corrosion in 3% salt solution. High-strength alloys having about 9% lithium and various quantities of aluminum, zinc, and other elements have a mixed hexagonal-plus-body-centered cubic structure. Such alloys generally have poorer corrosion resistance than the single-phase binaries. Three of the high-strength alloys were exposed for 32 months to the sea-coast atmosphere near Daytona Beach, Florida. For comparison purposes, samples of commercial AZ31A-H24 alloy were exposed at the same time. All alloys were in the form of 4 × 6 × 0.064 in. panels. The AZ31A sheet had corrosion resistance only slightly superior to that of an alloy containing Mg-8.7% Li-5% Al-8% Zn. The other two alloys, Mg-8.8% Li-7% Al-0.05% Sn-1% Mn and Mg-8.8% Li-7% Al-1% Sn, had much poorer corrosion resistance.

INTRODUCTION

Results of extensive research programs conducted in this country on magnesium-lithium-base alloys have been published in earlier papers (1–4). In addition to the work done in this country, investigations on magnesium-lithium alloys were carried out in England (5, 6) and in Russia (7).

The primary objective of the research in this country during the 1940's was to develop ultralight, high-strength alloys for structural applications. Although many alloys having high strength and good ductility were developed, their properties were not stable at temperatures above about 150°F. This instability, characteristic of all magnesium-lithium-base alloys, has prevented their use for structural purposes.

This paper describes the results of corrosion tests begun in June 1950, on several experimental structural-type alloys.

CORROSION TESTS

Lithium forms a series of solid solutions with magnesium. Alpha alloys, containing from 0 to 5.7% lithium, have a hexagonal close-packed structure; beta alloys, containing 10.3% or more lithium, are body-centered cubic. Between 5.7 and 10.3% lithium, a mixture of the alpha and beta phases exists.

Contrary to expectations, certain magnesium-lithium-base compositions have surprisingly good resistance to corrosion in 3% NaCl solution. Table I and Fig. 1 compare the relative corrosion resistance of several binary magnesium-lithium and ternary

magnesium-lithium-zinc alloys with that of a commercial magnesium-manganese composition in salt solution (1). The magnesium-manganese alloy corresponds to ASTM Alloy M1A, which is one of the more corrosion resistant commercial magnesium alloys. In this experiment the single-phase, beta Mg-11%Li alloy suffered the smallest weight loss and the least pitting attack of all the alloys tested. Thus, a magnesium-lithium alloy can have reasonably good corrosion resistance.

The marine-atmosphere corrosion tests, which comprise the main topic of this paper, were conducted on three high-strength magnesium-lithium-base alloys and the high-strength commercial Alloy AZ31A.[2] The alloys had the following nominal compositions:

Heat No.	Composition	Specific gravity
2611	Mg-8.8% Li-7% Al-1% Sn	1.56
2613	Mg-8.8% Li-7% Al-0.05% Sn-1% Mn	1.53
2615	Mg-8.7% Li-5% Al-8% Zn	1.65
AZ31A	Mg-3% Al-1% Zn-0.3% Mn	1.77

The three experimental alloys are of the alpha-beta type, containing appreciable quantities of the hexagonal phase. These were melted as 18-lb heats into ingots about 5 x 5 x 8 in. The ingots were homogenized 3½ hr at 720°F, scalped, and press forged.[3] The ingots were preheated 4 hr at 500°F and raised to 675°F for 1 hr prior to forging. They were upset and cross worked considerably and finally pressed into slabs approximately 1¼ x 6 x 21 in. These were scalped at Battelle and rolled into the sheet product at a temperature of about 625°–700°F. The panels

---

[2] Formerly designated as AZ31X.

[3] At Wyman-Gordon Co., Worcester, Mass.

TABLE I. *Relative corrosion resistance of several magnesium-lithium-base alloys in 3% NaCl solution at 95°F for 8 days**

Heat No.	Nominal composition, %				Average wt loss, mg/cm²/day
	Zn	Mn	Li	Mg	
875	4	—	10.6	Bal	2.83
690	4	—	9.0	Bal	2.81
874	—	—	11.0	Bal	0.57
873	—	—	9.3	Bal	0.77
872	—	—	4.0	Bal	4.44
871	—	—	2.0	Bal	4.92
251	—	1.26	—	Bal	0.62

* Alternate immersion test, ½-min immersion, 2-min emersion. Solutions were changed after 4 days. Specimens were tested as extruded and were approximately 6 x 1 x ¼ in. in size.

were exposed to the sea-coast atmosphere in the hot-rolled condition. In this condition, these alloys have a yield strength of about 28,000 psi. The commercial-alloy panels were all taken from the same sheet. They were exposed, as received, in the hard-rolled (H24) condition. The yield strength of this material, as hard rolled, is about 32,000 psi.

All specimens were in the form of sheet panels, 4 x 6 x 0.064 in. in size and weighing between 38
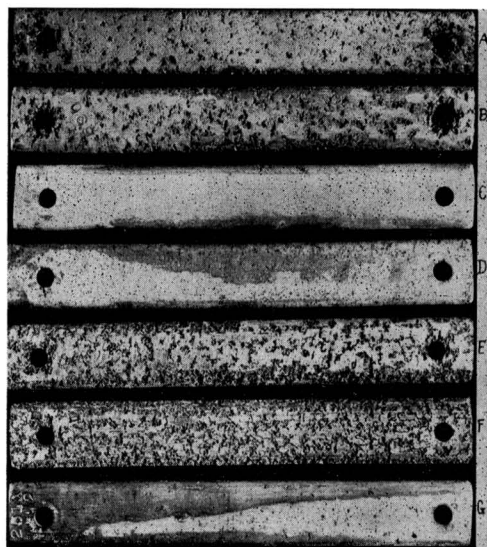
FIG. 1. Specimens of Mg-Li alloys compared with a commercial Mg-1.26%Mn alloy following cyclic immersion corrosion test in 3% NaCl at 95°F for 8 days. A—Heat No. 875, Mg-10.6%Li-4%Zn, lattice structure β; B—Heat No. 690, Mg-9%Li-4%Zn, lattice structure β; C—Heat No. 874, Mg-11%Li, lattice structure β; D—Heat No. 873, Mg-9.3% Li, lattice structure α-β; E—Heat No. 872, Mg-4%Li, lattice structure α; F—Heat No. 871, Mg-2%Li, lattice structure α; G—Heat No. 251, Mg-1.26%Mn, M1A alloy, lattice structure α.

and 46 g, depending on the alloy. After abrading with emery cloth to remove scale and degreasing, the panels were exposed, at the Battelle exposure station located about 12 miles south of Daytona Beach, Florida. This site is approximately 500 ft inland from the mean high tide line. At this point, the shoreline runs approximately northeast-southwest. The corrosion racks face south. The racks are dew coated about 9 out of 10 nights. The relative humidity in this area averages 82% and heavy fog occurs about 10% of the time. Thus, the panels were frequently wet.

Standard ASTM stainless steel corrosion racks were used. The panels were inclined 30 degrees from the horizontal and were supported at four points by porcelain insulators.

Ten panels of each alloy were exposed. Two panels of each were removed after intervals of 2, 4, 8, 16, and 32 months. The results of the tests are summarized graphically in Fig. 2. As might be expected, all four alloys corroded more rapidly during the early months of exposure. The corrosion rate reached a maximum in the Mg-Li-Al-Sn and Mg-Li-Al-Sn-Mn alloys after four months, whereas in the Mg-Li-Al-Zn and Mg-Al-Mn alloys the maximum occurred around two months or shortly thereafter. The commercial AZ31A alloy had the best corrosion resistance and the Mg-Li-Al-Zn alloy behaved very
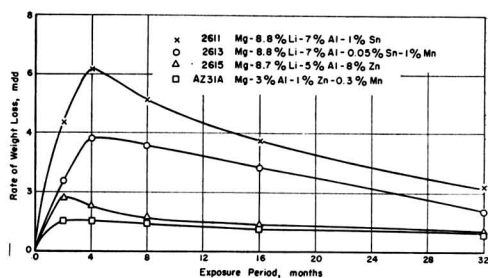
FIG. 2. Corrosion rate, expressed as weight loss, of experimental magnesium-lithium base alloys compared with commercial AZ31A alloy.
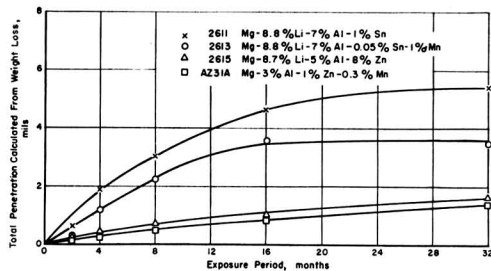
FIG. 3. Total penetration, calculated from weight loss, in experimental magnesium-lithium base alloys compared with commercial AZ31A alloy.

similarly. The Mg-Li-Al-Sn-Mn alloy had considerably poorer resistance; the Mg-Li-Al-Sn alloy had the highest corrosion rate of the four alloys.

Corrosion rates of the two more resistant alloys remained nearly constant after about eight months' exposure, whereas those of the two least resistant alloys decreased continuously during the same period. The trend is shown more strikingly when total penetration rather than penetration rate is plotted against the time abscissa, as in Fig. 3. Thus, the slopes of the corrosion curves for the Mg-8.7%Li-5%Al-8%Zn and Mg-3%Al-1%Zn-0.3%Mn alloys are essentially equal and constant between 8 and 32 months, but for the other two alloys the slopes decrease. This suggests that the two alloys which had the poorer corrosion characteristics in this experiment might appear to somewhat better advantage after exposures considerably longer than 32 months.

FIG. 8 (left). Underside of panel of the Mg-8.7%Li-5%Al-8%Zn alloy after 16 months' exposure; actual size before reduction for publication.
FIG. 9 (right). Same panel after removal of corrosion products.

FIG. 4 (left). Underside of panel of the Mg-8.8%Li-7%Al-1%Sn alloy after 16 months' exposure; actual size before reduction for publication.
FIG. 5 (right). Same panel after removal of corrosion products.
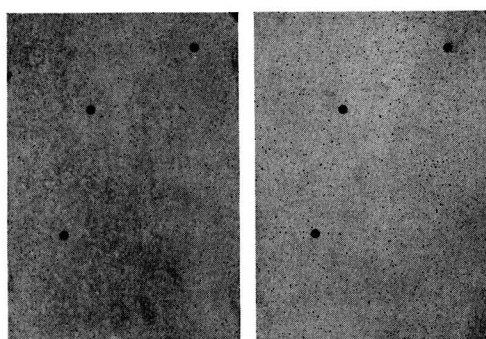
FIG. 10 (left). Underside of panel of the Mg-3%Al-1%Zn-0.3%Mn alloy after 16 months' exposure; actual size before reduction for publication.
FIG. 11 (right). Same panel after removal of corrosion products.

Photographs were taken of the underside of the panels exposed 16 months. These are shown in Fig. 4 through 11 before and after the corrosion products were removed.[4] The extent of the attack was invariably greatest on the underside of the panels throughout the entire experiment.

The appearance of the panels reflects the results shown by the graphical data. All panels were pitted, the first two alloys more severely than the last two. The commercial AZ31A alloy showed the least amount of attack. However, there was little difference in the appearance of this alloy and the Mg-8.7%Li-5%Al-8%Zn alloy. It might be added that unprotected carbon steel panels of the same thickness

FIG. 6 (left). Underside of panel of the Mg-8.8%Li-7%Al-0.05%Sn-1%Mn alloy after 16 months' exposure; actual size before reduction for publication.
FIG. 7 (right). Same panel after removal of corrosion products.

[4] Corrosion products were removed by immersing the panel for 1 min in a water solution of 232.6 g/l CrO_3 and 11.7 g/l $AgNO_3$ maintained at the boiling temperature.

exposed under similar conditions at the same site tend to disintegrate in less than 24 months.

Any discussion of this paper will appear in a Discussion Section to be published in the December 1955 JOURNAL.

REFERENCES

1. J. H. JACKSON, P. D. FROST, A. C. LOONAM, L. W. EASTWOOD, AND C. H. LORIG, *J. Metals*, **185,** 149 (1949).
2. P. D. FROST, J. G. KURA, AND L. W. EASTWOOD, *J. Metals*, **188,** 1277 (1950).
3. P. D. FROST, J. H. JACKSON, A. C. LOONAM, AND C. H. LORIG, *ibid.*, **188,** 1171 (1950).
4. R. S. BUSK, D. L. LEMAN, AND J. J. CASEY, *ibid.*, **188,** 945 (1950).
5. W. HUME-ROTHERY, G. V. RAYNOR, AND E. BUTCHERS, *J. Inst. Metals*, **71,** 589 (1945).
6. Unpublished discussions and communications with Prof. A. J. Murphy, Chairman Industrial Metallurgy Department, University of Birmingham, Birmingham, England.
7. F. L. SHAMRAI, *Bull. acad. sci. U.S.S.R.*, Section of Chemical Sciences, Part I, No. 6, 606 (1947); Part II, No. 1, 83 (1948); Part III, No. 3, 290 (1948).
8. G. GRUBE, H. VON ZEPPELIN, AND H. BUMM, *Z. Elektrochem.*, **40,** 160 (1934).

On The Nature of Lead Surfaces Passivated in Sulfuric Acid[1]

E. J. CASEY AND K. N. CAMPNEY

Defence Research Chemical Laboratories, Ottawa, Canada

ABSTRACT

Experimental results are presented which show that the rate of ennoblement of the electrochemical potential of lead which is passivating in sulfuric acid is markedly dependent on the concentration of hydrogen peroxide, whether formed by irradiation or added directly to the system. A study of factors which affect the ennobled potential of the sulfated or passivated lead is presented, as is a study of the conditions under which the sulfated lead shows rectifying properties. Results are interpreted in terms of the suggested presence of oxygen atoms sorbed into the lead sulfate layer.

INTRODUCTION

Considerable practical as well as theoretical importance attaches to the passivation of lead in sulfuric acid. In this paper are presented the results of some chemical, electrochemical, and electrical experiments which shed further light on the nature of the surface processes which give rise to the various observed phenomena. In particular, electrochemical effects observed during passivation by Müller (1), Haring and Thomas (2), and others have been puzzling. Thus, Müller has noted that lead pieces autocorroding in sulfuric acid show an electrochemical potential usually within 3 mv of the $Pb/PbSO_4$ reversible potential, but that when passivated they will exhibit a potential 0.50–0.65 v more noble than the $Pb/PbSO_4$ reversible potential. Müller has described this phenomenon in terms of a covering layer-pore theory (3), in which the ennobled potentials are described in terms of the electrolytic iR drop thought to exist in the pores in the film of $PbSO_4$. The potentials exhibited by such passivated electrodes, in terms of this theory, would be those measured between the metallic lead and the bulk electrolyte at the end of the pores, and would thus be (a) the potential of the local anode, the $Pb/PbSO_4$ electrode at the base of the pore, plus $i_L R_a$, where i_L is the local corrosion current and R_a is the electrolytic resistance of the pore; or (b) the potential of the local cathode, the nature of which is undetermined, but whose site is considered to be the whole $PbSO_4$-electrolyte interface; the local cathode is connected to metallic lead by the lead sulfate layer.

This theory leads to some difficulties. For instance, the theory does not adequately interpret the local cathode: what is the source of the driving energy for the maintenance of a local current of such a magnitude through such a high pore resist-

ance? If $R_a + R_c$ is so large that i_L is so small that no appreciable change in pore size occurs during local action, then, if $R_a \cong R_c$, any measurement made with a common potentiometer circuit would be insensitive because of high film resistances in the circuit; such is not the experimental observation. On the other hand, if $R_a \gg R_c$, say, the potentiometric measurement would be that of the local cathode which could not be sensibly polarized by the local current because the local current density through the cathode would be so small. Yet the potentials exhibited by the passivated pieces do not correspond to any of the common, known, redox systems. If, on the other hand, the local cathode is truly a strongly oxidizing electrode polarized down to the 0.50–0.65 v potential, then the implication in the Müller theory that unsealed pores exist on the passivated electrode is untenable.

The alternative argument, that pores do seal over while others are being formed by stress cracking of the surface film, to maintain open pores always of constant number and size, formed on different specimens which contain films of different thicknesses formed in different ways, which would have to be the case in order that the potential be reproducible, does not seem to be very likely either.

Haring and Thomas (2) considered the passivated lead to be completely covered with a layer of sulfate, and they considered the ennobled potential to be that of "an oxygen-depolarized hydrogen electrode," presumably a mixed potential of hydrogen and oxygen electrodes, both highly polarized, active at the lead sulfate-electrolyte interface. A detailed mechanism is not offered, however, for the formation and maintenance of the potential observed.

Experiments reported in the present paper have led to a new interpretation of the nature of the sulfated lead surface.

It is after the ennoblement of potential that the metal piece is defined, in the present paper, as passivated. This is perhaps a narrower definition of

passivation than is used by Pourbaix (4), but is the one used by Müller and his associates with reference to the type of electrochemical information herein reported.

EXPERIMENTAL RESULTS AND DISCUSSION

Lead samples were cut from Baker & Adamson lead metal sheet, which analyzed for: silver, 0.008%; bismuth, <0.001%; arsenic, <0.001%; copper, 0.06%; antimony, <0.005%. Surface preparation was effected by scraping the lead surface down to the bright metal by means of a glass edge, usually a microscope slide. The sulfuric acid and other chemicals were reagent grade.

Potential measurements were made with a Leeds & Northrup Type K potentiometer and with a General Radio type 715-A d-c amplifier plus Esterline-Angus recording milliammeter. Inverted lead-lead sulfate-sulfuric acid reference electrodes were made simply by covering the submerged, freshly prepared lead surface with lead sulfate crystals. Mercury-mercurous sulfate reference standards were prepared by a variation of the electro-oxidation method used by Harned and Hamer (5).

Rate of passivation.—Although lead sulfate, a good insulator, is formed on the surface of lead autocorroding in sulfuric acid, it is formed as small crystals. To a magnification of about 500 times the only apparent physical difference between an unpassivated and a passivated lead piece is the number and depth of the crystals (Fig. 1). The low current d-c resistance has increased markedly with passivation, but the electrode is by no means electrically insulated from the electrolyte by the lead sulfate layer, otherwise measurement would be impossible.

Fig. 2 shows a typical potential-time plot obtained with lead pieces allowed to autocorrode in 1.223 s.g. sulfuric acid. Potentials were measured against a $Pb/PbSO_4$ reference electrode, which was
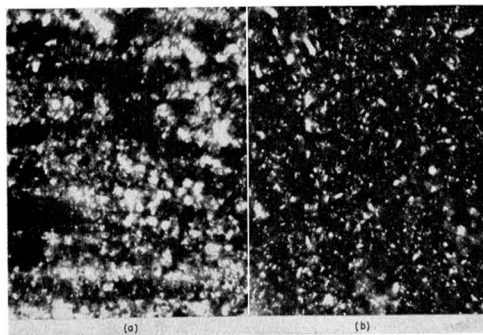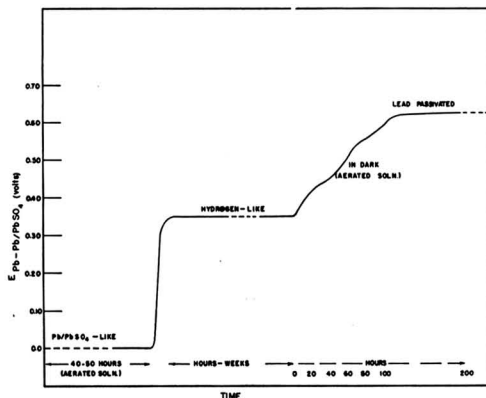
FIG. 2. Potential-time plot of lead pieces autocorroding in sulfuric acid.

frequently standardized against a Hg/Hg_2SO_4 reference electrode. Three distinct sections are noted in Fig. 2: (a) the time as a $Pb/PbSO_4$ electrode, when the corrosion is under cathodic control, before sulfation; (b) the time as a hydrogen-like electrode, when the rate may be anodically controlled by the covering layer of lead sulfate; and (c) the subsequent time as a fully passivated lead electrode, the nature of which was the subject of this investigation. The sulfation time, or the rate of attainment of sulfation, has been found previously by Müller and by Haring and Thomas to be transport-controlled, and the rate increases with increasing concentration of oxygen. Removal of the electrolyte-lead-air interface was found by Thomas (6) to reduce the sulfation time. It was concluded by Müller that diffusion of oxygen through the electrolyte toward the electrode controls sulfation. However, the existence of hydrogen-like electrodes on lead does not seem to have been noted previously.

After the electrodes have exhibited the hydrogen potential (0.35 v) for some time, the potential begins to rise slowly, and ultimately attains a value in the vicinity of 0.627 v more noble than the lead-lead-sulfate reference. Fig. 3 shows the general trend of the effects of irradiation (Hanovia, Type 30600, 140 w, mercury arc) on the rate of the passivation from 0.35 v toward 0.627 v. The stronger and more intense the radiation the faster is the rate of rise toward 0.627 v. If the radiation is very intense, the potential-time curve goes through a maximum; this perhaps indicates that some photochemical decomposition of the species which gives rise to the 0.627-v potential is occurring, or perhaps that photoconduction in the film exists. The bulk temperature of the electrolyte did not change appreciably during irradiation in these experiments. Pre-irradiation of the electrolyte before the immer-

FIG. 1. Photomicrograph (×500, approx) of lead surfaces: (a) unpassivated; (b) passivated.

sion of the 0.35-v electrode also increased the rate of the passivation to 0.627 v.

Since hydrogen peroxide is produced quite easily photochemically in many systems in the presence of certain sensitizers (7), and since possible sensitizers, such as iron, are commonly present in small amounts in sulfuric acid, analyses of the irradiated solutions for hydrogen peroxide were made. By the development of the characteristic color (absorption maximum at 4200 Å) of the titanium ion complex (8), it was established spectrophotometrically that in these irradiated solutions, whether or not a lead electrode was present, hydrogen peroxide was produced photochemically. It was found, further, that hydrogen peroxide was produced in greater quantity by irradiation of the air-electrolyte interface than by irradiation of a closed but aerated system through a quartz window. In the latter case, the production of a species which is not hydrogen peroxide and whose long wave-length absorption limit, about 3000 Å, is not different from that of persulfate ion (9), was evident. However, photochemical production of the SO_4^-–$S_2O_8^-$–SO_5^-–H_2O_2 system was not studied beyond these qualitative observations.

When hydrogen peroxide was added directly to even a freshly prepared lead piece, passivation time was reduced to nearly zero, and the hydrogen-like step was eliminated. Fig. 4 shows the effects on the potential of adding hydrogen peroxide directly to fresh lead pieces in sulfuric acid. Within a matter of seconds a transparent, glassy layer builds up on the lead surface. X-ray diffraction patterns of crystals taken from this surface layer were characteristic of pure lead sulfate. After some minutes this glassy ayer becomes covered with a second, whitish lead
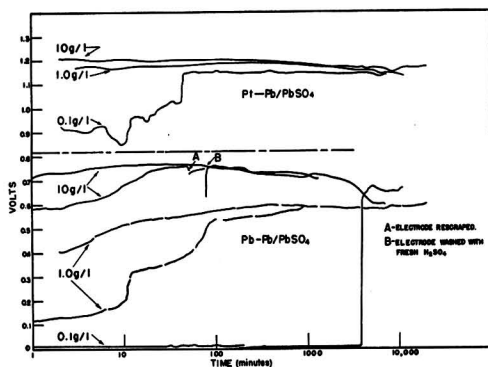
FIG. 4. Rate of ennoblement of potential as a function of H_2O_2 concentration.

FIG. 3. Effects of irradiation on the rate of passivation. 12″ and 2″: electrode 12″ and 2″, respectively, from u.v. source.

sulfate layer, the second layer bound only loosely to the first.

It was found that neither oxygen nor ozone has this effect on the rate of ennobling of the potential. This may be simply a question of rate of reaction or, alternatively, it may be a concentration effect, since O_2 and O_3 are gases with limited solubility in sulfuric acid solutions, while the liquid hydrogen peroxide is completely miscible and readily available to the surface. Although there existed spectrophotometric indication that $S_2O_8^-$ was present after irradiation, direct addition of $K_2S_2O_8$ to a sulfuric acid solution containing a fresh lead specimen did not result in the immediate passivation of lead to the 0.6-v potential, as did the addition of H_2O_2.

Factors which affect the potential of passivated surfaces.—The presence of oxygen (Fig. 2) or hydrogen peroxide (Fig. 4) seems to be a sufficient condition for the ennobled 0.6-v potential to be initiated. Therefore, the effects of oxygen concentration and hydrogen peroxide concentration were determined independently. Oxygen gas was bubbled into an electrolyte containing a 0.6-v lead electrode; then N_2; but other than Müller's "motor-electric" effect no change in the potential of the passivated lead was noted with changes in partial pressure of oxygen. In Table I are contained results which show that the passive potential is pressure independent and essentially temperature independent from 0°–55°C and from 40–760 mm mercury. This information seems to eliminate the possibility that O_2 species itself gives rise directly, even in part, to the potential measured. Platinum pieces in the same electrolyte, showing presumably the redox potentials of the electrolyte, were within a few millivolts of the O_2/H_2O_2 electrode, but the pressure and temperature independence of the potentials shown by both the platinum and passivated lead pieces seem to eliminate the possibility that O_2/H_2O_2 could be
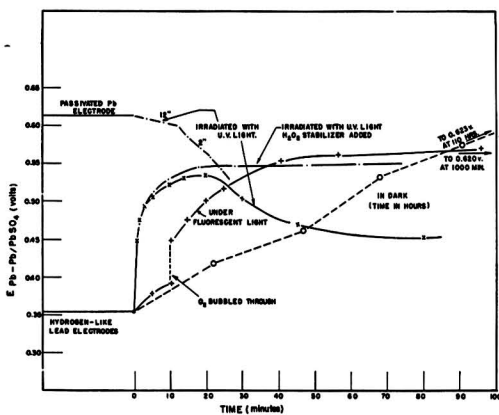
TABLE I. *Dependence of potential of passivated lead on temperature and on air pressure; also, results on Pt pieces under same conditions*

Pressure (mm)		$E_{Pb_{pass}-Pb/PbSO_4}$			$E_{Pt-Pb/PbSO_4}$	
		0°C	25°C	50°C	25°C	50°C
760	a	0.628 ± 0.008	0.627 ± 0.002	0.624 ± 0.002	c 1.039 ± 0.006	1.035 ± 0.003
	b		0.613 ± 0.004		d 1.000 ± 0.005	
					e 0.789 ± 0.005	0.789 ± 0.003
380	a		0.626 ± 0.002	0.627 ± 0.002	c 1.037 ± 0.002	
	b		0.613 ± 0.004			
100	a		0.627 ± 0.001	0.626 ± 0.004	c 1.036 ± 0.006	1.002 ± 0.002
	b		0.615 ± 0.005		d	1.018 ± 0.007
					e 0.809 ± 0.009	1.000 ± 0.015
40	a					
	b		0.610 ± 0.005			

Note: The limits assigned to each value express the range in which the electrode potential, as measured, drifted up and down during a time interval usually not less than 1–2 hr. a, b, etc., refer to experiments done at different times with different electrodes. Values read simultaneously against Hg/Hg₂SO₄ electrodes simply verified the above results and are not given.

the cathode of the Müller-type of local cell on the sulfated lead electrode.

Fig. 4 shows how the potential of a freshly prepared lead piece during passivation builds up in the presence of different concentrations of hydrogen peroxide. The peroxide was decomposing as the runs were made, so much so that at 10,000 min peroxide concentrations were all reduced to a common value. It was then established that the steady potential of the completely passivated lead becomes more noble with increasing hydrogen peroxide concentration. Typical results are contained in Table II; these figures are measurements made on several passivated pieces, each passed repeatedly and in random sequence into sulfuric acid solutions containing hydrogen peroxide of different concentrations. A plot of $E_{Pb_{pass}}$ vs. [H₂O₂] is sigmoidal after the manner of an adsorption curve. Peroxide breakdown with the evolution of oxygen begins at concentrations about 5 g/l in 30% acid. Results given in Table III show that the final potential, $E_{Pb_{pass}}$ (hydrogen scale), of lead pieces passivated in sulfuric acid containing hydrogen peroxide becomes more noble also with increasing concentration of sulfuric acid. The dependence of the passivated potential on [H₂O₂] and upon [H₂SO₄] is discussed in the last section of the paper.

That the passivated lead does not behave as an inert metal electrode (e.g., platinum) and exhibit the redox potential of the electrolyte was shown by the fact that in ferrous-ferric sulfate solutions in sulfuric acid the passivated lead did not exhibit the same potential values as did platinum pieces: thus, when E_{Pt} was 0.86 v more noble than the Pb/PbSO₄ reference, $E_{Pb_{pass}}$ was ~0.60 v, and when E_{Pt} was 1.14 v, $E_{Pb_{pass}}$ was ~0.61 v. Thus the passivated

TABLE II. *Dependence of potential of passivated lead upon H₂O₂ concentration*

H₂SO₄ sp gr 1.223 (4.35M, 7.7N)

Conc. (g/l)	Mean $E_{Pb_{pass}}^{*}$ (v)	Prob. error† of mean (v)
0.10	0.502	0.016
0.25	0.576	0.004
0.50	0.565	0.015
1.0	0.590	0.003
2.0	0.584	0.010
2.5	0.599	0.002
5.0	0.609	0.003
7.5	0.665	0.005
10.0	0.688	0.012
15.0	0.783	0.008

* Measured against Pb/PbSO₄/H₂SO₄ (7.7N) electrode.
† By Bessel's method (10).

lead is its own electrical buffer against changes in redox potential of the electrolyte. However, since the electrode responds to changes in concentration of H₂SO₄ and H₂O₂, the implication is strong that the surface of the passivated electrode is somewhat specific in the type of molecules or ions which can exchange electrons at the lead sulfate electrolyte interface.

In the presence of a passivated lead electrode the electrolyte was reduced cathodically, under nitrogen, on an auxiliary platinum cathode in a Pyrex system in which the anode and cathode compartments were separated by a closed, moist, ungreased stop-cock. Reduction at a cathode current density of 200 μa/cm² and voltage, with respect to Pb/PbSO₄, of about +0.07 v failed to alter the 0.627-v potential of the passivated lead. It was found, too, that passivated lead could be moved

TABLE III. *Dependence of potential of passivated lead on H$_2$SO$_4$ concentration*

% H$_2$SO$_4$	(Molality)	$a_{H_2SO_4}$ (activity)	$E_{Pb_{pass}}$ measured (v)	$E_{Pb_{pass}}$ reduced (v)	Probable error
1.0	0.103	0.028	0.372	0.062	0.011
15.0	1.80	0.22	0.495	0.158	0.007
30.0	4.35	0.78	0.584	0.232	0.010
36.6	5.74	1.5	0.688	0.327	0.009
50.0	10.2	(6.0)*	0.735	(0.37)	0.04

* From an extrapolation of the activity coefficient data.

The values given for $E_{Pb_{pass}}$ are mean values, of not less than seven independent experiments. Measurements were made against a Pb/PbSO$_4$/H$_2$SO$_4$ (m) electrode, and reduced to the hydrogen scale by means of the Nernst equation and the activity information of Harned and Hamer (11).

into successive fresh sulfuric acid electrolytes without any marked change in potential occurring. From these experiments it is inferred that the seat of the potential must be either (a) in or on the surface, the potential-determining species being very difficult to remove, or (b) in the solution, supplied continuously, if needed, by dissolution from the surface. In this latter case the rate of dissolution from the surface must be large enough to build up rapidly and thereafter maintain a saturation concentration of the potential-determining species. Thus, the electrode would exhibit behavior similar to that of a silver-silver chloride electrode placed in a chloride-free electrolyte.

Cathodic reduction, under nitrogen, of the passivated lead surface itself at 0.25 μa cm^{-2} resulted in no permanent alteration of the potential. But at 40· μa cm^{-2} the passage of the same number of coulombs did result in a temporary activation (that is, lessening of the potential to below 0.627 v). After some hours of idle stand, still under nitrogen, the potential had drifted upward again to 0.63 v. Hence, once the passivated potential is shown by a specimen, the presence of oxygen or hydrogen peroxide is not necessary for the re-ennoblement after the partial reduction of the surface: the unreduced surface resupplies the species needed to repassivate the reduced surface.

Rectification phenomena.—A striking fact is that for different specimens of passivated lead, all of which exhibited the passivated potential, the apparent electrical resistance, as determined from the voltage drop effected by the passing of 0.25 d.c. μa cm^{-2}, was found to vary over fiftyfold. It was also found that the apparent resistance measured when the passivated lead was made positive (oxidized) was two to three times higher than that measured when the lead piece was made negative (reduced). Thus the passivated lead surface in sulfuric acid

exhibits modified rectifying properties. With 60 cycles/sec alternating current a small ($\sim$10%) rectification of the current was observed on an oscilloscope when set up in the manner indicated in Fig. 5. The direction of the rectification of the current was found to be the same as that in an aluminum rectifier. The voltage across the passivated lead piece was also distorted in the same direction as that across the standard aluminum rectifier. Calibrations of the circuit were made on pure resistances and sufficient variations in cell construction made to eliminate the possibility that any factor other than the passivated lead surface was responsible for the observed rectification effects.

It was noted that, although the passivated potential of a lead piece would be established very soon (see Fig. 4) after the addition of H$_2$O$_2$ to the sulfuric acid electrolyte, the current rectification property developed very slowly, and was at its maximum value (5–10%) only after 24–36 hr. This suggests that the process responsible for the establishment of the passivated potential and the process responsible for the establishment of the properties of a rectifier are not identical. However, that the two processes must be related is shown by the facts that the appearance of the ennobled potential is a sufficient condition for the establishment of a rectifier, and that the rectifying property was never detected until the lead had become passivated. It was noted further that if hydrogen peroxide was added in excess (to concentration greater than 5 g/l) to the electrolyte which contained a rectifying electrode, peroxide breakdown accompanied by oxygen evolution occurred on the lead surface, and the rectification which formerly was exhibited by the passivated lead surface was thereby destroyed.

In contrast with the behavior of aluminum rectifiers, at the higher currents ($\sim$0.8–1.0 ma cm^{-2}) and higher impressed voltages, the rectification of
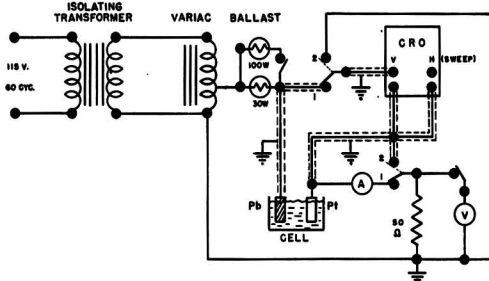
FIG. 5. Electrical circuit used to follow rectifying properties. With the switches closed to positions marked "1" the voltage variations of the electrode are displayed. Closed to positions "2", the current through the cell is displayed.

the passivated lead piece decreased and disappeared within about one minute after the current was turned on. This loss of the rectifying power was found usually to be not permanent, and would return by an idle stand of some minutes or hours.

DISCUSSION

It would seem that penetration of current carriers through thick layers of lead sulfate on the surface would be highly unlikely. Suppose that even at the bottom of the cracks, pores, or holes in the lead sulfate layer the lead surface was converted to lead sulfate by local action until the pores had sealed over completely. The authors assume that it is lead sulfate at the bottom of the pore because PbO is neutralized rather quickly by H_2SO_4 and because the presence of H_2O_2 (shown above to be a sufficient constituent for the establishment of the ennobled potential of Pb in H_2SO_4) has been found in this laboratory to accelerate greatly the rate of conversion of any of the lead oxides into lead sulfate. The increase in potential of the passivated lead as the concentrations of H_2O_2 and/or H_2SO_4 increase only serves to emphasize the possible reaction products, persulfate ($S_2O_8^-$) and monopersulfate (SO_5^-) ions. It is reasonable to suppose, then, that the outer part of the surface of the sulfated electrode is oxidized sulfate, containing SO_5^-, perhaps, or the stoichiometric equivalent, $SO_4^- + O$. It would thus seem possible for oxygen atoms to be absorbed into the lead sulfate surface and thence perhaps to penetrate further into the lead sulfate lattice by diffusion. These impurity centers in the lead sulfate would make the lead sulfate a defect-type semiconductor (12). This layer of oxygen atoms in the lead sulfate layer at or near the electrolyte-lead sulfate interface (see Fig. 6) is pictured as being the negative analog of the Schottky-type barrier layer which exists in semiconductor materials near the metal-semi-

FIG. 7. Freundlich-type plot of potential of passivated lead as a function of H_2O_2 concentration.
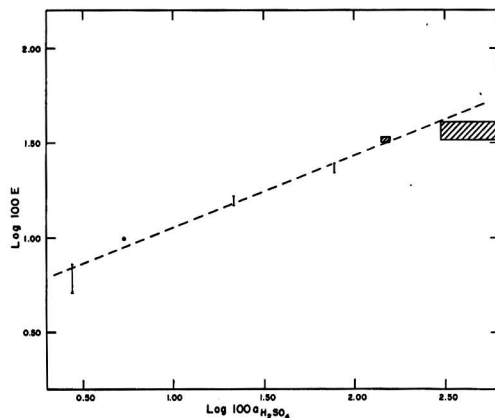
FIG. 8. Freundlich-type plot of potential of passivated lead as a function of activity of H_2SO_4.

conductor interface. A detailed consideration of the oxygen atom layer reveals properties which are strikingly analogous to the properties of the Schottky-type barrier. Thus the highest concentration of positive charge in the Schottky-type barrier is near the metal semiconductor interface, and falls off rapidly into the semiconductor. The highest concentration of negative charge of the oxygen barrier is near the lead sulfate-electrolyte interface, and falls off rapidly into the lead sulfate. Thus the direction of the rectification effects should be the same for both cases, as was found experimentally.

The oxygen barrier layer differs from the Schottky-type in the strength with which the barrier layer is held by the surface. Strong reduction of the electrolyte on an auxiliary cathode and even mild direct reduction of the passivated surface fail to disturb the potentials exhibited; however, the layer

FIG. 6. Idealized model of passivated lead surface

is disturbed by strong reduction of the surface, by H_2O_2 breakdown accompanied by oxygen gas evolution at the surface if the concentration of H_2O_2 is made too high, or by high alternating currents.

Further evidence of adsorption of oxygen atoms during passivation is provided from a study of the dependence of potential upon concentration of H_2O_2 and upon concentration of H_2SO_4. As noted earlier, results in Table II show that the dependence of potential upon $[H_2O_2]$ is sigmoidal. If one assumes that the potential measured during the passivated state is a measurement of the amount of oxygen atoms adsorbed, then the Freundlich adsorption isotherm should be applicable. Fig. 7 shows a plot of log $10E$ vs. log 10 $[H_2O_2]$. Three distinct regions are noted. Above 5 g/l, H_2O_2 increases the thickness of the adsorbed layer beyond the stability limit, and oxygen gas is released. Below about 0.25 g/l, not enough H_2O_2 is present to mend the cracks which occur due to strains in the film during short-term experiments. Between 0.25 and 5.0 g/l the Freundlich equation describes adequately the results found, although the variation of potential with concentration is so slight that the surface must be nearly saturated over this range of concentration.

A remarkable fact is the strong dependence of potential on activity of sulfuric acid. The experimental points are not described even remotely by the Nernst equation when applied to any of the known lead redox systems (13) or the known oxygen or hydrogen peroxide systems (14). In terms of the Freundlich expression, Fig. 8 shows log 100 $E_{Pb_{pass}-hyd.}$ vs. log 100 $a_{H_2SO_4}$. Linearity within the limits of the probable error, and the strong dependence of potential upon concentration suggest the adsorption of a second potential-determining species, perhaps SO_4^-, whose adsorption in the range of concentrations studied was considerably below saturation. Thus it seems reasonable to conclude that the passivated potentials observed are those of one of the equilibria of the $SO_4^- - S_2O_8^- - SO_5^- - H_2O_2$ system, about which very little thermodynamic information at present exists.

The response of the passivated surface to changes in concentration of H_2O_2 and of H_2SO_4, and the lack of response to wide changes in the redox potential of the electrolyte (produced by changes in the

Fe^{++}-Fe^{+++} additions) warrant a further comment. This behavior suggests that the electrical response of the surface is specific to those redox species which can, for steric reasons, be preferentially sorbed into the surface. In a metal-electrolyte system the source or sink of electrons is pictured as being right at the interface; but in the semiconductor-electrolyte system an electron transfer must be made at a defect center. Thus, in the present case, the potential-determining species must be able to penetrate right into the oxygenated sulfate of the surface. Hence the steric factor may well be quite critical.

ACKNOWLEDGMENTS

REFERENCES

1. W. J. MULLER, *Kolloid-Z.*, **86**, 150 (1939).
2. H. E. HARING AND U. B. THOMAS, *Trans. Electrochem. Soc.*, **48**, 293 (1935).
3. W. J. MULLER AND W. MACHU, *Korrosion u. Mettalschutz*, **16**, 187 (1940).
4. M. POURBAIX, "Thermodynamics of Dilute Aqueous Solutions," Edward Arnold & Co., London (1949).
5. H. S. HARNED AND W. J. HAMER, *J. Am. Chem. Soc.*, **57**, 31 (1935).
6. U. B. THOMAS, Private communication, April 1953.
7. *See, e.g.,* E. BAUR AND C. NEUWEILER, *Helv. Chim. Acta*, **10**, 901 (1927); M. C. MARKHAM AND K. J. LAIDLER, *J. Phys. Chem.*, **57**, 363 (1953).
8. *See, e.g.,* F. G. PALILLA, N. ADLER, AND C. F. HISKEY, *Anal. Chem.*, **25**, 926 (1953).
9. J. L. R. MORGAN AND R. H. CRIST, *J. Am. Chem. Soc.*, **49**, 338 (1927).
10. W. N. BOND, "Probability and Random Errors," E. Arnold & Co., London (1935).
11. H. S. HARNED AND W. J. HAMER, *J. Am. Chem. Soc.*, **57**, 27 (1935).
12. N. F. MOTT AND R. W. GURNEY, "Electronic Processes in Ionic Crystals," 2nd ed., Oxford University Press, New York (1948).
13. P. DELAHAY, M. POURBAIX, AND P. VAN RYSSELBERGHE, *This Journal*, **98**, 57 (1951); J. J. LANDER, *ibid.*, **98**, 213 (1951).
14. W. K. LATIMER, "The Oxidation States of the Elements and Their Potentials in Aqueous Solutions," 2nd ed., Prentice-Hall, Inc., New York (1952).

Stress During the Electrodeposition of Copper on Copper Substrate[1]

Hussein Sadek, M. Halfawy, and S. G. Abdu

Chemistry Department and Institute of Industrial Chemistry, Alexandria University, Alexandria, Egypt

ABSTRACT

The stress in electrodeposits of copper on a copper substrate was investigated. Copper strips, coated on one side by petroleum jelly wax mixtures, were used as cathodes and the deflection they suffered during electrodeposition was measured. Maximum deflection was obtained at a current density of 2 amp/dm² using 60% wax coating. The deflection does not vary linearly with the time during electrodeposition but becomes linear during anodic attack.

Introduction

Electrodeposition of metals is widely used to provide the substrate metal with a more corrosion-resistant or a better wearing surface. Most metals are normally electrodeposited in a state of stress. Not only does stress occur during electrodeposition, but it often increases on standing (1). An understanding of the various factors that cause and control stress in electrodeposited metals is of both theoretical and technical importance.

Various authors (1–3) have studied the stress of several electrodeposited metals using different substrates, various bath conditions, and addition agents. Results obtained, however, differ among the different authors. It is believed that the type of solution is a factor more important than the operating conditions in determining the physical properties of the deposits (4). However, no adequate explanation of the causes of the stress has yet been given. The present paper is one of a series which summarizes work undertaken to elucidate the nature of the phenomenon.

Experimental

Electrolytic copper strips[2] were used as substrates. They were 10 mm wide, 0.3 mm thick, and were bent at an angle of 90° at one end so as to leave a length of 10 cm for electrodeposition. Before electrodeposition, the strips were annealed for ½ hr at 500°C, dipped in dilute nitric acid (1:1) for 3 sec, thoroughly rinsed with water and alcohol, dried between filter paper, checked for weight and modulus of elasticity, and finally bent and waxed on one side. The modulus of elasticity was checked by clamping the strip firmly at one end in a horizontal position and measuring the deflection produced on hanging a weight of one gram at the other end. Only strips which gave the same deflection (within 2%) were chosen for the stress measurements. Following the procedure of Van der Sommen (3), wax

was applied by a warm spatula to produce a fairly thin and uniform coating. After being waxed, the strip was etched in 3% solution of KCN, rinsed, immersed in dilute HCl (1:20), and rerinsed. The strip was then weighed after standing for ½ hr in a desiccator. To insure uniform thickness of the wax on each strip, differences in weight before and after waxing were always compared. They showed a deviation of the order of 1% which was considered quite satisfactory. A light-weight glass fiber about 4 cm long was fixed at the extreme free end of the strip by gently warming the wax locally. This fiber served as a pointer whose movement could be followed easily by a vernier microscope, accurate to 0.01 mm. The same pointer was used throughout the whole series of measurements.

The electrolytic cell was a shallow porcelain vessel of about 600 cc capacity. The plating bath containing 150 g/l of $CuSO_4 \cdot 5H_2O$ and 50 g/l of concentrated sulfuric acid was prepared from analytically pure reagents. The effect of the very small amounts of impurities could not be of primary importance in comparing the stress values, since the same bath was used throughout.

The strip was held in a horizontal position by a clamp with the unwaxed side facing the copper anode made of electrolytic copper. The tip of the pointer was always above the wall of the cell and its deflection (Δ) was followed by the travelling microscope. Plating was carried out at room temperature 25° ± 2°C for 18 min.

Results

In all cases it was observed that, when the strips were coated electrolytically, they contract and become concave on the coated side. Comparison of the deflection (Δ) of the strip rather than the calculated stress was made since all substrate strips were exactly the same, and the deposit and substrate were of the same metal. The variation of the deflection as a function of time of deposition at various current densities is shown in Fig. 1. It is obvious that the
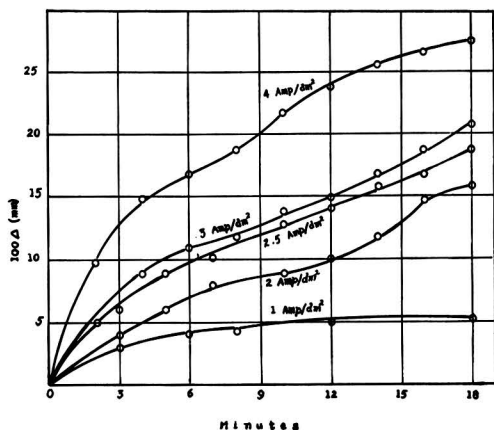
FIG. 1. Variation of the deflection (Δ) with time at several current densities.
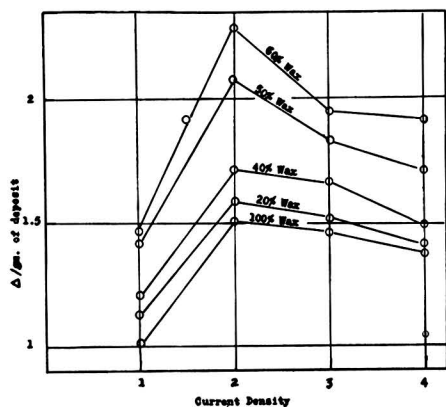
FIG. 2. Dependence of specific deflection on the composition of coating.

deflection after a given time is greater the greater the current density. All the curves are almost linear in the early stages of deposition.

The deflection at a given current density, after 18 min of deposition, varies with the composition and, hence, with the mechanical properties of the coating material. The highest deflection was obtained when a coating of 60 % wax and 40 % petroleum jelly was applied (Fig. 2). This coating (mp, 48°C) was used throughout the work. It will be noticed that the highest specific deflection (Δ/g Cu deposited) for any one coating is obtained at a current density of 2 amp/dm².

Although the total deflection of the strip after 18 min of deposition was greater at higher current density, the relation was not linear, as can be seen from Fig. 3. The weight of copper deposited at each current density is also shown in the same figure, and is seen to vary linearly with current density as required by Faraday's laws. Similar results, using other coatings of the wax-petroleum jelly mixtures,

were obtained. The cathode efficiency was found to be $100 \pm 0.1\%$.

Anodic attack of the deposit in the same bath resulted in a linear decrease of the deflection with time of attack, as shown in Fig. 4. In this case, the strip was first coated on one side with a copper deposit at 5.5 amp/dm² for 18 min, weighed, and then made anode in the same bath and attacked at the same current density. The deflection and weight of the
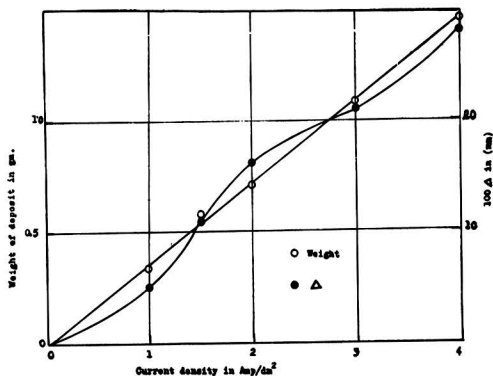
FIG. 3. Variation of weight of deposit and of deflection with current density.
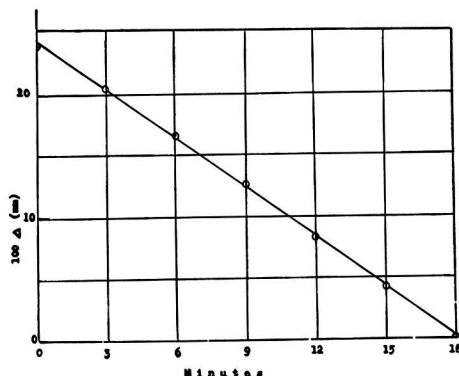
FIG. 4. Plot of deflection against time during anodic attack.
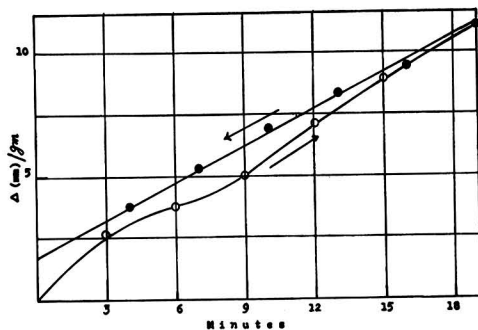
FIG. 5. Variation of (Δ/g) during deposition and anodic attack with time.

strip were determined every 3 min. The linearity of the anodic attack curve as compared to the non-linearity during cathodic deposition indicates hysteresis in the phenomenon. This result is clearly shown in Fig. 5 by plotting the specific deflection for each 3-min interval for both deposition and attack. This result has been repeatedly confirmed and cannot be attributed to experimental error. The anode efficiency in this case was found to be $99.8 \pm 0.1\%$. Work in progress in this laboratory has indicated that this hysteresis phenomenon is even more pronounced when zinc is electrodeposited on a copper substrate and then anodically attacked.

DISCUSSION

Jacquet (2) investigated the effect of very small but variable concentrations of addition agents, such as gelatin, on the amount of stress in electrodeposited copper. He found that such addition agents affected the stress in varying degrees according to their nature and concentration. These agents are known to produce fine-grained deposits probably because they are adsorbed on the crystal nuclei and thus prevent their growth. The consequent discharge of ions must lead, therefore, to the formation of new nuclei. Piontelli (5) showed that, during deposition of a metal on the same metal, the formation of new nuclei implies changes of configuration and of energy of the base metal. The former change involves disappearance of a portion of the original and formation of a new surface between nuclei and liquid. The latter change involves sublimation energy of the deposited metal (when an incomplete lattice plane is formed) and adsorption as well as interfacial energies (when two-dimensional nuclei are formed). Moreover, deformation of metallic crystal faces usually takes place when subjected to a stress (6). Furthermore, Yang (7) has proved by electron diffraction studies that the stress is in no way connected with a favored orientation of the crystals of the deposit on the substrate surface. Such a view was previously held by Bozorth (8) and Wyllie (9).

In the present case of deposition of copper on copper substrate it cannot be argued that the stress is in any way connected with the difference in lattice constants between deposit and substrate. The explanation that seems most reasonable is that the observed tensile stress is due to the forces of attraction parallel to the surface between adjacent crystallites. Fig. 2 shows that tensile stress increases with increase in current density up to 2 amp/dm². This result may be explained as being due to an increase in the density of the deposit as it grows in thickness, and hence the attractive forces between crystallites increase. Such attractive forces are responsible for sintering in metals, which is largely due to increase in particle size. On this basis one can explain the

readiness with which condensed nickel atoms on glass surfaces sinter at 100°C (10). The decrease in the tensile stress above a current density of 2 amp/dm² may be attributed to a decrease in the density of the deposit and, hence, to a fall in the attractive forces. The effect may be linked to a decrease in density of a cold-rolled metal (11). The same sort of effect occurs when a bag of sand which has been well shaken is compressed. The grains are disturbed from their equilibrium positions and the net effect is to increase the volume they occupy and thus reduce the density.

The kinetics of electrode processes at metal surfaces has been discussed by Lorenz (12) from the standpoint of the theory of crystal growth. He distinguishes electrolytic crystal growth from growth out of the gas phase or from melts in that, in the former, separations of electrically charged particles depend on the moving electric field forming within the electrolyte. A clear understanding of the cathodic process of crystal growth and of the nature of the bonding between deposit and substrate might throw more light on the nature of the interatomic forces in the deposit.

The hysteresis phenomenon shown in Fig. 5 may be explained by the heterogeneity of metallic surfaces (13). The last crystals to grow by cathodic deposition are not necessarily the first to be attacked anodically. It has been shown by tracer technique that the surface layer of electrodeposited copper includes sulfur as SO_4^{-2} which could be bound either electrostatically or by adsorption, causing favorable orientation of crystallites (14).

Any discussion of this paper will appear in a Discussion Section to be published in the December 1955 JOURNAL.

REFERENCES

1. A. W. HOTHERSALL, *J. Inst. Metals*, Reprint 1082, 107 (1947); *C.A.*, **42**, 465 (1948).
2. P. A. JACQUET, *Compt. rend.*, **194**, 456, 870 (1932).
3. J. VAN DER SOMMEN, *Proc. 3rd Intern. Electrodep. Conference*, London, 195 (1947).
4. A. BRENNER, V. ZENTNER, AND C. W. JENNINGS, *Plating*, **39**, 865 (1952).
5. R. PIONTELLI, *Proc. 3rd Intern. Electrodep. Conference*, London, 157 (1947).
6. A. T. STEER, *Proc. 3rd Intern. Electrodep. Conference*, London, 165 (1947).
7. L. YANG, Ph.D. Thesis, London University, London (1948).
8. R. M. BOZORTH, *Phys. Rev.*, **26**, 390 (1925).
9. M. R. J. WYLLIE, *J. Chem. Phys.*, **16**, 52 (1948).
10. O. BEECK, A. E. SMITH, AND A. WHEELER, *Proc. Roy. Soc. London*, **177A**, 162 (1940).
11. A. TAYLOR, "An Introduction to X-ray Metallography," p. 233, Chapman and Hall, London (1947).
12. W. LORENZ, *Z. physik. Chem.*, **202**, 275 (1953).
13. H. SADEK AND H. S. TAYLOR, *J. Am. Chem. Soc.*, **72**, 1168 (1950).
14. F. G. HOUTERMANS, D. VICENT, AND G. WAGNER, *Z. Elektrochem.*, **56**, 944 (1952).

On the Behavior of Rapidly Diffusing Acceptors in Germanium[1]

F. van der Maesen and J. A. Brenkman

Philips Research Laboratories, N. V. Philips' Gloeilampenfabrieken, Eindhoven, Netherlands

ABSTRACT

The acceptor activity of Cu and Ni and their diffusion in germanium have been investigated. Their acting as acceptors as well as recombination centers gives reason to believe that impurity atoms are placed substitutionally in the lattice. However, the value of 10^{-5} cm²/sec of the diffusion constant makes it likely that the diffusion goes interstitially. This leads to the concept of an equilibrium existing between substitutional and interstitial atoms. The fact that the diffusivity is dependent on the range of diffusion can be explained qualitatively on the basis of the picture given above.

INTRODUCTION

A number of investigations have been made recently on the influence of impurities such as copper, nickel, and elements other than 3rd or 5th column elements, on the properties of germanium. Investigations by Theuerer and Scaff (1) on "thermal conversion," experiments by Fuller and Struthers on acceptor activity and on the saturation concentration and diffusion of copper in germanium (2), as well as the authors' work on these subjects (3) are mentioned. Investigations on the influence of Cu and Ni on the lifetime of holes and electrons have been reported recently (4).

Experiments with Ni in the authors' laboratory have shown that Ni behaves similarly to Cu. The saturation concentration of Ni in germanium at high temperatures (800°C) is about one-tenth of the value for Cu at the same temperature and the diffusivity is of the same order of magnitude.

Prolonged heating of samples saturated with Ni or Cu at 500°C restores the original resistivity; there is also evidence that the lifetime is then increased (5).

Diffusion experiments show that the diffusion coefficient D of Cu and Ni is not simply a constant: D increases from the beginning toward the end of the diffusion range in all cases.

In this paper the authors propose that copper and nickel may be present at both normal and interstitial lattice positions. These two forms are in a thermodynamic equilibrium. They will explain how the diffusion experiments can be understood by assuming different diffusion constants for substitutional and interstitial atoms.

EFFECT OF HEAT TREATMENTS

It is well known that copper produces in Ge an acceptor level with an activation energy of 0.04 ev

(6). According to Burton (4), one should ascribe to Cu also an acceptor level with a rather high activation energy of 0.25 ev which also acts as recombination center (7). The acceptor properties of Cu and the fact that a negative Cu ion in itself would be too large for an interstice suggest that the Cu concerned is placed *substitutionally* in the lattice.

On the other hand, copper has a remarkably high diffusion constant of 10^{-5} cm²/sec at 800°C (8) (for normal donors and acceptors this value is about 10^{-12} cm²/sec). These facts give strong support to the idea that the diffusion proceeds *interstitially*.

The above considerations lead to the concept that both substitutional (Cu_s) and interstitial (Cu_i) atoms are present. The two forms will be in a temperature dependent equilibrium:[2]

$$Cu_i \rightleftarrows Cu_s + Q \qquad \text{(I)}$$

One assumes that only the substitutional atoms will show an electrical (i.e., acceptor) activity.[3]

Prolonged heating at 500°C for 48 hr nearly restores the original resistivity. In view of the phase diagram Cu—Ge it is likely that the excess of Cu is precipitated, presumably as Cu_3Ge:

$$3Cu_i + Ge \rightleftarrows Cu_3Ge \qquad \text{(II)}$$

---

[1] Manuscript received October 20, 1954. This paper was prepared for delivery before the Chicago Meeting, May 2 to 6, 1954.

[2] Just before the completion of our work, an extended article appeared by Fuller et al. from Bell Telephone Laboratories (9). Comparing the total saturation concentrations ($Cu_i + Cu_s$) determined *with radioactive* Cu *with the concentration* (Cu_s) *derived* from direct resistivity measurements from figure 5 of their paper, it is clear that at 600°C these two quantities have nearly the same value, whereas at 800°C $Cu_i + Cu_s$ is about twice Cu_s. This can be explained by a shift of the equilibrium toward an increase of interstitial Cu at higher temperatures. At the same time the direction of the shift should indicate that the thermochemically denoted Q has a positive sign.

[3] It is possible that the situation is more complicated; e.g., one might think of Cu_i as a donor. The general idea however will not be affected.

TABLE I. Cu

Time (t) min	12			15			20		
x (mm)	$\lambda = x/\sqrt{t}$, $10^{-3}\frac{cm}{sec^{1/2}}$	C_{Cu}, $10^{14}\frac{at}{cm^3}$	D, $10^{-5}\frac{cm^2}{sec}$	$\lambda = x/\sqrt{t}$, $10^{-3}\frac{cm}{sec^{1/2}}$	C_{Cu}, $10^{14}\frac{at}{cm^3}$	D, $10^{-5}\frac{cm^2}{sec}$	$\lambda = x/\sqrt{t}$, $10^{-3}\frac{cm}{sec^{1/2}}$	C_{Cu}, $10^{14}\frac{at}{cm^3}$	D, $10^{-5}\frac{cm^2}{sec}$
0.00	0	140.0	0.5	0	140.0	1.0	0	140.0	2.0
0.50	1.9	50.6	3.1	1.7	58.1	4.1	1.4	68.8	3.7
1.00	3.7	40.6	3.3	3.3	43.5	4.5	2.9	56.8	3.9
1.50	5.6	33.6	3.5	5.0	37.0	4.7	4.3	49.3	4.1
1.75									
2.00	7.4	27.5	3.6	6.7	28.9	4.9	5.8	40.5	4.2
2.38	8.7	17.4	3.9						
2.50	9.3	12.9	4.0	8.3	21.5	5.2	7.2	35.5	4.3
2.88							8.3	27.2	4.5
3.00	11.1	12.2	4.1	10.0	16.8	5.3	8.7	23.2	4.6
3.50	13.0	9.3	4.2	11.7	15.0	5.5	10.1	19.4	4.7
3.90				13.0	10.9	5.6			
4.00	14.8	5.8	4.3	13.3	7.6	5.7	11.5	16.6	4.6
4.50	16.7	3.3	4.5	15.0	7.1	5.8	13.0	12.3	4.8
5.00	18.5	0.5	4.8	16.7	6.1	5.7	14.4	8.1	4.9
5.50				18.3	4.9	5.9	15.9	4.6	5.1
6.00				20.0	3.9	6.0	17.3	2.7	5.2
6.50							18.8	1.0	5.3
7.00							20.2	0.2	5.5
		0.0	6.2		0.0	8.3		0.0	6.5

In equation (II) the symbol Cu_i is used in order to show that the compound will be formed mainly from interstitial Cu atoms, because they can move easily through the lattice. After heat treatment the compound Cu_3Ge will be distributed throughout the germanium in a dispersed phase. The two equations describe the general behavior of copper in germanium. Annealing at 500°C causes reaction (II) to go to the right, and therefore reaction (I) shifts to the left: the acceptor activity disappears and the lifetime increases. On the other hand, reheating at 800°C of such an annealed piece of germanium will restore the Cu_s concentration quite quickly throughout the whole crystal, a fact which is confirmed by experiment: after reheating only two minutes, followed by quenching, a sample was p-type throughout the whole crystal (3, 9). One can repeat this cycle of annealing and restoring the acceptor activity.

DIFFUSION

The diffusivity D of Cu does not seem to be a constant along the range of diffusion. A comparison of the measurements of Fuller and Struthers (2) with those of Fuller, Theuerer, and van Roosbroeck (8) shows that the D value computed from measurements at short diffusion times is 8 times smaller than the D value found from an experiment with a long diffusion time.

It is to be noted that the latter authors can fit their data on the diffusion-penetration curve with a constant D of 8×10^{-5} cm²/sec, but with an effective starting concentration of one-tenth the saturation concentration of Cu at the given temperature. Furthermore, the work of Esaki (10) on the diffusion of thermal acceptors is of interest. He gives the value of 37,000 cal/mole for the activation energy, which is large compared to the value 12,000 cal/mole found by Fuller, Theuerer, and van Roosbroeck (8).[4]

A number of experiments were carried out by the authors to investigate these phenomena. Penetration curves (concentration C vs. depth x) of Cu and Ni diffusing in germanium at 800°C at different diffusing times were obtained from resistivity measurements. In making the experiments, samples were first thoroughly cleaned with pure HNO_3 in a soxhlet in the manner described earlier (3), then covered with copper on one side and heated. The cleaning step is necessary in order to avoid copper diffusion from side and rear surfaces. In later work a solution of Complexon III was used. Results for copper are given in Table I. Here it is assumed that each acceptor gives one hole in the valence band.[5]

[4] According to a more recent paper by Fuller and co-workers (9) this value should not exceed 4500 cal/mole.

[5] This does not have to be necessarily true if each Cu atom provides a second acceptor level with a rather high activation energy. In that case the number of acceptors will be dependent on the position of the Fermi level. In
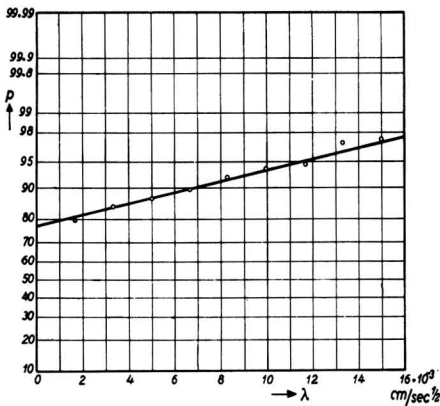
FIG. 1. Copper diffusion in germanium at 800°C during 15 min. $p = 50(2 - C/C_0)$ as a function of $\lambda = x/\sqrt{t}$.

Ordinary diffusion processes are governed by Fick's second law. In this case

$$\frac{\partial C}{\partial t} = \frac{\partial}{\partial x}\left(D \frac{\partial c}{\partial x}\right) \qquad \text{(III)}$$

or, for constant D,

$$\frac{\partial C}{\partial t} = D \frac{\partial^2 C}{\partial x^2} \qquad \text{(IV)}$$

The experimental conditions are that at $x = 0$, the concentration is equal to the saturation concentration C_0 for all times, and the internal concentration C is equal to zero at $t = 0$. In that case the solution of (IV) can be written as

$$\frac{C}{C_0} = 1 - \text{erf}\,\frac{x}{2\sqrt{Dt}} \equiv 1 - \text{erf}\,\tau = \text{erfc}\,\tau$$

$$\text{erf}\,\tau = \frac{2}{\sqrt{\pi}}\int_0^t e^{-z^2}\,dz \qquad \tau = \frac{x}{2\sqrt{Dt}} \qquad \text{(V)}$$

Introducing $\dfrac{x}{\sqrt{t}} = \lambda$, (V) can be rewritten as

$$\frac{C}{C_0} = 1 - \text{erf}\,h\lambda = \text{erfc}\,h\lambda \text{ and } h = \frac{1}{2\sqrt{D}} \qquad \text{(VI)}$$

When the experimental concentration C is plotted as a function of λ, the curves do not seem to follow the ordinary error function denoted by (VI). This indicates that D is not simply a constant.

It was shown by Boltzmann that, in case D is a function of C, the solution of Fick's law under the same initial conditions as given above is still of the

form $C = C\left(\dfrac{x}{\sqrt{t}}\right)$. Then D at various C can be found by integration of (III) leading to (11)

$$D = -\frac{1}{2}\frac{d\lambda}{dC}\int_0^c \lambda\,dC \qquad \text{(VII)}$$

An expedient method of computing D has recently been reported by Hall (12). One can plot C/C_0 on probability paper and see whether one obtains a straight line. In all cases for Cu and Ni the authors found that the greatest part of the penetration curve plotted in this way gives a straight line; an example is given in Fig. 1: the values of Table I for $t = 15'$ are used.

The straight line can be expressed as:

$$C/C_0 = \text{erfc}\,(h\lambda + k) = \text{erfc}\,u \qquad \text{(VIII)}$$

Applying (VII) to (VIII) leads to

$$D = \frac{1}{4h^2} - \frac{k\sqrt{\pi}}{4h^2}e^{u^2}\,\text{erfc}\,u \qquad \text{(IX)}$$

the constants h and k are the slope and intercept, respectively, of the straight line in Fig. 1 and $k = 0$ gives the ordinary error function (VI) with a constant D. The values of D in Table I are those calculated from (IX). D varies appreciably.[6]

Results on Ni diffusion are listed in Table II. According to the authors' measurements of the resistivity and Hall effect of Ni-saturated samples, Ni atoms produce one acceptor level lying 0.23 ev above the valence band. This is in agreement with values of 0.25–0.30 ev given by Burton (4).

In calculating the values of C from the resistivity measurements it has been taken into account that acceptors with such a high energy are not completely exhausted. The fraction α of the acceptors which give free holes is given in the table.

The question arises as to whether C is a function of $\dfrac{x}{\sqrt{t}} = \lambda$ or not. Fig. 2 and 3 show penetration curves for various diffusion times for Cu and for Ni, respectively; C is plotted as a function of λ. It is apparent that the curves do not coincide; this is very clear in the case of Ni. The curves show a shift downward when t decreases; hence C is not a function of λ alone.

It should be mentioned that if C is not a function of λ alone, D is not a function of C alone. Therefore, D calculated from (VII) is not a real diffusivity but

---

experiments with Ni this is taken into account by calculation (Table II). Experiments with Cu have shown that the number of acceptors for a given concentration of Cu is, to a large extent, independent of the position of the Fermi level. (To be published in *Physica*.) This holds also in the case of the diffusion experiments.

[6] According to Fuller and coworkers (9) equation (IV) is obeyed, and D, therefore, should be a constant. With respect to this it should be noted that the C_0 values the authors used are taken from direct resistivity measurements of the interior of saturated samples. Fuller and collaborators use C_0 values obtained by extrapolation of the diffusion experiments.

TABLE II. Ni

x (mm)	Time (t) (min) 10.5					Time (t) (min) 15				
	$\lambda = x/\sqrt{t}$, $10^{-3} \frac{cm}{sec^{1/2}}$	$(p-n+N_d)$ $10^{14} \frac{at}{cm^3}$	α	C_{Ni}, $10^{14} \frac{at}{cm^3}$	D, $10^{-8} \frac{cm^2}{sec}$	$\lambda = x/\sqrt{t}$, $10^{-3} \frac{cm}{sec^{1/2}}$	$(p-n+N_d)$ $10^{14} \frac{at}{cm^3}$	α	C_{Ni}, $10^{14} \frac{at}{cm^3}$	D, $10^{-8} \frac{cm^2}{sec}$
0				15.95					15.95	0.4
0.25	1.0	2.72	0.970	2.80	2.8	0.8	5.96	0.921	6.47	3.5
0.50	2.0	2.67	0.971	2.75	2.8	1.7	5.49	0.929	5.91	3.6
0.75	3.0	2.40	0.975	2.46	3.0	2.5	5.08	0.935	5.44	3.8
1.00	4.0	2.18	0.979	2.23	3.0	3.3	4.80	0.940	5.10	3.9
1.25	5.0	2.14	0.979	2.18	3.1	4.1	4.51	0.944	4.78	3.9
1.50	6.0	2.04	0.981	2.08	3.1	5.0	4.23	0.949	4.45	4.0
1.75	7.0	1.94	0.982	1.98	3.2	5.8	3.90	0.954	4.09	4.1
2.00	8.0	1.87	0.983	1.90	3.2	6.7	3.40	0.962	3.53	4.2
2.20	8.8	0.93	1.00	0.93	3.9					
2.25	9.0	0.58	1.00	0.58	4.2	7.5	3.14	0.966	3.25	4.3
2.50	10.0	0.55	1.00	0.55	4.3	8.3	2.81	0.971	2.89	4.4
2.75	11.0	0.51	1.00	0.51	4.3	9.2	2.41	0.977	2.47	4.6
3.00	12.0	0.48	1.00	0.48	4.3	10.0	2.21	0.980	2.26	4.6
3.25	13.0	0.43	1.00	0.43	4.4	10.8	2.08	0.982	2.12	4.7
3.50	14.0	0.34	1.00	0.34	4.5	11.7	1.95	0.984	1.98	4.7
3.75	15.0	0.29	1.00	0.29	4.5	12.5	1.80	0.988	1.82	4.8
3.90						13.0	1.07	1.00	1.07	5.0
4.00	16.0	0.21	1.00	0.21	4.7	13.3	0.81	1.00	0.81	5.1
4.25	17.0	0.20	1.00	0.20	4.8	14.1	0.78	1.00	0.78	5.1
4.50	18.0	0.11	1.00	0.11	4.9	15.0	0.72	1.00	0.72	5.1
4.75	19.0	0.08	1.00	0.08	5.1	15.8	0.62	1.00	0.62	5.3
5.00	20.0	0.07	1.00	0.07	5.1	16.7	0.52	1.00	0.52	5.3
5.25						17.5	0.47	1.00	0.47	5.3
5.50						18.3	0.41	1.00	0.41	5.4
5.75						19.2	0.37	1.00	0.37	5.4
6.00						20.0	0.33	1.00	0.33	5.6
∞					8.1					7.6

an apparent one. The variation of the apparent D with λ calculated according to (IX) shows in all cases the same behavior and is represented for Cu and Ni in Fig. 4, the values being taken from the tables at $t = 900$ sec.

The experimental facts just presented indicate that the diffusion process is more complicated than one would expect.

For an ordinary diffusion process of one kind of particles one would not expect any influence of the concentration upon D because this quantity is very small. It is quite possible, however, that diffusion of just one kind of particles does not occur in this case, and that a diffusion of two species, namely, Cu_i and Cu_s, must be considered. Moreover, if these two can interchange, it is clear that application of Fick's second law as given in (III) is not permissible.

Giving these considerations a more strict form one arrives at the following picture which makes it possible to understand a variation of the apparent D regardless of the small concentration of the impurities.

1. Cu_s and Cu_i atoms have different constants D_s and D_i, where it is likely that $D_s < D_i$.

2. During diffusion, the Cu_s and Cu_i atoms are subjected to the reactions

$$Cu_i \underset{k_2}{\overset{k_1}{\rightleftarrows}} Cu_s$$
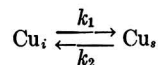
where k_1 and k_2 are reaction constants.

Accordingly, the concentrations N_s and N_i of Cu_s and Cu_i have to obey the following equations:

$$\frac{\partial N_s}{\partial t} = D_s \frac{\partial^2 N_s}{\partial x^2} + k_1 N_i - k_2 N_s$$

$$\frac{\partial N_i}{\partial t} = D_i \frac{\partial^2 N_i}{\partial x^2} - k_1 N_i + k_2 N_s$$

In the following, two extreme cases will be considered: (a) k_1 and k_2 very large; (b) k_1 and k_2 very small.

(a) If the rate of exchange between Cu_i and Cu_s is very large (k_1 and $k_2 \to \infty$), the ratio of N_i and N_s is equal to k_2/k_1 for every x and t. In that case,
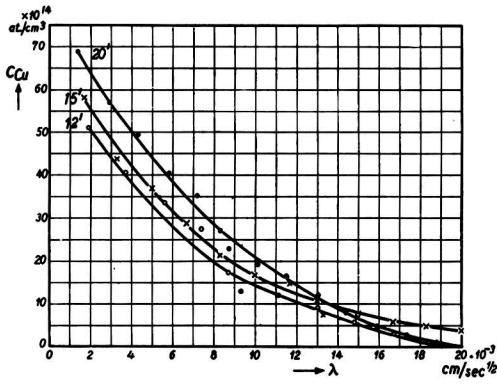
FIG. 2. Copper concentration as a function of $\lambda = x/\sqrt{t}$ at different times.
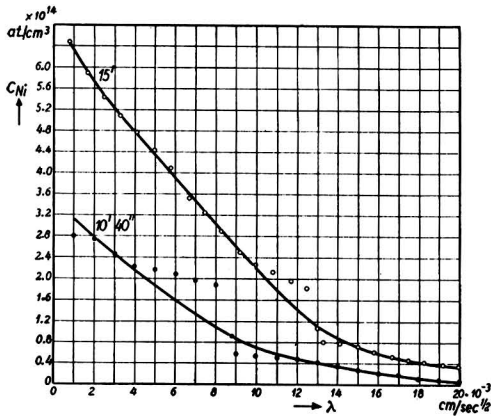
· FIG. 3. Nickel concentration as a functon of $\lambda = x/\sqrt{t}$ at different times.

solutions for the total concentration N_{tot} and the concentrations N_i and N_s are error functions:

$$N_{tot} = N_0 \, \text{erfc} \, \tau$$

$$N_i = \frac{k_2}{k_1 + k_2} N_0 \, \text{erfc} \, \tau, \quad N_s = \frac{k_1}{k_1 + k_2} N_0 \, \text{erfc} \, \tau \quad \text{(XI)}$$

N_0 is the total concentration at $x = 0$, which is supposed to be constant for all t, furthermore

$$\tau = \frac{x}{2\sqrt{Dt}} \quad D = \frac{k_2 D_i + k_1 D_s}{k_1 + k_2} = \text{constant}$$

(b) An approximate solution for small reaction constants k_1 and k_2 can be written as

$$N_s = \frac{k_1}{k_1 + k_2} N_0 \, \text{erfc} \, \tau_s + \frac{k_1 k_2 N_0 t}{k_1 + k_2} \frac{1}{1 - \gamma^2}$$

$$\left[\frac{2}{\sqrt{\pi}} \gamma^2 \tau_s e - \tau_s^2 + (1 + 2\tau_i^2)(\text{erf} \, \tau_s - \text{erf} \, \tau_i) \right.$$

$$\left. - \frac{2}{\sqrt{\pi}} \tau_i e - \tau_i^2 \right] \quad \text{(XII)}$$
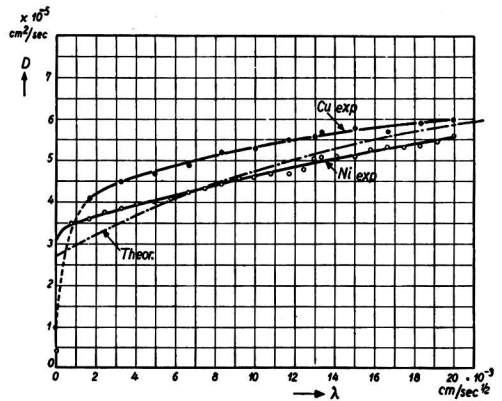
FIG. 4. The diffusion coefficient D for Cu and Ni at 800°C as a functon of $\lambda = x/\sqrt{t}$.

where

$$\tau_s = \frac{x}{2\sqrt{D_s t}} \quad \tau_i = \frac{x}{2\sqrt{D_i t}} \quad \gamma = \sqrt{\frac{D_s}{D_i}}$$

At $x = 0$, the quotient $N_s/N_i = k_1/k_2$ is supposed to be a constant.

When $D_s \ll D_i$, i.e., $\gamma \to 0$, τ_i will be small compared to τ_s. For a given time (XII) can be simplified to

$$N_s = \text{const.} \left[(1 + 2\tau_i^2) \, \text{erfc} \, \tau_i - \frac{2}{\sqrt{\pi}} \tau_i e - \tau_i^2 \right] \text{(XIII)}$$

$$= \text{const.} \, i^2 \, \text{erfc} \, \tau_i$$

i^n erfc τ_i denotes the n times integrated error function. One can replace (XII) by (XIII) except for very small x.

With (VII) D can be calculated from (XIII) as a function of τ_i. The result is

$$\frac{D}{D_i} = \frac{1}{3} \frac{4\tau_i^3 \, \text{erfct} \, \tau_i + (1 - 2\tau_i^2) \dfrac{2}{\sqrt{\pi}} e - \tau_i^2}{2i^1 \, \text{erfc} \, \tau_i} \quad \text{(XIV)}$$

If one assumes D_i to be a certain value, say, $8.1 \cdot 10^{-5}$ cm²/sec, D can be calculated from (XIV) as a function of λ. For τ_i or $\lambda = 0$, $D/D_i = \frac{1}{3}$; for τ_i or $\lambda = \infty$, $D/D_i \rightleftharpoons 1$. D as a function of λ is plotted in Fig. 4 (theoretical curve).

The experimental and theoretical curves show an agreement; it must be pointed out, however, that validity of (XII) can only be expected when the k_2 value is small, that is, of the order of 10^{-3} sec⁻¹. In this way the diffusion experiments give support to the general picture given above.

Any discussion of this paper will appear in a Discussion Section to be published in the December 1955 JOURNAL.

REFERENCES

1. H. C. THEUERER AND J. H. SCAFF, *J. Metals*, **191,** 59 (1951).
2. C. S. FULLER AND J. D. STRUTHERS, *Phys. Rev.*, **87,** 526 (1952).
3. F. V.D. MAESEN, P. PENNING, AND A. V. WIERINGEN, *Philips Research Repts.*, **8,** 241 (1953); F. V.D. MAESEN AND J. A. BRENKMAN, *ibid.*, **9,** 225 (1954).
4. J. A. BURTON, G. W. HULL, F. J. MORIN, AND J. C. SEVERIENS, *J. phys. Chem.*, **57,** 853 (1953).
5. D. NAVON, R. BRAY, AND H. Y. FAN, *Proc. I.R.E.*, **40,** 1342 (1952).
6. F. J. MORIN AND J. P. MAITA, *Bull. Am. Phys. Soc.*, **28,** 8 (1953).
7. W. SHOCKLEY AND W. T. READ, *Phys. Rev.*, **87,** 835 (1952).
8. C. S. FULLER, H. C. THEUERER, AND W. VAN ROOS-BROECK, *Phys. Rev.*, **85,** 678 (1952); W. C. DUNLAP, JR., *ibid.*, **94,** 1531 (1954).
9. C. S. FULLER, J. D. STRUTHERS, J. A. DITZENBERGER, AND K. B. WOLFSTIRN, *ibid.*, **93,** 1182 (1954).
10. L. ESAKI, *ibid.*, **89,** 1026 (1953).
11. C. MATANO, *J. Phys. (Japan)*, **8,** 109 (1933); "Atom Movements," Chicago (1950).
12. L. D. HALL, *J. Chem. Phys.*, **21,** 87 (1953).

Polarographic Studies in Acetonitrile and Dimethyl-formamide

II. Behavior of Aromatic Olefins and Hydrocarbons[1]

S. Wawzonek, E. W. Blaha,[2]

R. Berkey,[2] and M. E. Runner[3]

Department of Chemistry, State University of Iowa, Iowa City, Iowa

ABSTRACT

Stilbene, anthracene, and 9-anisylidenefluorene are reduced stepwise polarographically in anhydrous acetonitrile and in dimethylformamide. Triphenylethylene, tetraphenylethylene, styrene, and 1,1-diphenylethylene give only one reduction wave. Large-scale electrolytic reductions in these solvents indicate that carbanion intermediates exist for a short period of time. 1,2,3,4-Tetraphenylbutane and *meso*-diphenyl succinic acid have been prepared electrolytically from stilbene in dimethylformamide.

Introduction

Previous work on the polarographic behavior of inorganic salts in acetonitrile (1) has indicated that this solvent is suitable for studies in this field. The work has now been extended to the study of aromatic olefins and hydrocarbons, examples of irreversible organic systems. Since the results in dimethylformamide were quite similar to those obtained in acetonitrile, data obtained in both solvents are treated together.

Experimental

Polarograms were obtained in a manner similar to that described previously (1). Characteristics for the dropping mercury electrode used in acetonitrile were the same as given before (1). The dropping mercury electrode for the studies in dimethylformamide was used at 60 cm pressure and had a drop time of 3.91 sec (open circuit). The $m^{2/3} t^{1/6}$ value was 1.77 $mg^{2/3}$ $sec^{-1/2}$. The resistance of the electrolysis cell using using dimethylformamide as a solvent with $0.2M$ tetrabutylammonium iodide as the supporting electrolyte was found to be 500 ohms.

Materials

Dimethylformamide was purified in the following manner. A sample dried over anhydrous potassium carbonate for several days was distilled through an 80 cm Fenske column. The first 200 ml of the distillate was discarded and the fraction boiling at

151.5°–153°C collected. Tetrabutylammonium iodide was prepared according to directions in the literature (2). Tetrabutylammonium bromide was prepared by a variation of the directions of Hager and Marvel (3). A solution of tri-*n*-butylamine (156 g) and *n*-butyl bromide (116 g) in anhydrous ethyl acetate (400 ml) was refluxed for 48 hr. The resulting solution on cooling gave crystalline tetra-*n*-butylammonium bromide. Several recrystallizations from anhydrous ethyl acetate gave a product (64 g) melting at 115°–116°C.

The acetonitrile was purified in a similar fashion to that reported previously (1).

Experimental Techniques of Electrolyses

Electrolyses were carried out in a cell similar in construction to that used by Lingane (4) with a 7 mm tube fitted with a stopcock connecting the two flasks at their mid-points. The purpose of this additional tube was to counteract the electrical osmosis which occurred during the electrolyses; the solution flowed from the anode to the cathode compartment. Purified nitrogen was passed through both compartments for an hour to remove the dissolved oxygen. The mercury pool used as a cathode had an area of approximately 50 cm². The anode was either a stirred mercury pool or a platinum electrode with an area of 65 cm². The direct current obtained from an 85 v generator was not controlled. Electrolyses were carried out with stirring and with cooling by an ice bath to prevent loss of the solvent; otherwise, heat was usually generated in a run and caused the solvent to boil. Analysis of gases given off during the electrolysis was accomplished by an absorption train attached to the cell, consisting of an ice trap, a 10% hydrochloric acid trap, an ascarite tube, an anhydrone tube, and a dry ice trap. The effluent

---

[1] Manuscript received August 13, 1954. The greater part of this research was done under A.E.C. Contract AT(11-1)-72, Project No. 6.

[2] Abstracted in part from the Ph.D. Theses of E. W. Blaha (1954) and R. Berkey (1955).

[3] National Institute of Health Postdoctorate Fellow 1949–50. Present address: Department of Chemistry, Illinois Institute of Technology, Chicago, Illinois.

gases were then passed through a column of iodine pentoxide at 155°. Iodine, formed from the oxidation of hydrogen and carbon monoxide liberated in the electrolysis, was condensed in an air-cooled tube and the resulting water and carbon dioxide collected in anhydrone and ascarite tubes, respectively, after purification by passing over a plug of silver wool at 350°C to remove any traces of iodine carried over.

Electrolyses in Dimethylformamide

Following is a typical electrolysis in dimethylformamide. To the reduction cell containing a stirred mercury pool cathode and a platinum anode was added a solution of stilbene (10 g) in dimethylformamide (350 ml) which was 0.155M with respect to tetrabutylammonium iodide. The solution in both compartments was deaerated with nitrogen for one hour. Direct current was passed through the cell for 22 hr starting with a value of 0.42 amp and gradually decreasing to 0.17 amp at the end of the electrolysis. During the electrolysis a violet-black color streamed from the sintered glass disk into the catholyte. This color varied with the compound reduced and the inert electrolyte used.

After the electrolysis, anolyte and catholyte were combined and distilled under reduced pressure to remove the dimethylformamide and other volatile substances. From this distillate there could be isolated tri-n-butylamine (3.4–5.7 g) by acidifying with dilute hydrochloric acid, removing the dimethylformamide under reduced pressure, and neutralizing the residue with alkali. Identification was made by forming tri-n-butylmethylammonium iodide, mp 178°C (5).

The residue from the distillation was steam distilled and the distillate extracted with ether. The ether solution gave, after removal of traces of tri-n-butylamine with acid, pure bibenzyl (6.37 g), mp 52°C. The residue from steam distillation when extracted with ether gave 1,2,3,4-tetraphenylbutane and, occasionally, stilbene. Separation of the two hydrocarbons was accomplished by reducing the stilbene to bibenzyl with sodium (23.0 g) in absolute ethanol (200 ml) and steam distilling. The nonvolatile 1,2,3,4-tetraphenylbutane, after one recrystallization from ethanol, melted at 86° and proved identical with the lower melting isomer obtained by the sodium-alcohol reduction of 2,3,4,5-tetraphenylthiophene (6).

The steam distillation residue left after the ether extraction of the hydrocarbons proved to be a mixture of ditetrabutylammonium tetraiodomercurate, tetrabutylammonium iodide, and tetrabutylammonium triiodide (1.8 g). Separation was effected by dissolving the residue in hot ethanol. The ditetrabutylammonium tetraiodomercurate (2–6 g)

crystallized and melted at 132°C. The alcohol filtrate gave tetrabutylammonium iodide when treated with an excess of ether. Removal of the solvent from the filtrate gave tetrabutylammonium triiodide (1.8 g) which melted at 69°C after one crystallization from ethyl acetate (7).

The liquid (0.5–0.8 g) collected in the dry ice trap proved to be a mixture of butene-1 and n-butane. The butene-1 was identified by conversion to 1,2-dibromobutane. Presence of n-butane was demonstrated by combustion in an Orsat gas analyzer after removal of the butene-1 with concentrated sulfuric acid.

Carbon monoxide and hydrogen were determined by oxidation with iodine pentoxide to carbon dioxide and water and collecting these substances.

meso-Diphenylsuccinic acid.—A solution (200 ml) of 0.155M tetrabutylammonium iodide in dimethylformamide containing stilbene (3.0 g) was electrolyzed, using a stirred mercury cathode and a platinum anode. For one hour prior to electrolysis and during the electrolysis, carbon dioxide was passed through the solution. The electrolysis was carried out for 19 hr using a current of 0.32 amp. The catholyte remained colorless throughout this period. Removal of the solvent under reduced pressure was followed by the addition of 10% sodium hydroxide (100 ml) and steam distillation. From the distillate a small amount of bibenzyl (0.1 g) was obtained. The solution left in the distillation flask was filtered from the precipitated tetrabutylammonium iodide and ditetrabutylammonium tetraiodomercurate and acidified with excess dilute hydrochloric acid. Crystals obtained after one crystallization from methanol melted at 229°C and proved to be *meso*-diphenylsuccinic acid by comparison with an authentic sample (8), yield, 4.1 g (92%).

1,1,2-Triphenylethane.—Triphenylethylene (3.0 g) in a dimethylformamide solution (280 ml) of 0.193M tetrabutylammonium iodide was reduced electrolytically for 19 hr in a cell similar to that described for the reduction of stilbene. The current, which was 0.53 amp at the beginning, gradually decreased to 0.36 amp at the end of the electrolysis. The catholyte assumed a bright violet color during this period.

Removal of the solvent under reduced pressure gave a brown residue (22.9 g) which was extracted with ether. The ether extract after removal of tri-n-butylamine with dilute acid gave 1,1,2-triphenylethane (2.8 g). Recrystallization from ethanol gave a sample melting at 53°–54°C (9).

Electrolyses in Acetonitrile

The following procedure was used for the reduction of stilbene and triphenylethylene. Stilbene

(5.0 g) was reduced electrolytically in acetonitrile (300 ml) which was 0.45M in tetrabutylammonium iodide. The current, which was passed through the cell for 10 hr, started at 0.52 amp and gradually decreased to 0.34 amp. The catholyte turned a bright green; if the current was turned off, the green changed to red which then faded to a light yellow. Removal of the solvent from the combined catholyte and anolyte gave a brown residue which was steam distilled. The distillate yielded bibenzyl (4.0 g), mp 51°–52°C. The residue from the steam distillation when dissolved in hot ethanol gave, on cooling, ditetrabutylammonium tetraiodomercurate (11 g), mp 131°–132°C. The alcohol filtrate upon removal of the solvent gave a solid, from which 4-amino-2,6-dimethylpyrimidine (0.02 g) sublimed when heated at 200°C under reduced pressure (1 mm). A mixture of this compound with an authentic sample (10) melted at the same point.

Electrolysis of a similar solution without stilbene gave ditetrabutylammonium tetraiodomercurate, 4-amino-2,6-dimethylpyrimidine, and tri-*n*-butyl-amine. No hydrogen butane or 1-butene were detected.

Substitution of a mercury anode for the platinum anode in the reduction of stilbene gave a comparable yield of bibenzyl.

Use of tetrabutylammonium bromide as the inert electrolyte in the reduction of stilbene gave only bibenzyl and 4-amino-2,6-dimethylpyrimidine.

1,1,2,2-Tetraphenylethane.—A suspension of tetraphenylethylene (5.0 g) in acetonitrile (250 ml) which was 0.175M in tetrabutylammonium iodide, was electrolyzed for 23.5 hr. The current was 0.5 amp at the beginning and gradually decreased to 0.12 amp at the end. During this time, a dark violet color was produced in the cathode compartment. The resulting solution was filtered from the unchanged tetraphenylethylene (0.4 g) and gave, after removal of the solvent, a brown residue (25.4 g). Treatment of this material with hot ethanol (100 ml) gave the insoluble 1,1,2,2-tetraphenylethane which was recrystallized from a benzene-ethanol mixture; yield, 2.4 g; mp 204°–206°C. The alcohol filtrate upon cooling gave ditetrabutylammonium tetraiodomercurate (1.8 g). Removal of alcohol, followed by steam distillation, gave diphenylmethane (2.0 g), mp 25°–26°C. The melting point was not depressed when this compound was mixed with an authentic sample (11).

1,2-Diphenylbutane.—A solution of stilbene (5 g) and ethyl iodide (23 ml) in acetonitrile (250 ml), which was 0.175M in tetrabutylammonium iodide, was electrolyzed for 19 hr. The current which started at 0.64 amp gradually decreased to 0.02 amp at the end of the run. Removal of the solvent gave a brown residue (20 g) which was taken up in ether and washed with dilute hydrochloric acid. The residue obtained after removing the ether was subjected to fractional distillation under reduced pres-

TABLE I. *Half-wave potentials, diffusion currents, and diffusion current constants of various compounds in solutions indicated*

Compound	Conc, milli-moles/liter	i_d, μa		I_d*		$E_{1/2}$ (v) vs. Hg pool		$0.059/n$**	
		1st wave	2nd wave	1st wave	2nd wave	1st wave	2nd wave	1st wave	2nd wave
Acetonitrile—0.1M tetrabutylammonium bromide									
$(C_6H_5)_2C{=}C(C_6H_5)_2$	1.0	6.56	—	4.31	—	−1.62	—	0.028	—
$(C_6H_5)_2C{=}CHC_6H_5$	1.0	7.36	—	4.84	—	−1.67	—	0.089	—
$(C_6H_5)_2C{=}CH_2$	1.0	8.65	—	5.69	—	−1.92$_5$	—	0.032	—
$C_6H_5CH{=}CHC_6H_5$(trans)	1.0	4.67	2.68	3.07	1.76	−1.73	−2.06	0.078	0.086
$C_6H_5CH{=}CHC_6H_5$(cis)	1.0	5.57	2.29	3.66	1.50	−1.81	−2.11	0.025	0.095
Anthracene	1.0	4.77	2.88	3.14	1.89	−1.48	−2.06	0.073	0.078
Ethyl iodide	8.28	88.0		6.15		−1.85			
Dimethylformamide—0.2M Tetrabutylammonium iodide									
$C_6H_5CH{=}CH_2$	2.31	13.1	—	3.21	—	−1.96	—	0.145	—
$C_6H_5CH{=}CHC_6H_5$(trans)	1.20	4.10	3.21	1.92	1.51	−1.61	−2.02	0.069	0.075
$C_6H_5CH{=}CHC_6H_5$(trans)†	1.20	3.55	2.67	—	—	−1.64	−2.02	0.068	0.075
9-p-$CH_3OC_6H_4CH{=}CC_{12}H_8$‡	1.20	3.40	3.02	1.64	1.42	−1.17	−1.56	0.057	0.050
CO_2§	—	—	—	—	—	−2.05	—	—	—

* $I_d = \dfrac{i_d}{C_m{}^{2/3}\, t^{1/6}}$

** From current-voltage curve analysis.

† Hg height = 40 cm instead of 60 cm.

‡ *p*-Anisylidenefluorene.

§ Concentration not known.

TABLE II. *Effect of proton donors on the polarographic behavior of hydrocarbons in acetonitrile—0.175M tetrabutylammonium bromide*

Compound[a]	Water added to 20 ml soln (ml)	$i_d\mu_a$		$E_{1/2}(v)$ vs. Hg pool		$0.059/n$[b]	
		1st wave	2nd wave	1st wave	2nd wave	1st wave	2nd wave
Anthracene	0	4.77	2.88	−1.48	−2.06	0.073	0.078
	0.1	4.97	3.78	−1.49	−2.06	0.062	0.098
	0.2	5.27	3.28	−1.54	−2.10	0.043	0.095
	0.5	5.87	2.58	−1.58	−2.13	0.076	0.085
	1.0	7.36	1.0[c]	−1.63	−2.2[c]	0.060	—[c]
Stilbene (trans)	0	4.67	2.68	−1.73	−2.06	0.078	0.086
	0.2	7.26	1.5[c]	−1.80	−2.2[c]	0.069	—[c]
	0.5	8.75	—	−1.81	—	0.033	—
Stilbene (cis)	0	5.57	2.29	−1.81	−2.11	0.025	0.095
	0.1	7.95	1.2[c]	−1.80	−2.1[c]	0.056	—[c]
	0.5	8.65	—	−1.84	—	0.038	—
p-Anisylidenefluorene[d]	0	2.91	2.52	−1.17	−1.56	0.057	0.050
Benzoic acid[d, e]	0	6.74	—	−1.58	—	—	—
p-Anisylidenefluorene and benzoic acid[d, f]	0	4.76	—	−1.11	—	—[g]	—

[a] $0.001M$ solutions.
[b] From current-voltage curve analysis.
[c] Supporting electrolyte discharge interferes.
[d] In dimethylformamide containing $0.2M$ $(C_4H_9)_4NI$.
[e] $0.003M$ solution.
[f] 0.985 Millimoles of p-anisylidene fluorene and 3.32 millimoles of benzoic acid.
[g] Maximum present.

TABLE III. *Large-scale electrolytic reductions of hydrocarbons in acetonitrile and dimethylformamide*

Amount of hydrocarbon	Electrolyte	Anode	Colors observed	Current used amp		Time of electrolysis (hr)	Products formed
				Start	Finish		
5.0 g Stilbene	CH_3CN − $0.145M$ $(C_4H_9)_4NI$ (300 ml)	Pt	Green-red-yellow	0.5	0.05	22	$C_6H_5CH_2CH_2C_6H_5$ (3.9 g) $C_6H_5CH=CH_6C_6H_5$ (0.8 g)
3.0 g Stilbene	CH_3CN − $0.175M$ $(C_4H_9)_4NI$ (200 ml)	Hg	Greenish-black	0.5	0	24	$C_6H_5CH_2CH_2C_6H_5$ (2.5 g)
5.0 g Triphenylethylene	CH_3CN − $0.154M$ $(C_4H_9)_4NI$ (300 ml)	Pt	Bright violet	0.5	0.12	22	$(C_6H_5)_2CHCH_2C_6H_5$ (5.0 g)
3.0 g Triphenylethylene	$HCON(CH_3)_2$ − $0.193M$ $(C_4H_9)_4NI$ (280 ml)	Pt	Bright violet	0.53	0.36	19	$(C_6H_5)_2CHCH_2C_6H_5$ (2.8 g)
5.0 g Tetraphenylethylene (partially insoluble)	CH_3CN − $0.175M$ $(C_4H_9)_4NI$ (250 ml)	Pt	Dark violet	0.40	0.12	23.5	$(C_6H_5)_2CHCH(C_6H_5)_2$ (2.4 g) $(C_6H_5)_2CH_2$ (2.0 g) $(C_6H_5)_2C=C(C_6H_5)_2$ (0.4 g)

sure and fractional crystallization. The lower boiling fraction upon steam distillation gave an oil which, after two distillations at atmospheric pressure, had the physical properties of 1,2-diphenylbutane, bp 288°C, n_D^{20} 1.554 (12).

Anal. calc'd for $C_{16}H_{18}$: C, 91.37; H, 8.63
Found: C, 91.21; H, 8.64

The amount isolated was insufficient to make a solid derivative.

Ditetra-n-butylammonium tetraiodomercurate.—Mercuric iodide (2.0 g) and tetra-n-butylammonium iodide (3.2 g) were refluxed in 50% ethanol (50 ml) until the mercuric iodide turned white. More ethanol (25 ml) was added and the solution heated

TABLE IV. *Electrolyses products from stilbene in dimethylformamide—0.155M* $(C_4H_9)_4$ *NI in millimoles*

Stilbene used	Bibenzyl formed	1,2,3,4-Tetraphenylbutane Formed	H₂ required for stilbene reduction	CO obtained	H₂ obtained	CO due to stilbene reduction	H₂ due to stilbene reduction
0	0	0	0	6.4	13.0	0	0
13.9	12.6	0.8	13.4	23.5	46.4	17.1	33.0
27.8	24.7	1.4	26.1	33.5	69.9	27.1	56.9
55.6	13.2	6.4	19.6	25.5	51.0	19.1	38.0
55.6	35.6	8.8	44.4	35.5	71.0	29.1	58.0

to reflux. Cooling gave a white curdy precipitate which was recrystallized from ethyl acetate, yield, 4.9 g, mp 131°–132°C.

Anal. calc'd for $C_{32}H_{72}N_2HgI_4$: C, 32.25; H, 6.05; N, 2.35.

Found: C, 32.23; H, 5.93; N, 2.40

Results

Polarographic data obtained for the various hydrocarbons in acetonitrile and dimethylformamide containing tetrabutylammonium iodide and bromide are given in Table I. The waves in all cases were well defined. Since the availability of protons in these solvents is very poor, the effect of water and benzoic acid upon the polarographic waves was studied and is given in Table II.
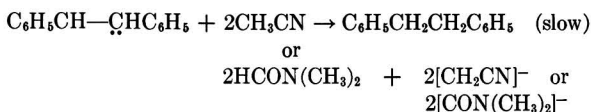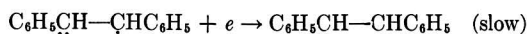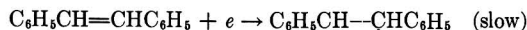
To help formulate electrode reactions, large-scale reductions of the various hydrocarbons were carried out in acetonitrile and dimethylformamide, and the products are summarized in Table III. In the electrolyses in dimethylformamide, hydrogen and carbon monoxide were obtained as by-products. The amounts of these obtained in the reduction of varying amounts of stilbene are given in Table IV.
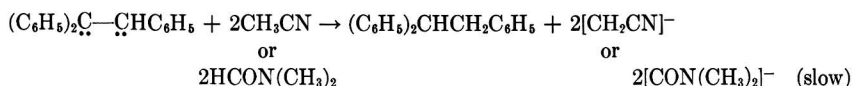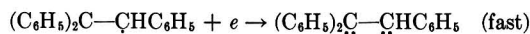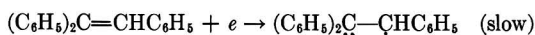
DISCUSSION OF RESULTS

Examination of results in Table I indicates that the polarographic behavior of aromatic olefins and hydrocarbons in acetonitrile and dimethylformamide is similar to that observed in 75% dioxane (3, 13) except for the behavior of three compounds. Stilbene, 9-anisylidenefluorene, and anthracene are reduced stepwise and give two polarographic waves. The sum total of the two waves, however, is approximately equal to the height of the one wave observed with triphenylethylene which shows a normal behavior.

The two waves for these compounds are markedly affected by the addition of small amounts of water or benzoic acid as is shown in Table II. At a high enough concentration (2.44%) of water, the two waves for stilbene are replaced by one wave with a height equal approximately to the combined heights of the two waves obtained in anhydrous media. Benzoic acid exerts its effect on the waves of *p*-anisylidenefluorene at a much lower concentration. This behavior is in agreement with the more acidic nature of benzoic acid. It was not possible to use this proton donor with stilbene because the discharge of hydrogen ions occurred before the reduction of the olefin.

These results indicate that the following mechanism of reduction, using stilbene as an example, applies to these three compounds:

$$C_6H_5CH{=}CHC_6H_5 + e \rightarrow C_6H_5\overset{\cdot}{C}H{-}\overset{\cdot}{C}HC_6H_5 \quad (slow)$$

$$C_6H_5\overset{\cdot}{C}H{-}\overset{\cdot}{C}HC_6H_5 + e \rightarrow C_6H_5\overset{\cdot\cdot}{C}H{-}\overset{\cdot\cdot}{C}HC_6H_5 \quad (slow)$$

$$C_6H_5\overset{\cdot\cdot}{C}H{-}\overset{\cdot\cdot}{C}HC_6H_5 + 2CH_3CN \rightarrow C_6H_5CH_2CH_2C_6H_5 \quad (slow)$$

$$\text{or}$$

$$2HCON(CH_3)_2 \quad + \quad 2[CH_2CN]^- \quad or$$
$$2[CON(CH_3)_2]^-$$

Analyses of the current-voltage curves were not consistent; the majority of the values, however, approximated 0.059. Varying the height of the mercury reservoir for stilbene indicated that the currents for both waves were diffusion-controlled.

The reduction of the other hydrocarbons, which show only one polarographic wave, must differ from the above in that the second step, illustrated with triphenylethylene, is a rapid reaction.

$$(C_6H_5)_2C{=}CHC_6H_5 + e \rightarrow (C_6H_5)_2\overset{\cdot\cdot}{C}{-}\overset{\cdot}{C}HC_6H_5 \quad (slow)$$

$$(C_6H_5)_2\overset{\cdot\cdot}{C}{-}\overset{\cdot}{C}HC_6H_5 + e \rightarrow (C_6H_5)_2\overset{\cdot\cdot}{C}{-}\overset{\cdot\cdot}{C}HC_6H_5 \quad (fast)$$

$$(C_6H_5)_2\overset{\cdot\cdot}{C}{-}\overset{\cdot\cdot}{C}HC_6H_5 + 2CH_3CN \rightarrow (C_6H_5)_2CHCH_2C_6H_5 + 2[CH_2CN]^-$$

$$\text{or} \qquad\qquad\qquad\qquad\qquad \text{or}$$

$$2HCON(CH_3)_2 \qquad\qquad\qquad\qquad 2[CON(CH_3)_2]^- \quad (slow)$$

In the presence of water or other acidic materials the mechanism of reduction must be the following:

$$C_6H_5CH=CHC_6H_5 + e \rightarrow C_6H_5\overset{.}{\underset{.}{C}}H-\overset{.}{C}HC_6H_5 \quad \text{(slow)}$$

$$C_6H_5\overset{.}{\underset{.}{C}}H-\overset{.}{C}HC_6H_5 + H_2O \rightarrow C_6H_5CH_2\overset{.}{C}HC_6H_5 + OH^- \quad \text{(fast)}$$

$$C_6H_5CH_2-\overset{.}{C}HC_6H_5 + e \rightarrow C_6H_5CH_2\overset{..}{C}HC_6H_5 \quad \text{(fast)}$$

$$C_6H_5CH_2\overset{..}{C}HC_6H_5 + H_2O \rightarrow C_6H_5CH_2CH_2C_6H_5 + OH^- \quad \text{(fast)}$$
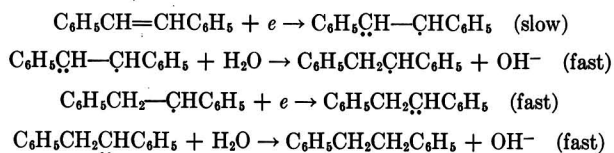
The second step under these conditions involves a rapid reaction with water to give a free radical which is reduced immediately. These steps must

$$2C_6H_5\overset{..}{C}H-\overset{.}{C}H-C_6H_5 \rightarrow C_6H_5\overset{..}{C}H-CH(C_6H_5)CH(C_6H_5)\overset{.}{C}HC_6H_5$$

$$C_6H_5\overset{..}{C}H-CH(C_6H_5)CH(C_6H_5)\overset{..}{C}HC_6H_5 + 2HCON(CH_3)_2 \rightarrow$$
$$C_6H_5CH_2CH(C_6H_5)CH(C_6H_5)CH_2C_6H_5 + 2[CON(CH_3)_2]^-$$

also occur in the reduction of the hydrocarbons in 75% dioxane solution rather than those previously suggested (2).

Reaction between the anion-free radical and either acetonitrile or dimethylformamide must occur to a certain extent and form the free radical which is reduced immediately since the two waves obtained are not of equal heights. At the first wave, which is the higher of the two, some anion-free radical would diffuse away from the electrode and

formamide, however, it was possible to isolate, in addition to the bibenzyl, up to a 30% yield of the lower melting isomer of 1,2,3,4-tetraphenylbutane (6). This product would arise from a dimerization of the intermediate anion-free radical postulated

The formation of this dimer solely in dimethylformamide is made possible no doubt by the fact that dimethylformamide is a weaker acid than acetonitrile.

Further evidence for the stable anion intermediates proposed is the formation of *meso*-diphenylsuccinic acid from the reduction of stilbene in dimethylformamide in the presence of carbon dioxide. The reaction under these conditions probably goes by a step-wise addition of electrons and carbon dioxide.

$$C_6H_5CH=CHC_6H_5 + e \rightarrow C_6H_5\overset{..}{C}H-\overset{.}{C}HC_6H_5 \quad \text{(slow)}$$

$$C_6H_5\overset{..}{C}H-\overset{.}{C}HC_6H_5 + CO_2 \rightarrow C_6H_5CH-\overset{.}{C}HC_6H_5 \quad \text{(fast)}$$
$$\overset{|}{C}OO^-$$

$$C_6H_5CH-\overset{.}{C}HC_6H_5 + e \rightarrow C_6H_5CH-\overset{..}{C}HC_6H_5 \quad \text{(fast)}$$
$$\overset{|}{C}OO^- \qquad\qquad\qquad \overset{|}{C}OO^-$$

$$C_6H_5CH-\overset{..}{C}HC_6H_5 + CO_2 \rightarrow C_6H_5CH-CHC_6H_5 \quad \text{(fast)}$$
$$\overset{|}{C}OO^- \qquad\qquad\qquad \overset{|}{C}OO^- \quad \overset{\diagdown}{C}OO^-$$
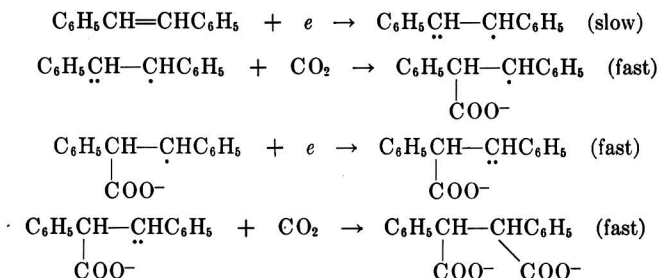
some would react with the solvent and be immediately reduced further. The difference in the two wave heights found in dimethylformamide is smaller than that found in acetonitrile and indicates that dimethylformamide is less acidic than acetonitrile. This behavior is in accord with the structure of these two solvents.

Evidence for the mechanisms proposed is the nature of the products isolated in the large-scale reductions of these hydrocarbons and the colors observed during the large-scale electrolysis. Triphenylethylene gave, in both acetonitrile and dimethylformamide, using tetra-*n*-butylammonium iodide as the inert electrolyte, 1,1,2-triphenylethane as the sole product. Stilbene in acetonitrile under similar conditions gave bibenzyl. In dimethyl-

More, but less conclusive, evidence for anion intermediates is the formation of 1,2-diphenylbutane in a poor yield in the electrolysis of stilbene in acetonitrile in the presence of ethyl iodide. In this example ethyl iodide is reduced at only a slightly more negative potential than stilbene and the possibility therefore exists that the resulting product, an ethyl free radical or anion, may add to the stilbene and give the same product as would be obtained by alkylating the stilbene anion-free radical with ethyl iodide. In the previous example cited carbon dioxide does not have this disadvantage since it is reduced at a more negative potential than stilbene.

Colors observed (Table III) for the intermediates formed during the electrolyses were dependent on

the hydrocarbon and the solvent used. In general, colors were lighter than those reported for disodium derivatives of the hydrocarbons in ether (14).

A possible explanation for the different polarographic behaviors observed for the hydrocarbons is that the group, which gives a two-step reduction, with the exception of p-anisylidenefluorene, is symmetrical in structure. The other examples, which give only one wave, are unsymmetrical in structure with the exception of tetraphenylethylene. The symmetry present in stilbene and anthracene allows a greater resonance stabilization of the intermediate anion-free radical since the forms are equivalent.

$$C_6H_5\overset{..}{C}H—\overset{.}{C}HC_6H_5 \leftrightarrow C_6H_5\overset{.}{C}H—\overset{..}{C}HC_6H_5$$
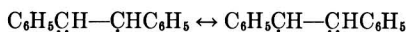
p-Anisylidenefluorene does not have such a symmetrical structure but contains groups which may help stabilize free radicals.

Symmetry is apparently not the only factor necessary for a two-step reduction. The ability of the intermediate to assume a planar arrangement is also important. Tetraphenylethylene is an excellent

phenylethyl from the disodium derivative of tetraphenylethylene and triphenylmethyl chloride (16).

The availability of protons in acetonitrile is indicated by the isolation of 4-amino-2,6-dimethyl pyrimidine. This compound is usually made by treating acetonitrile with strong base (10) and points to the formation of the carbanion $[CH_2CN]^-$ in the electrolysis.

The role of the solvent in the electrolytic reductions in dimethylformamide is not clear. Inspection of Table IV indicates that approximately one mole of carbon monoxide and two moles of hydrogen are liberated for each mole of hydrogen consumed in the reduction. Participation of the inert electrolyte in the reaction is indicated by the formation of butene-1 and n-butane. These hydrocarbons may be formed both by deposition of the tetrabutylammonium ion and by interaction of this ion with carbanions formed in the electrolysis. Possible reactions, which would explain the formation of the carbon monoxide and hydrogen but not the ratios of these found, are the following:

$$\overset{\diagdown}{\underset{\diagup}{}}C{:}^- \ + \ H\overset{\overset{O}{\|}}{C}—N(CH_3)_2 \ \rightarrow \ \overset{\diagdown}{\underset{\diagup}{}}CH \ + \ [\overset{\overset{O}{\|}}{C}—N(CH_3)_2]^-$$

$$[\overset{\overset{O}{\|}}{C}—N(CH_3)_2]^- \ \rightarrow \ CO \ + \ [N(CH_3)_2]^-$$

$$N(CH_3)_2{}^- \ - \ e \ \xrightarrow{\text{anode}} \ \cdot N(CH_3)_2$$

$$2(CH_3)_2N\cdot \ \rightarrow \ H_2 \ + \ 2CH_3N{=}CH_2$$
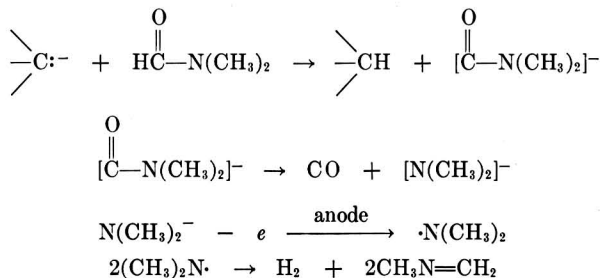
illustration of this point since it is symmetrical but is reduced in a single two-electron step. The intermediate anion-free radical, because of the four bulky phenyl groups, cannot assume the planar arrangement necessary for resonance stabilization and is, therefore, reduced further and rapidly to a dianion. Evidence for this mechanism is the large-scale reduction of tetraphenylethylene to 1,1,2,2-tetraphenylethane and diphenylmethane. The last hydrocarbon apparently arises from the dissociation of the intermediate dianion into an anion free radical followed by a reaction of the latter with the solvent.

$$(C_6H_5)_2\overset{..}{C}—\overset{..}{C}(C_6H_5) \rightleftarrows 2(C_6H_5)_2\overset{..}{C}\cdot$$

This dissociation is no doubt due to the highly arylated structure and the electrostatic repulsion of the two negative charges present in the molecule. Such an equilibrium may also be the basis for the cleavage of 1,1,2,2-tetraphenylethane with sodium-potassium alloy (15) and for the formation of penta-

The tetrabutylammonium tetraiodomercurate and tetrabutylammonium triiodide isolated are products of the reactions of tetrabutylammonium iodide with the mercuric iodide and iodine formed in the electrolysis.

The demonstration of the carbanion intermediates in anhydrous dimethylformamide and acetonitrile indicates that direct electron addition to organic compounds occurs in electrolytic reductions. A similar mechanism is indicated for aromatic olefins and hydrocarbons in solutions containing water since the differences in half-wave potentials for the various hydrocarbons are similar to those observed in anhydrous media.

REFERENCES

1. S. WAWZONEK AND M. E. RUNNER, *This Journal*, **99**, 457 (1952).
2. H. A. LAITINEN AND S. WAWZONEK, *J. Am. Chem. Soc.*, **64**, 1765 (1942).

3. F. D. HAGER AND C. S. MARVEL, *ibid.*, **48,** 2689 (1926).

4. J. J. LINGANE, C. G. SWAIN, AND M. FIELDS, *ibid.*, **65,** 1348 (1943).

5. G. S. FORBES AND C. E. NORTON, *ibid.*, **48,** 2278 (1926).

6. E. BERGMANN, *J. Chem. Soc.*, **1936,** 505.

7. R. E. BUCKLES AND J. P. YUK, *J. Am. Chem. Soc.*, **75,** 5048 (1953).

8. A. LAPWORTH AND J. A. McRAE, *J. Chem. Soc.*, **121,** 1699 (1922).

9. A. KLAGES AND S. HEILMANN, *Ber.*, **37,** 1433 (1904).

10. A. R. RONZIO AND W. B. COOK, *Org. Syntheses*, **24,** 6 (1944).

11. T. ZINCKE, *Ann.*, **159,** 367 (1871).

12. V. N. IPATIEFF, H. PINES, AND R. E. SCHAAD, *J. Am. Chem. Soc.*, **66,** 816 (1944).

13. S. WAWZONEK AND H. A. LAITINEN, *ibid.*, **64,** 2365 (1942).

14. W. SCHLENK AND E. BERGMANN, *Ann.*, **463,** 1 (1928).

15. J. B. CONANT AND B. S. GARVEY, JR., *J. Am. Chem. Soc.*, **49,** 2599 (1927).

16. W. SCHLENK AND H. MARK, *Ber.*, **55,** 2285 (1922).

Preliminary Investigation of Hafnium Metal by the Kroll Process[1]

H. L. Gilbert[2] and M. M. Barr

Northwest Electrodevelopment Laboratory, U. S. Bureau of Mines, Albany, Oregon

ABSTRACT

Several hundred pounds of hafnium metal of better than 98% purity have been produced by the Kroll process of magnesium reduction of the tetrachloride. A discussion of the process from oxide to metal stages is given with thermodynamic values for chlorination and reduction. Metal produced to date is hot malleable but not cold ductile.
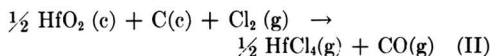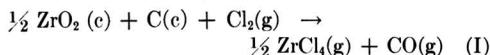
Preliminary Investigation

The Kroll process (1) has been employed in the production of titanium and zirconium metals with great success (2–4). While application of the process to the production of other metals may be postulated, recent production of several hundred pounds of relatively pure hafnium metal is of particular interest due in part to the rarity of this element in the pure state.

Hafnium is normally associated with zirconium ores to the extent of about 2%, and while as common as beryllium, germanium, and uranium, and more plentiful than mercury, tantalum, niobium (columbium), and silver (5), it is far more unusual in the pure form because of the great difficulty encountered in separating it from zirconium. It has been reported that the separation may be accomplished through fractionation of mixtures of hafnium-zirconium chloride-phosphorous oxychloride addition compounds (6) and by fractional crystallization of the mixed zirconium-hafnium fluoride-potassium fluoride double salts. Selective precipitation (7), ion exchange, and liquid-liquid exchange (8) are known to give reasonable separations, but no method is without disadvantages.

The material employed in this work was prepared by the Oak Ridge National Laboratory Materials Chemistry Division through methods employed in isotopic separations (9).

The thermodynamics involved in converting hafnium oxide to the metal may be compared with zirconium on a relative basis by the following calculations of Kelley (10):

$$\tfrac{1}{2} \text{ZrO}_2 \text{ (c)} + \text{C(c)} + \text{Cl}_2\text{(g)} \rightarrow \tfrac{1}{2} \text{ZrCl}_4\text{(g)} + \text{CO(g)} \quad \text{(I)}$$

$$\tfrac{1}{2} \text{HfO}_2 \text{ (c)} + \text{C(c)} + \text{Cl}_2 \text{ (g)} \rightarrow \tfrac{1}{2} \text{HfCl}_4\text{(g)} + \text{CO(g)} \quad \text{(II)}$$

	ΔH 1200	ΔF° 1200
Zirconium	1700	−32,600
Hafnium	−9700	−43,100

$$\tfrac{1}{2} \text{ZrCl}_4 \text{ (g)} + \text{Mg (l)} \rightarrow \tfrac{1}{2} \text{Zr (c)} + \text{MgCl}_2\text{(l)} \quad \text{(III)}$$

$$\tfrac{1}{2}\text{HfCl}_4 \text{ (g)} + \text{Mg (l)} \rightarrow \tfrac{1}{2} \text{Hf (c)} + \text{MgCl}_2 \text{ (l)} \quad \text{(IV)}$$

	ΔH 1150	ΔF° 1150
Zirconium	−39,300	−26,600
Hafnium	−26,200	−14,700

Free energy values favor reaction (II) over reaction (I) and reaction (III) over (IV), meaning that hafnium oxide is more readily chlorinated than is zirconium oxide, but the tetrachloride formed is less efficiently reduced by magnesium than is the tetrachloride of zirconium. Both of these predictions were borne out by reaction behavior in the plant runs.

Experimental

The hafnium material received was first calcined at 800°C to assure the conversion of any compounds present to the oxide. Tests showed that carbiding of the oxide by the reaction

$$\text{HfO}_2 + 3\text{C} \rightarrow \text{HfC} + 2\text{CO}$$
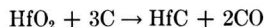
proceeded satisfactorily, but formation of a dense crystalline material so familiar with zirconium (11) could not be attained readily in the case of the hafnium carbide, due perhaps to the higher melting point of the latter material. Since chlorination of a noncrystalline material is difficult, hafnium oxide was chlorinated directly according to the reaction.

$$\text{HfO}_2 + 2\text{C} + 2\text{Cl}_c \rightarrow \text{HfCl}_4 + 2\text{CO}$$

It must be noted that other products, particularly carbon dioxide and phosgene, also are formed, showing that the reaction probably is more complicated than indicated (12).

A chlorination mixture was prepared as follows: hafnium oxide, 81.5%; carbon black, 9.5%; dextrine, 4.5%; water, 4.5%.

This mixture was blended in a ribbon mixer and then stored for 24 hr to allow the moisture to become diffused throughout the mass. Briquetting was accomplished in a Belgian roll type machine which produced very hard, dense briquets about $1\frac{3}{8}$ x 1 x $\frac{3}{4}$ in. These were dried at 140°C and chlorinated at 900°C in an experimental 12-in. diameter shaft chlorinator previously described (12).

Crude hafnium tetrachloride as produced was a buff-colored powder which sublimed at 317°C and was sensitive to oxidation and hydrolysis, fuming when exposed to the atmosphere, even at room temperature. By the time this fluffy mass had been transferred to the purification furnace considerable oxidation and hydrolysis had taken place, partly bec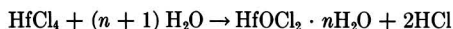ause of the finely divided state of the material. The more troublesome reaction is the hydrolysis to form hafnyl chloride:

$$HfCl_4 + (n + 1) H_2O \rightarrow HfOCl_2 \cdot nH_2O + 2HCl$$

Prior to reduction, this material must be removed from the tetrachloride since much of the success of the entire process depends upon the extent of its removal. Best results were found with a combination of thermal decomposition and vacuum treatment to remove the water liberated:

$$HfOCl_2 \cdot nH_2O \rightarrow HfO_2 + 2HCl + nH_2O$$

Under parallel circumstances in the zirconium process rather complete elimination of volatile oxide-bearing compounds is effected, but with hafnium it would appear that the oxychloride has sufficient stability in the anhydrous form ($HfOCl_2$) to permit some carry-over in subsequent sublimation. Attempts to establish the existence of a volatile oxychloride were not successful, in part because of difficulties encountered in the analysis for oxygen.

By careful heating and evacuation, the bulk of the moisture was removed from the raw hafnium tetrachloride at an ultimate temperature of 200°C. The furnace was then filled with helium and the crude tetrachloride transferred by sublimation to a water-cooled coil where it collected in a dense massive form.

The purified tetrachloride was transferred to a reduction furnace and there sublimed under helium into molten magnesium. The effect of the lower free energy of the reaction coupled with apparent insolubility of the hafnium metal in molten magnesium required a magnesium excess of 40% over the stoichiometric amount. Operating temperature during reduction was 850°C.

Separation of the hafnium formed from the excess magnesium and by-product magnesium chloride was accomplished in the standard vacuum distillation furnace employed in processing zirconium.
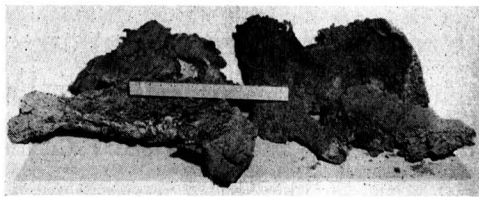
FIG. 1. Hafnium sponge after vacuum distillation step
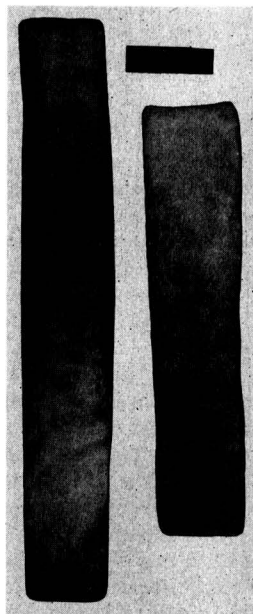
FIG. 2. Hafnium sheet hot rolled from arc melted ingot

The sponge metal shown in Fig. 1 was very heavy, since hafnium has a density of 13.3, but did not appear to have coalesced to the extent that is found with zirconium. Several observations tend to show a very low comparative solubility of hafnium in magnesium which could impede crystal growth, and the considerably higher transformation temperature of hafnium (1550° vs. 861°C) might also contribute to the crystalline form.

The physical state of the hafnium sponge made it rather reactive when exposed to air. Initial exposure was to an air-helium mixture which prevented actual ignition of the sponge while allowing the more pyrophoric materials to oxidize slowly to such an extent that the furnace could be opened and the sponge removed without loss. Handling, cutting, and cleaning of the sponge was done in a helium atmosphere box.

Hafnium sponge was melted by consumable electrode arc methods and the ingots forged and rolled to sheet as shown in Fig. 2. All metal had a

hardness of Rockwell C 20 to 25 which is indicative of oxygen contamination. At such hardnesses the metal may not be considered cold ductile. The sponge can be purified by the iodide dissociation method to give metal having a reported hardness of Rockwell B 78 (5).

Analysis of three test lots of sponge metal was as follows:

Sample No.	$\dfrac{Zr}{Hf + Zr}$	Analysis ppm							
		O₂	Fe	N₂	Cl	Al	Cu	Pb
1	1.4	650	400	10	150	30	100	30
2	1.4	850	400	20	100	30	100	30
3	1.3	950	400	30	200	50	50	20

	Zn	Cr	Co	Mn	Ni	Si	Ti	V	Mo
1	5	100	10	30	5	100	50	20	10
2	5	100	10	30	5	100	50	20	10
3	50	5	10	30	5	20	50	20	10

All residues and metal scrap were burned in large porcelain dishes to hafnium oxide for recycling in the process.

Several modifications in the process are under consideration, and it is hoped that by means of these and the exercise of extreme care throughout the process the hardness of the metal may be reduced to more satisfactory levels.

Conclusions

Hafnium metal may be produced in zirconium plant equipment without modification. Greater sensitivity of hafnium tetrachloride to atmospheric moisture and higher stability of hafnyl chloride required some additional care and effort in chloride purification. Magnesium in the amount of 40% over stoichiometric is employed in reducing the

chloride. Magnesium chloride by-product and excess magnesium were removed by vacuum distillation. Sponge metal was somewhat reactive in air. Metal ingots had a hardness of Rc 20 to 25 but could be hot forged and rolled to sheet.

Any discussion of this paper will appear in a Discussion Section to be published in the December 1955 JOURNAL.

References

1. W. J. KROLL, U. S. Pat. 2,205,854.
2. H. C. FULLER, D. H. BAKER, AND F. S. WARTMAN, U. S. Bur. Mines Rept. Investigation 4879, June 1952.
3. S. M. SHELTON AND E. DON DILLING, "Zirconium and Zirconium Alloys," p. 82, American Society for Metals, Cleveland (1953).
4. D. I. BROWN, *Iron Age*, **170**, 260 (1952) et seq.
5. F. B. LITTON, *This Journal*, **98**, 488 (1951).
6. D. M. GRUEN AND J. J. KATZ, *J. Am. Chem. Soc.*, **71**, 3843 (1949).
7. H. H. WILLARD AND H. FREUND, *Ind. Eng. Chem.* (Anal. Ed.), **18**, 195 (1946).
8. E. H. HUFFMAN AND L. J. BEAUFAIT, U. S. Pat. 2,566,665.
9. E. C. MILLER, "Zirconium and Zirconium Alloys," p. 337, American Society for Metals, Cleveland (1953).
10. K. K. KELLEY, Private communication.
11. W. J. KROLL, W. W. STEPHENS, AND J. P. WALSTAD, *Trans. Am. Inst. Mining Met. Engrs.*, **188**, 1394 (1950).
12. W. W. STEPHENS AND H. L. GILBERT, *J. Metals*, **4**, 733 (1952).
13. A. E. VAN ARKEL AND J. H. DE BOER, *Z. anorg. u. allgem. Chem.*, **141**, 289 (1924).

The Influence of Impurities in the Electrolyte in Chlorine-Caustic Electrolysis by the Mercury Cell Process

V. Further Investigation of the Influence of Metals on the Cathodic Current Efficiency[1]

Gösta Angel, Tage Lundén, Stig Dahlerus, and Rolf Brännland

Division of Applied Electrochemistry, Royal Institute of Technology, Stockholm, Sweden

ABSTRACT

In a number of electrolysis experiments the influence of mixtures of certain common metals, such as vanadium, magnesium, and aluminum, was investigated. A theory is developed for the action of those metals which have previously been shown to interfere with electrolysis in mercury cells.

Introduction

A number of metals have been examined with respect to their influence on the cathodic current efficiency in mercury cells (1), but in each experiment only one metal was added. Certain amalgam decomposition experiments indicated, however, that two metals may interfere in an unexpected manner; therefore, another series of experiments was made with extraneous metals combined in groups of two.

The experiments were performed in the same way as those previously described (1); the current was 10 amp (25 amp/dm²), the brine flow rate 7.5 ml/min, the mercury flow rate 8–10 ml/min, and the temperature generally 38°–42°C.

Experimental

Vanadium and iron.—As previously reported (2), amalgam decomposition experiments showed that the influence of vanadium on decomposition rate was promoted very much by comparatively small quantities of iron. Since vanadium, and iron above all, may be present in industrial brines, this pair of metals was thoroughly investigated by electrolysis experiments.

The somewhat surprising results of these experiments are reproduced in Fig. 1. In the presence of comparatively large quantities of iron, the influence of vanadium was very much reduced, contrary to what might be predicted from the amalgam decomposition experiments.

During the experiments, the mercury surface was bright, and all the hydrogen evolution was concentrated at the glass wall and the mercury lock. In the presence of only 1–2.5 mg/l iron, a gas "spot"

was formed after some time at the cathode surface, and the current efficiency began to decrease markedly.

In a special series of experiments it was found that, after it had once started, hydrogen evolution due to vanadium could not be nullified by addition of iron-containing brine. It was also observed that ferric hydroxide was precipitated in the cell during electrolysis; this phenomenon may explain why vanadium was de-activated by iron under conditions prevailing in a mercury cell.

Experiments with magnesium as one constituent.—With magnesium mixed with a number of other metals, a series of experiments was performed as shown by the table below:

	Ti	Al	Cu	Fe	Ni	Mn	Ca
Mg	+	+	+	+	+	+	O

"+" means that the influence of both metals together is stronger than that of any of them alone; "O" means that no increased influence was observed.

In the experiments with brine containing 5 mg/l magnesium and 5 mg/l titanium, hydrogen gas evolution occurred within 2 min, and after 15 min the current efficiency had decreased to about 30% This result does not agree with those obtained from brines containing a titanium salt alone.

With 2.5 mg/l magnesium and 5 mg/l aluminum simultaneously present in the brine, the cathodic reaction was similarly affected; hydrogen gas evolution started within 1 min and current efficiency was 29% in 20 min.

Using 5 mg/l magnesium and 5 mg/l copper, cathodic current efficiency was 47% after 20 min.

Experiments were made with magnesium and iron simultaneously present in varying concentrations. The results of typical runs with 10 mg/l iron mixed with 10 and 25 mg/l magnesium, respectively, are demonstrated in Fig. 2. Although

ห้องสมุด กรมวิทยาศาสตร์

246

neither iron nor magnesium was able to cause any hydrogen evolution separately, they decreased the current efficiency considerably when present together. In the experiments it was also observed that the mercury surface was completely covered by a thick layer of iron and magnesium hydroxide, possibly mixed with some amalgam.

With 5 mg/l magnesium and 5 mg/l nickel a similar phenomenon occurred; in 10 min the current efficiency had decreased to about 40%. With the same quantities of magnesium and manganese the same result was obtained, and after 15 min the current efficiency was only 50%.

In the simultaneous presence of magnesium and calcium, however, no interference with the cathodic current efficiency was observed.

Experiments with aluminum as one constituent.— Results of the experiments with aluminum as one constituent are given in the following table:

	V	Ti	Cu	Fe	Ni	Mn	Ca
Al	+	+	+	O	O	O	O

"+" means that the influence of both metals together is stronger than that of any of them alone; "O" means that no increased influence was observed.

With 12.5 mg/l aluminum and 0.5 mg/l vanadium the influence was considerably greater than with vanadium alone. Thus the current efficiency decreased to 4% in 1 hr, and it is therefore clear that vanadium is not de-activated by the formation of aluminum hydroxide.

With 5 mg/l aluminum and 0.3 mg/l titanium, hydrogen evolution occurred immediately after the start of the experiment and after 10 min the current efficiency had decreased to 76%.

With 5 mg/l aluminum and 5 mg/l copper, the hydrogen evolution started after about 2 min of electrolysis, then the current efficiency decreased to 20% in 18 min. After the experiment was finished, a reddish brown film was observed on the mercury surface.

With 5 mg/l aluminum and either 5 mg/l iron, 5 mg/l nickel, 50 mg/l manganese, or 50 mg/l calcium, no effect was observed.

Experiments with copper as one constituent.—As well as the previously described combination experiments with copper mixed with either magnesium or aluminum, experiments on mixtures of copper with the following metals were carried out:

	Ti	Fe	Ni	Mn	Ca
Cu	+	O	O	O	O

"+" means that the influence of both metals together is stronger than that of any of them alone; "O" means that no increased influence was observed.

With 0.5 mg/l copper and 5 mg/l titanium,
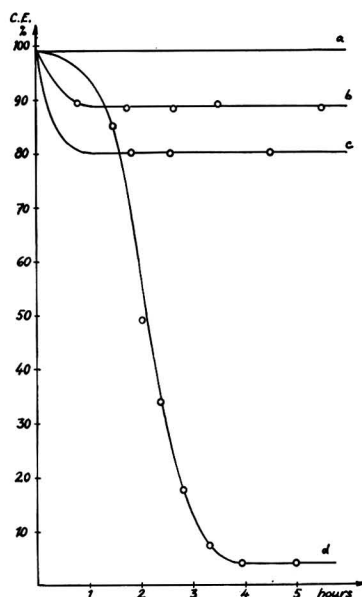
FIG. 1. Current efficiency in presence of vanadium and iron. Curve a, 12.5 mg/l Fe; curve b, 0.5 mg/l V + 12.5 mg/l Fe; curve c, 1.0 mg/l V + 12.5 mg/l Fe; curve d, 0.5 mg/l V.
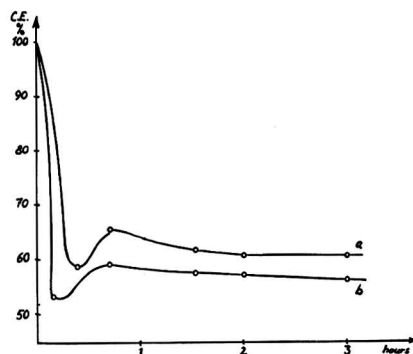
FIG. 2. Current efficiency in presence of magnesium and iron. Curve a, 10 mg/l Mg + 10 mg/l Fe; curve b, 25 mg/l Mg + 10 mg/l Fe.

hydrogen evolution occurred a few seconds after the start of electrolysis. After 13 min the current efficiency had decreased to 0%. Also in this case a reddish brown film was found at the cathode surface after the experiment.

With the other metals in the table no interference with the cathode reaction was obtained.

Experiments with sodium silicate.—In a previous paper (3) it was reported that sodium silicate or silicic acid had a strongly de-activating influence on vanadium and molybdenum in the amalgam decomposition experiments. The influence of silicate

FIG. 3. Current efficiency in presence of silicate and molybdenum. Curve a, 1.5 mg/l Mo; curve b, 1.5 mg/l Mo + 25 mg/l Si; curve c, 1.5 mg/l Mo + 100 mg/l Si.

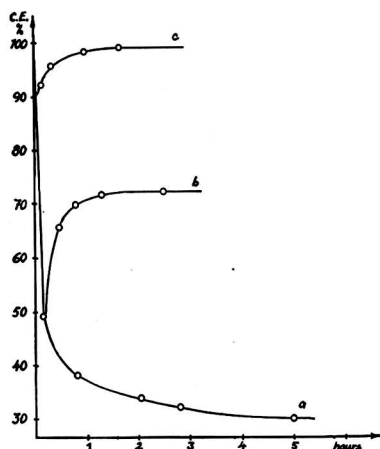with respect to certain interfering metals was also investigated by electrolysis experiments, typical results of which are presented in Fig. 3.

The experiments show that 25 mg/l silicon is sufficient to de-activate 0.5 mg/l vanadium or the same concentration of chromium. With 1.5 mg/l molybdenum and 25 mg/l silicon the current efficiency was, however, decreased to 49% in 8 min, and 100 mg/l silicon was needed in order to de-activate this quantity of molybdenum.

The effect of silicate addition to brine containing 10 mg/l iron and 25 mg/l magnesium was also investigated, but in this case the current efficiency still decreased to about 57%.

In the electrolysis experiments with silicate some observations were made which are of great importance for an explanation of the reaction mechanism and for the possible use of silicate as de-activator of vanadium.

It was found that silicate had no effect on metals belonging to the vanadium group, if the silicate was added when gas evolution had once started at the cathode. This indicates that vanadium ions may be absorbed by silicic acid and thus removed from solution.

Experiments with silicate show that comparatively large quantities are required to de-activate completely the interfering metals, 25–40 times the concentration of the metal in question. But experiments with large concentrations of silicic acid have also shown that the mercury cathode may be covered with a film of silicic acid, which acts as a diaphragm and impedes the sodium ion transport to the cathode, thus causing hydrogen gas evolution and a decrease of current efficiency. With 30 mg/l

silicon a maximum hydrogen content of 30% was obtained.

However, if silicate-treated brine was allowed to stand for a few hours before the electrolysis, no disturbance was observed, and brines with 100 mg/l silicon could then be electrolyzed without any film formation. The phenomenon is probably caused by cataphoretic deposition of colloidal silicic acid at the cathode. If on the other hand the brine is allowed to stand, the silicic acid flocculates and cannot move in the electric field.

DISCUSSION

Metals investigated may be arranged with respect to their influence on cathodic current efficiency into two groups: one of strong influence (vanadium, molybdenum, chromium, titanium), and one of slight or no influence (magnesium, calcium, barium, iron, etc.).

With regard to the strong effect of the vanadium group, the polyvalent character of these metals is striking. It might be assumed that, under certain conditions, hydrogen ions could be reduced by metal ions of low valency, which were then reduced again at the cathode, according to the formulas:

$$2H^+ + Me^{n+} = H_2 + Me^{(n+2)+} \qquad (I)$$

$$Me^{(n+2)+} + 2e^- = Me^{n+} \qquad (II)$$
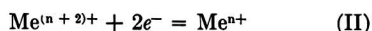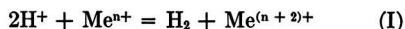
In that case, reaction (I) would take place in the cathode film and reaction (II) at the mercury surface. However, most of the active metals were added as anions, and, although the same reactions would take place, the ions would have to be transported to the cathode by diffusion alone. On account of the violent gas evolution, which makes the concentrating of active metals in the cathode film difficult, and because of certain observations accounted for below, this explanation seems improbable.

Of course, it is very convenient to characterize the action of the vanadium group as catalysis. According to this hypothesis, the active metal ions should lower the hydrogen overvoltage on mercury by catalyzing one of the steps in the reaction chain:

$$H_3O^+ \rightarrow H^+ \rightarrow H \rightarrow H_2 \text{ (adsorbed)} \rightarrow H_2 \text{ (gas)}$$
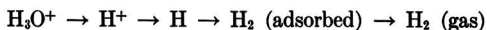
However, experiments described later show that the hypothesis cannot be correct in this form, but must be modified to an assumption of deposition of the metal in question on the mercury surface. In this case, the reaction no longer involves hydrogen overvoltage on mercury but on the deposited metal.

This theory thus presumes that: the active metal can be electrochemically deposited at the actual cathode potential; the deposited metal remains at

the mercury surface and is not amalgamated, dissolved, or dispersed; the hydrogen overvoltage upon the deposited metal is lower than that upon mercury.

Cathode potentials.—According to Latimer (4) the following standard potentials apply to the metals discussed. For vanadium,

$$V^{2+} + 2e^- = V \qquad\qquad e^0 = -1.18 \text{ v}$$

$$V^{3+} + e^- = V^{2+} \qquad\qquad e^0 = -0.25 \text{ v}$$
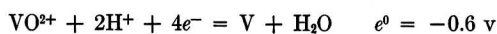
$$VO^{2+} + 2H^+ + e^- = V^{3+} + H_2O \qquad e^0 = 0.36 \text{ v}$$
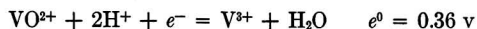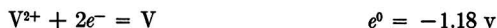
These equations may be combined according to Luther's rule:

$$VO^{2+} + 2H^+ + 4e^- = V + H_2O \qquad e^0 = -0.6 \text{ v}$$

With $a_{VO^{2+}} = 10^{-6}$ and pH 12, the reversible cathode potential at 50°C is -1.2 v.

For molybdenum, $H_2MoO_4 + 6H^+ + 6e^- = Mo + 4H_2O$ $e^0 = 0.0$ v (approx). With $a_{H_2MoO_4} = 10^{-6}$ and pH 12, the reversible cathode potential at 50°C is about -0.9 v.

For chromium, $Cr^{3+} + 3e^- = Cr$ $\quad e^0 = -0.74$ v With $a_{Cr^{3+}} = 10^{-6}$, the reversible potential at 50°C is -0.87 v.

For titanium, $TiO^{2+} + 2H^+ + 4e^- = Ti + H_2O$ $e^0 = -0.88$ v With $a_{TiO^{2+}} = 10^{-6}$ and pH 12, the reversible potential at 50°C is approximately -1.4 v.

For magnesium, calcium, barium, and iron, the standard potentials are below -2 v, but the reduction is depolarized by amalgam formation and, according to Kolthoff and Lingane (5), the actual standard potentials are:

$$Mg^{2+} + 2e^- + Hg = Mg(Hg) \qquad e^0 = -1.9 \text{ v}$$
$$\text{(approx.)}$$

$$Ca^{2+} + 2e^- + Hg = Ca(Hg) \qquad e^0 = -1.95 \text{ v}$$

$$Ba^{2+} + 2e^- + Hg = Ba(Hg) \qquad e^0 = -1.70 \text{ v}$$

$$Fe^{3+} + 3e^- = Fe \qquad e^0 = -0.036 \text{ v}$$
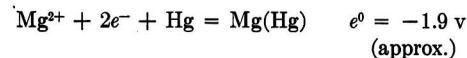
De Nora (6) reported that the cathode potential is about -1.75 v in industrial electrolysis of saturated NaCl solutions with mercury cathode. Thus most of the metals mentioned above may be electrochemically deposited even if they occur in concentrations of 1 γ/l.

Solubility in mercury.—Irving and Russel (7) studied the solubility of vanadium, molybdenum, and chromium in mercury and found that they were practically insoluble: vanadium, $5 \times 10^{-5}\%$; molybdenum, $2 \times 10^{-5}\%$; chromium, $5 \times 10^{-5}\%$; titanium, $10^{-5}\%$.

The solubility of amalgams formed by magnesium, calcium, and barium is comparatively high (8–10).

The solubility of iron in mercury has been studied very extensively, but the results are partly contradictory. The general opinion is that iron is quite insoluble and merely forms a suspension in the mercury (11). Thus the iron particles in a mercury suspension are influenced by a magnetic field (12). Katoh (13) examined an iron "amalgam" by x-ray analysis and found that the iron particles consisted of α-iron. The iron concentration in mercury may be so high that a solid mixture is formed (amalgam butter), corresponding to an iron content of more than 2%.

Hydrogen overvoltage.—According to investigations by Thiel and Hammerschmidt (14) the minimum hydrogen overvoltage is: mercury 0.570 v, vanadium 0.135 v, molybdenum 0.157 v, chromium 0.182 v, titanium 0.236 v.

Important Observations for Establishing the Reaction Mechanism Theory

In the electrolysis experiments, some observations were made which must be taken into consideration when the hypotheses given above are discussed.

1. The addition of absorbing substances, such as silicic acid and ferric hydroxide, has no effect if they are added when gas evolution, caused by vanadium, for example, has once occurred. This phenomenon indicates that the active metal is no longer present in the solution, but precipitated at the electrode surface.

2. In the presence of moderate quantities of vanadium, molybdenum, or chromium, the gas evolution is concentrated to only a part of the cathode surface (gas spot). If the electrolysis is interrupted and this gas spot is removed by suction together with some mercury, gas evolution will not occur again when the electrolysis is continued. It is probable that, if a metal, insoluble in mercury, is deposited at the cathode, the metal forms a coherent film owing to the surface forces, the area of which increases with the quantity of metal deposited and at which the gas evolution is located.

3. If the electrolysis of a salt solution polluted with vanadium, molybdenum, or chromium is interrupted, the brine carefully sucked off, and the cell rinsed with distilled water, then a violent gas evolution nevertheless occurs when fresh *pure* brine is supplied and the electrolysis is continued.

4. In experiments with about 5 g/l vanadium, a dark, tough film was obtained at the cathode after a few minutes of electrolysis.

In addition to the electrolysis experiments described above, some amalgam decomposition experiments were performed in order to show that vanadium is removed from the solution with the amalgam. The experiments included shaking the
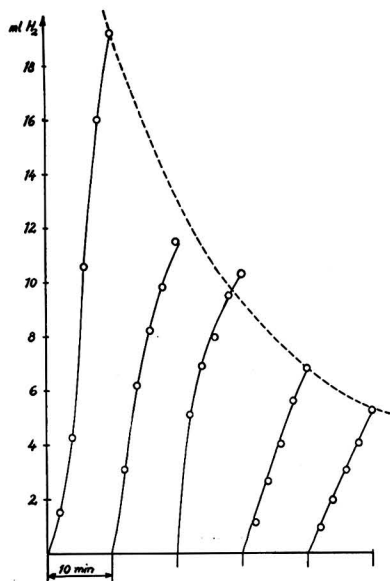
FIG. 4. Amalgam decomposition experiment with vanadium-containing brine and addition of fresh amalgam at 10 min intervals.

polluted salt solution with sodium amalgam for 10 min. The solution was then decanted, acidified with hydrochloric acid to pH 6.5, and again shaken with a quantity of fresh amalgam for 10 min, etc. This was repeated 5 times, and in the course of the experiment the gas evolution decreased steadily (cf Fig. 4). The experiment shows that vanadium is removed from the solution to a considerable extent and presumably deposited at the amalgam surface.

CONCLUSIONS

Theoretical considerations show that the electrochemical reduction of vanadium, molybdenum, and chromium to the metallic state is possible. The deposited metals are not soluble in mercury but remain at the cathode surface and, since the hydrogen overpotential is lower on these metals than on mercury, hydrogen evolution is promoted.

As to the action of magnesium, this metal is probably reduced to some extent and amalgamated but, more important, the hydroxide is precipitated in the alkaline cathode film and forms a diaphragm there, which makes the passage of sodium ions difficult while the smaller hydrogen ions migrate more easily and are discharged at the cathode. The diaphragm is further reinforced if other hydroxides are coprecipitated.

The observations accounted for above support the assumption that certain mercury-insoluble metals are deposited in small quantities at the cathode and form there active spots where hydrogen ions exclusively are discharged.

As to mixtures of interfering metals, experiments have shown that interaction between, e.g., magnesium and metals of the vanadium group, may very well occur, so that the cathode film is rendered more alkaline by the hydrogen ion discharge, more hydroxide is precipitated, the sodium ion migration is made still more difficult, etc.

Yet, the literature (15) shows that two metals may interfere in the mercury phase so that their solubility in mercury is considerably decreased. A film of the interfering metal is then formed at the cathode, and hydrogen evolution is promoted.

Results of the electrolysis experiments are directly applicable to the industrial chlorine-caustic electrolysis in mercury cells. Thus, vanadium has been proved to be the most dangerous of the impurities examined, and the vanadium influence is greater in brine purer with respect to certain other substances, such as ferric iron and silicic acid, which decrease the influence of vanadium to a considerable extent. Therefore, the previously mentioned, serious interruptions in 1949 at two Swedish chlorine plants were no doubt caused by vanadium dissolved from the graphite anodes employed (2). The less serious disturbances at other chlorine plants may be explained by the assumption that the brine in those cases contained certain impurities which have been shown to inhibit vanadium influence.

SUMMARY

A number of electrolysis experiments are described, in which the influence of mixtures of certain metals was investigated under normal operating conditions: current density 25 amp/dm², brine depletion 15%, and amalgam concentration 0.14%. In each experiment the brine was polluted with salts of two metals so that the combined effect of these metals could be studied. It is shown that:

1. Magnesium interferes with the cathode reaction when iron, nickel, titanium, copper, aluminum, or manganese is simultaneously present.

2. Aluminum promotes hydrogen ion discharge when either titanium or copper is also present in the brine.

3. Silicate or silicic acid in adequate quantities reacts with vanadium, molybdenum, and chromium, so that these metals are de-activated and sodium ion discharge proceeds undisturbed.

A theory is developed for the action of metals belonging to the vanadium group and for other metals. The former are assumed to be electrochemically deposited and to remain at the surface, thus decreasing hydrogen overvoltage and promoting

the discharge of these ions. Magnesium, on the contrary, is supposed to act quite mechanically by the formation of a hydroxide diaphragm reinforced by other metal hydroxides, which makes the sodium ion migration difficult.

Any discussion of this paper will appear in a Discussion Section, to be published in the December 1955 JOURNAL

REFERENCES

1. G. ANGEL, T. LUNDÉN, S. DAHLERUS, AND R. BRÄNNLAND, *This Journal*, **102**, 124 (1955).
2. G. ANGEL AND T. LUNDÉN, *This Journal*, **99**, 435 (1952).
3. G. ANGEL, T. LUNDÉN, AND R. BRÄNNLAND, *ibid.*, **100**, 39 (1953).
4. W. M. LATIMER, "The Oxidation States of the Elements and Their Potentials in Aqueous Solutions," Prentice-Hall, New York (1952).
5. I. M. KOLTHOFF AND J. J. LINGANE, "Polarography," Interscience Publishers, New York (1952).
6. V. DE NORA, *This Journal*, **97**, 346 (1950).
7. N. M. IRVIN AND A. S. RUSSEL, *J. Chem. Soc. London*, **1932**, 891.
8. A. SMITS AND R. P. BECK, *Proc. Acad. Amsterdam*, **23**, 975 (1921).
9. H. MOISSAN AND G. CHAVONNE, *Compt. rend.*, **140**, 125 (1905).
10. A. SCHÖLLER, *Z. Elektrochem.*, **5**, 259 (1898).
11. T. W. RICHARDS AND R. N. GARROD-THOMAS, *Z. phys. Chem.*, **72**, 181 (1910).
12. M. RABINOWITSCH AND P. B. ZYWOTINSKI, *Koll.-Z.*, **52**, 31 (1930).
13. N. KATOH, *J. Chem. Soc. Japan*, **64**, 1079 (1943).
14. A. THIEL AND W. HAMMERSCHMIDT, *Z. anorg. u. allgem. Chem.*, **132**, 15 (1923).
15. H. HOHN, *Österr. Chem.-Ztg.*, **49**, 15 (1948).

Electrolytic Reduction of Titanium Monoxide[1]

M. E. Sibert, Q. H. McKenna, M. A. Steinberg, and E. Wainer

Horizons Incorporated, Cleveland, Ohio

ABSTRACT

An electrolytic method for preparation of titanium metal from titanium monoxide is described. The process is carried out in alkaline earth halide melts under an inert atmosphere. The inert atmosphere cell and its operation are described. Methods for preparation of reduced titanium oxides are also discussed. These include reactions of titanium carbide with ZnO or MgO, carbon reduction of TiO_2, and electrolytic reduction of TiO_2. Electrolytic titanium prepared from TiO is deposited as a crystalline metal powder in a salt matrix and is recovered by aqueous techniques. Although metal so prepared has not generally been acceptable from a purity standpoint, revision in cell design and procedure could offer improvement in this respect.

INTRODUCTION

Considerable effort has been expended on the development of new processes for titanium metal preparation, much of this effort toward electrolytic processes.

Probably the biggest problem is that of a source electrolyte. Such a material should preferably be obtainable as an ore or be readily processed, be stable under normal conditions, and lend itself readily to electrolysis. The most logical material is TiO_2 since naturally occurring rutile, anatase, and ilmenite are easily converted to pure TiO_2. However, there is no known single stage reductant capable of producing metal from the dioxide even by thermal reaction. Thus, it was decided to investigate methods of preparing the lower oxides and their electrolysis.

Four methods were developed for production of the monoxide or sesquioxide. Since a one-step reduction (Ti II to Ti) is preferable to a two-step (Ti III to Ti II to Ti), and since the monoxide is about as easy to prepare as the sesquioxide, the electrolytic effort was concentrated on the monoxide.

An electrolytic method for reduction of the monoxide to metal was subsequently developed. The procedure entails a high temperature electrolysis of TiO in a melt of an alkaline earth halide. For most of the work anhydrous $CaCl_2$ has been employed.

A protective atmosphere of argon or helium is a requirement of the process, both for protection of produced titanium metal and the TiO in the bath.

With this process titanium up to 99% purity has been produced. The metal can be arc melted and hot worked although, in general, it does not meet commercial specifications at this stage of the

development. The only significant impurities present are oxygen and carbon.

Titanium Metal Preparation

A review of the literature on the electrolytic preparation of titanium reveals a varied array of attempts, but little in the way of substantial results. A number of these have been carried out in aqueous solution, but it is improbable that pure titanium can ever be isolated in this manner.

Titanium films of 1 μ thickness on copper were deposited from sulfanilic acid—$Ti(OH)_4$ solutions (1) as were thin black films of titanium on lead, zinc, and antimony by electrolysis of TiO_2 in H_2SO_4—Na_2SO_4—$10H_2O$ solutions (2), or from $Ti_2(SO_4)_3$ solutions (3).

There are patents on electroplating titanium from strongly alkaline solutions of TiO_2 or $Ti(OH)_4$ on iron or copper (4) and for treatment of base metals by anodization in baths containing colloidal suspensions of Si, Al, Zr, or a "rare earth oxide" (including TiO_2) and a conducting salt or acid (5). An anion must be present to form an insoluble salt of the metal being treated.

Titanium plating has been reported from $Ti(C_4H_4O_6)_2$ solutions at room temperature (6). Electrolysis of titanium salicylates have been attempted (7) where titanium apparently formed an anionic complex. Negative results are reported using solutions of $TiCl_4$ in CH_3OH, C_2H_5OH, pyridine, and other organic solvents (6).

Deposition of titanium and other reactive metals on mercury by shaking with an acidified salt of the metal has been claimed (8). Another use of a mercury cathode was reported as an analytical method for quantitative determination of titanium in silica-aluminum by electrolysis (9). An unsuccessful attempt was made to plate titanium from aqueous solution as well as a number of other high dielectric constant electrolytes (10). The metal

could only be plated from highly ionized complexes as opposed to the simple salts employed in the work described. It has been claimed that titanium can be electroplated from solutions of complex organic titanium salts where the concentration was 35 g Ti/l or more (11). Titanium was said to have been plated on Hg from a solution of $TiCl_2$ in $2N$ HCl (12).

A number of summaries of attempts to produce titanium electrolytically have been written. Andrieux (13, 14) considered the fused salt field. Others, covering varying aspects of the whole field, include those by Keeney (15) and Spence (16).

Attempts have been made to produce the metal directly by electrolysis of ores, e.g., titanoferrous ores (17) or the aluminum by-product "red mud" as an electrolytic feed material (18).

Others have produced alloys successfully by electrolytic methods. A patent entailing electrolysis of a fused mixture of alkali, alkaline earth, and titanium halides and employing the cathode as alloying metal has been obtained (19).

Binary and ternary alloys have been prepared (1) using baths of $AlCl_3$—NaCl and NaCl—NaF with TiO_2 as a source electrolyte. The alloying metal was derived from the anode in most cases; Zn—Ti was commonly used.

There are numerous reports of titanium preparation by fused salt electrolysis. A reasonably pure product was claimed from electrolysis of TiO_2 in $CaCl_2$ (20). Electrolysis of pure rutile later failed (21). The use of 1 mole of TiO_2 in 10 moles of K_2SiF_6 produced only $TiSi_2$ and Ti_2O_3 (22). Only lower oxides were obtained with TiO_2 in a variety of fused salts and salt mixtures and with K_2TiF_6 in a mixture of NaCl—KCl (23).

A process for producing Ti by electrolysis of $TiCl_4$ in one or more of NaCl, KCl, $CaCl_2$, and $MgCl_2$ using a cell of special design has been described recently (24). Dendritic powder has been formed from $TiCl_3$ dissolved in a mixture of LiCl and KCl at 550°C under a hydrogen atmosphere (25) and Ti powder has been prepared from baths of K_2TiF_6—NaCl—KCl, $TiCl_3$—NaCl—KCl, and TiF_3—NaCl—KCl at 850°–900°C under an inert atmosphere (26). A further process involving electrolysis of $TiCl_4$ in a LiCl—KCl mixture at 400°C has been reported (27).

The present authors have reported on the electrolysis of K_2TiF_6 in NaCl producing a very pure titanium powder (28). A major difference in this work and that of earlier investigation (23) was the use of a controlled inert atmosphere.

TiO *Preparation*

Claims for the formation of TiO by reduction of TiO_2 by carbon (29–31), by Zn (32, 33), by Mg (34), and by Na (35) have been made. The possibility of TiO in slags from the smelting of titaniferrous ores has been described (36).

In all of these studies the TiO was generally not pure; some (33, 32) found it to have an indigo-blue color, while another obtained it as a black crystalline mass prepared by heating the TiO_2 with carbon in the electric arc furnace. Newberry and Pring (37) found that under a pressure of 150 atm hydrogen reduces titanic acid at 2000°C to the monoxide.

One mole of TiO_2 was reacted with two moles of Mg powder at a red heat in a current of hydrogen, the reduction taking place with incandescence (38). The product was cooled in an atmosphere of hydrogen, washed in glacial acetic acid, dried at a moderate heat, then completely dried in a current of hydrogen at 150°C. A brown powder was obtained which contained no metallic material but a lower oxide of the metal, mixed with magnesium in the form of magnesium titanate. From the quantity of oxygen taken up on heating the reduction product, it appears that the reduction takes place according to the equation $2TiO_2 + Mg = TiO + MgTiO_3$. When sodium vapor is passed over heated TiO_2, the product is a mixture of TiO and Ti_2O_3 (35).

TiO was obtained as a brown powder by heating an intimate mixture of TiO_2 and metallic Ti (38), but no information was given regarding the properties of TiO. Carstens (36) prepared TiO as described above. X-ray analysis (39) of TiO prepared this way (36) showed that it belongs to the cubic system (NaCl type) with the cube edge $a_o = 4.235$ Å. The calculated specific gravity lies between 5 and 6.

Others (40) prepared TiO in a like manner, but were unable to confirm the formation of TiO as a solid phase by the reduction of TiO_2 with carbon. Junker (41) also assumed that the reduction of TiO_2 with carbon merely yields mixtures of Ti_2O_3 and TiC.

Dawihl and Shroeter (42) also prepared TiO by reaction of Ti and TiO_2. The mole for mole mixture was pressed into rods and heated in a vacuum of 1×10^{-3} mm Hg at 1700°–1750°C. It was later found that 1550°C was high enough. These rods were golden yellow in color, and broke with a coarsely crystalline fracture. X-ray analysis showed it to have an NaCl structure with $a_o = 4.154$ Å (see above).

Metallographic examination revealed that the TiO rods were porous but consisted of a homogeneous yellow coarsely crystalline phase, as is confirmed by x-ray examination.

TiO dissolves slowly in dilute H_2SO_4 and in HCl with evolution of H_2. It does not dissolve in HNO_3, but is rapidly oxidized to TiO_2 in the boiling acid.

When finely powdered and heated in air for one hour at 400°C, it is converted, with about 1% weight increase, into a dark-blue crystalline material; when heated one hour at 600°C, it becomes gray-green in

color, with about 5% weight increase; above 800°C oxidation to TiO_2 proceeds rapidly.

Determination of the specific gravity of finely powdered TiO samples shows a value of 4.93, considerably lower than that calculated from the edge length of the elementary unit or by x-ray analysis (39). The melting point of TiO, determined by the Pirani-Altertheim bore-hole method (43) was found to be 1750°C. The electrical conductivity at room temperature averages 2490 reciprocal ohm cm.

Many of the literature references to TiO are in error. Observations of color alone illustrate this. It has been reported to be blue, green, black, violet, and golden. Pure TiO is a stable golden yellow compound and is essentially inert to most chemical attack (38, 42). This is borne out by the work described herein.

EQUIPMENT

Thermal reactions.—High temperature thermal reactions were initially carried out in high temperature Pyrex glass furnaces. The units were modifications of a design of Guldner and Beach (44). The unit is essentially a 3 in. Pyrex glass envelope fitted with a vacuum side arm, sight glass window, and a side arm magnetic crucible loading device. A fused clear quartz tube 2 in. in diameter is supported on glass hooks inside the Pyrex tube by platinum wire. A $\frac{3}{4}$ in. ID x 3 in. graphite crucible is inserted inside this tube surrounded by graphite filings for insulation. Pelleted reaction mixtures are dropped in the crucible from the side arm above.

The furnace unit is heated by a $3\frac{1}{8}$ in. ID induction coil powered by a 6 kw Ajax converter. A flat glass plate on the furnace bottom is removable for loading. A large Pyrex funnel fits over the bottom of the furnace; an air jet blows through this for cooling.

The furnace is connected through a dry ice-acetone cold trap to an Eimac oil diffusion pump (HVI). A Cenco Megavac is used as forepump. Ionization and thermocouple gauges are in the line between the trap and diffusion pump. The system is capable of attaining a vacuum of 10^{-4} mm of mercury at 1500°C. Temperatures in excess of 2000°C are possible.

This equipment was employed for sintering or melting of small titanium samples as well as for thermal reactions.

When larger amounts of monoxide were required, the vacuum thermal reactor was scaled up to produce TiO in 100 g lots. The components were the same, except that the diffusion pump was eliminated. A quartz tube furnace with lampblack insulation was used. The graphite crucible was $1\frac{3}{4}$ in. ID by 7 in. high and was molybdenum-lined to eliminate TiC formation. The rest of the vacuum line was composed

of welded steel fittings. An ultimate vacuum of $10–15\mu$ was used and temperatures to 2500°C were possible.

Electrolytic Cells

Two sizes of cells have been utilized in this work, but both are of similar design. One has a 100 g salt capacity and the other a 2250 g capacity. The cell has several specific functions: (a) be capable of temperatures to 1000°C; (b) provide an inert air free atmosphere; (c) be resistant to chlorine and salt corrosion; and (d) provide for d-c electrodes.

Graphite is the principle material of construction being used for the entire interior of the cell including a crucible container for the melt. A steel outer shell is used but this is protected against chlorine by an insulating layer of calcined lampblack. A graphite retaining inner shell holds the lampblack in place. A machined graphite resistance heating element is located just inside this shell. Water cooled external copper leads are employed to feed alternating current to the element. The graphite crucible fits inside the element, and rests on a graphite pedestal. This pedestal in turn rests on a nickel post welded through the bottom of the steel shell. This enables the crucible to serve as an anode. The top of the furnace is fitted with a removable head allowing insertion of the crucible. Holes are provided for admission of the cathode, charging of the salts, and observation. These are normally closed with graphite plugs. Argon is admitted through the bottom of the cell. A.C. power is supplied by a 7.5 kva transformer coupled with a variable voltage transformer. D-C power is furnished by a 400 amp motor generator. Argon used was 99.9% pure, but was further purified by passing through a P_2O_5 tower and a hot titanium sponge tower.

Cells of this type have been further described in a previous article (45).

Arc melting furnace.—A small arc melting unit was constructed in order to consolidate the metal powders produced for evaluation. A water cooled copper hearth anode is used with a water cooled tungsten tipped cathode. A Pyrex cylinder encloses the unit and is sealed against the copper with neoprene gaskets. A 400 amp motor generator powers the unit which can melt up to 50 g of titanium per melt. The cathode is silver soldered to a copper head through a bellows arrangement allowing flexibility; vacuum and argon inlets are also made through this head. Melting is done under about 200 mm of argon pressure.

PREPARATION OF TiO

Initially, TiO was prepared by a 1200°–1400°C solid-state reaction between the metal and dioxide.

This produces a very pure monoxide when the reaction is carried out under vacuum or argon.

$$Ti + TiO_2 \rightarrow 2TiO$$

After the process fundamentals were established other methods of preparation were investigated. Three successful reactions were found. It was prepared from titanium carbide by reaction with zinc or magnesium oxide and by direct carbon reduction of the dioxide. All were run under high vacuum to enable removal of by-product gases as rapidly as formed to prevent recombination with titanium. In all cases, reactants were mixed by micropulverizing and ball milling, and then compressed into pellets. Reactions were carried out in molybdenum-lined graphite vessels.

Zinc oxide and magnesium oxide react with the carbide nearly identically according to the reactions,

$$2ZnO + TiC \rightarrow \rightarrow \rightarrow TiO + 2Zn + CO$$

$$2MgO + TiC \rightarrow \rightarrow \rightarrow TiO + 2Mg + CO$$
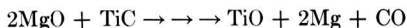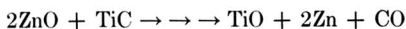
Zinc or magnesium starts to come off at about 900°C. The metal is collected in a special condensing trap between the furnace and pump. Evolution of metal and CO is complete at 1350°–1400°C. The reaction is stepwise, first going to Ti_2O_3. The first stage of the reaction accomplishes removal of all of the Zn or Mg and most of the CO.

$$5TiC + 10ZnO$$

$$\rightarrow \rightarrow \rightarrow 2Ti_2O_3 + TiC + 10Zn + 4CO$$

·A temperature of 1730°–1740°C is required for the sintering operation to insure complete reaction of the Ti_2O_3 in the second stage of the reaction.

$$2Ti_2O_3 + TiC \rightarrow \rightarrow \rightarrow 5TiO + CO$$
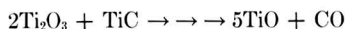
The TiO as produced by this method is a uniform golden yellow in color with a near lustrous characteristic of the crystals. Typical TiO ingots are illustrated in Fig. 1. It has a melting point of slightly more than 1775°C. When touched to a grinder, orange yellow sparks are emitted. A small amount of Ti_2O_3 present greatly reduces this sparking.

The exact pressure maintained in the system is not critical as long as it is substantially reduced and the atmosphere is free of air and moisture. Successful runs have been made where the pressure was never less than 1000 μ.

The mixtures employed were not strictly stoichiometric. Extra ZnO was added, e.g., to allow for its moisture content and to compensate for free carbon in the TiC. The TiC as received contains several per cent of iron. This is leached out with acid or ferrofiltered prior to mixing with the oxides.
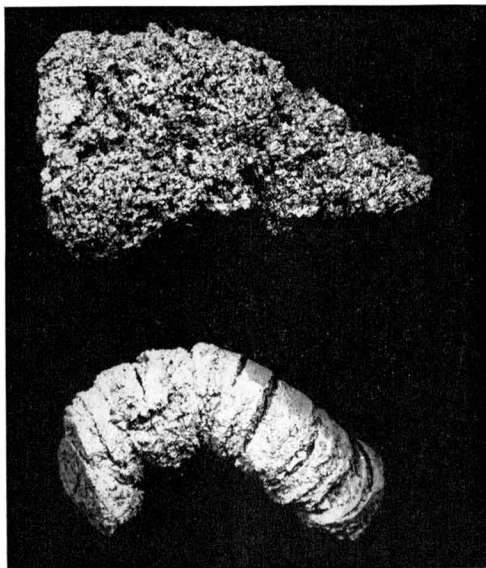

Fig. 1. Typical TiO ingots. Above, from tamped ZnO-TiC mix; below, pressed from ZnO-TiC mix

The sesquioxide may be prepared in like manner using a 2:5 ratio of TiC to ZnO or MgO.

These reactions are particularly attractive since only the product oxide remains in the crucible. Products so formed are of near theoretical composition, and low in all impurities.

The alternative thermal method is more direct, since the intermediate TiC formation is unnecessary.

$$TiO_2 + C \rightarrow TiO + CO$$
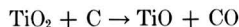
This reaction is carried out in the same manner and in the same equipment as the oxide-carbide reactions. It is run just under the melting point of TiO which is about 1750°C. This is also a stepwise reduction going through the Ti_2O_3 stage. High vacuum is essential to prevent reversal of the reaction.

Typical data for preparation of TiO by thermal reactions involving the reaction of TiC with zinc or magnesium oxides and reduction of TiO_2 with carbon is given in Table I.

A further alternative method for TiO preparation is attractive in light of the process for metal preparation. This is an electrolytic procedure involving electrolysis of TiO_2 dissolved in $CaCl_2$ under an inert atmosphere. At 1000°–1100°C, under 4–5 v, TiO is deposited cathodically from such a melt per the reaction

$$CaCl_2 + TiO_2 \rightarrow TiO + CaO + Cl_2$$
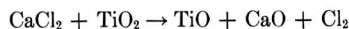
Melts consisting of 80 % $CaCl_2$ and 20 % TiO_2 have been used. The TiO deposits as a golden yellow crystalline mass interspersed with salts. It is re-

TABLE I. *Preparation of TiO by thermal reaction*

| Run No.	Furnace charge	Temp, °C	Time, min	Pressure Min	Pressure Max	Yield TiO %	Remarks
				μ	μ		
4447-1	28.3 g TiC 41.5 g MgO*	1400-1700	90	10	600	98.5	No Mg evolved after 45 min
4476-1	47 g TiC 41.5 g MgO*	1500-1700	90	10	700	98	
83-17	198 g TiC 256 g ZnO	RT-780 862-1100 1175-1200	43 142 138	150 3800 760	790 >5000 2800	ND†	P break 862°-heavy Zn reaction over 142 min
		RT-1590 1600-1730	52 39	100 5500	>5000 >5000	ND†	Sintering step
83-36	198 g TiC 256 g ZnO	RT-750 965-1075+	35 140	160 5000	1500 >5000	ND†	P break <965°-heavy Zn
		RT-1160 1160-1720	39 45	90 1900	570 >5000	ND†	Sintering step
83-82	5900 g TiO₂ 890 g C	RT-1115 1165-1540	57 206	170 1500	1700 >5000		Heavy gassing
		RT-1160 1160-1750	92 285	150 150	150 1000	84	Shrinkage noted
83-103	6000 g TiO₂ 900 g C	RT-1145 1150-1400	203 170	80 1900	4800 >5000		P break 925°, 99 min
		RT-950 1145-1520	100 220	50 40	170 1300	74	

* 91.8% MgO.
† Not determined.

TABLE II. *Electrolytic preparation of TiO*

Run No.	Electrolyte composition	Temp, °C	Time, min	E volts	Current density amp/dm²	Total amp hr	Current efficiency %	Total yield %
2286-D1	80% CaCl₂ 20% TiO₂	975-1050	45	5.0	200	20	48	97
2273-B1	80% CaCl₂ 20% TiO₂	1200-1250	15	7.5	400	12	ND	ND
2273-B2	80% CaCl₂ 20% TiO₂	1150-1200	30	6.5	300	20	46	95

covered by crushing the mass and washing in hot water and dilute HCl. The latter wash serves to remove any occluded CaO. Data for TiO₂ electrolysis are shown in Table II.

PREPARATION OF TITANIUM METAL

Titanium metal is produced from the monoxide by electrolysis in molten anhydrous CaCl₂. The over-all cell reaction is

$$CaCl_2 + TiO \rightarrow Ti + CaO + \overline{Cl_2}$$
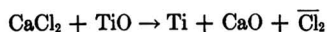
The exact mechanism of the process has not been conclusively demonstrated, but a number of facts and observations can be listed.

TiO is soluble only to about 0.5 % in CaCl₂, at 850°C. However, this would be sufficient to satisfy a reaction mechanism dependent upon the solubility factor. It is reasonably certain that the TiO solubility is a factor in this process, either chemically or electrically. As the process is carried out, the CaCl₂ is first melted and the TiO charged on top of the
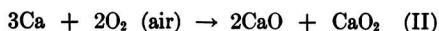
melt. The bulk of the TiO settles to the bottom becoming part of the anode.

A purification electrolysis is usually run prior to addition of TiO to further purify the $CaCl_2$. A graphite cathode is employed for this purpose. Any deposit is discarded.

The main electrolysis is carried out using a rod cathode of steel, molybdenum, titanium, or zirconium. The portion of the cathode above the bath level is protected from chlorine by a graphite sleeve. Electrolysis is run under 3–5 v at 850°–900°C using a current density of 200–500 amp/dm². A concentration of 5–10 wt% TiO is generally employed.

It is possible that the reaction is a two-step procedure, TiO going into solution as an ion, probably TiO^{2+}, and migrating to the cathode where it interacts with calcium metal produced there, which in turn reduces the titanium ion to metal. This explanation is somewhat justified by the following.

At the start of the electrolysis, a great deal of fuming takes place. This is largely CaO (from Ca metal vapor) with some CaO_2 and $TiCl_4$. Calcium is formed and floats on the bath surface, some of it volatilizing and oxidizing as it leaves the cell.

$$Ca^{2+} + 2e \rightarrow Ca \qquad (I)$$

$$3Ca + 2O_2 \text{ (air)} \rightarrow 2CaO + CaO_2 \qquad (II)$$

$$2CaCl_2 + 2TiO \rightarrow 2CaO + TiCl_4 + Ti \qquad (III)$$

After 10–15 min of electrolysis the process proceeds quietly and fuming ceases. If TiO is oxidized anodically, it can migrate to the cathode as an ion:

$$TiO \rightarrow \rightarrow TiO^{2+} + 2e \qquad (IV)$$
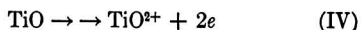
Calcium liberated at the cathode according to (I) can then reduce this ion.

$$Ca + TiO^{2+} + 2e \rightarrow CaO + Ti \qquad (V)$$
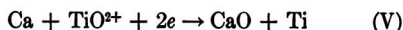
The lime so formed is not too soluble in $CaCl_2$ and much of this would precipitate out; such is found on the bath surface. As solubility permits, some is added to the electrolyte and broken down in preference to $CaCl_2$. Any oxygen so evolved would be liberated as CO at the anode.
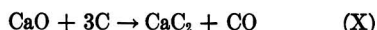
$$C + O^{2-} \rightarrow CO + 2e \qquad (VI)$$
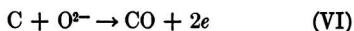
Chlorine must also evolve at the anode if Ca is produced.

$$2Cl^- \rightarrow Cl_2 + 2e \qquad (VII)$$

Certain side reactions take place to some extent causing some contamination. The most serious of these are carbide formation and liberation of free carbon.

$$TiO + 2C \rightarrow TiC + CO \qquad (VIII)$$
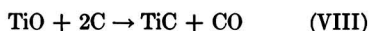
Lime or calcium may react with carbon to form CaC_2. Titanium oxide then can react with this CaC_2 producing further TiC impurity, or perhaps elemental carbon.
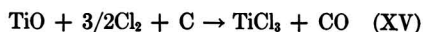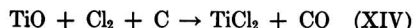
$$Ca + 2C \rightarrow CaC_2 \qquad (IX)$$

$$CaO + 3C \rightarrow CaC_2 + CO \qquad (X)$$

$$TiO + CaC_2 \rightarrow TiC + CaO + C \qquad (XI)$$

$$TiO + CaC_2 \rightarrow Ti + CaO + 2C \qquad (XII)$$

Calcium metal can also reduce CO, and this may occur to some extent.

$$3Ca + 2CO \rightarrow CaC_2 + 2CaO \qquad (XIII)$$

Any rechlorination of calcium or titanium will, of course, reduce the efficiency of the process.
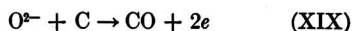
If this sort of mechanism prevails, then titanium is actually produced from a +4 valence change. All efficiencies are calculated on the basis of a divalent change however (0.8935 g/amp-hr).

It is frequently observed, particularly above 900°C, that very little chlorine is evolved from the cell for the amount of metal produced. This suggests that the above mechanism is not valid and that a straight electrolytic mechanism would prevail. This could involve a chlorination of the TiO at the anode to $TiCl_2$, $TiCl_3$, or both which is subsequently broken down electrolytically.

$$TiO + Cl_2 + C \rightarrow TiCl_2 + CO \qquad (XIV)$$

$$TiO + 3/2Cl_2 + C \rightarrow TiCl_3 + CO \qquad (XV)$$

$$Ti^{x+} + xe \rightarrow Ti \qquad (XVI)$$

This would then account for the excess Ca formed and subsequent CaC_2 and also the lack of chlorine evolution in many runs; it would also explain the formation of some $TiCl_4$ early in the run.

A third mechanism might involve ionization of TiO and a direct electrolysis to yield CO and Ti.

$$TiO \rightleftarrows Ti^{2+} + O^{2-} \qquad (XVII)$$

$$Ti^{2+} + 2e \rightarrow Ti \qquad (XVIII)$$

$$O^{2-} + C \rightarrow CO + 2e \qquad (XIX)$$
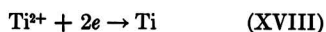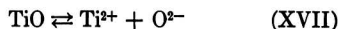
CO is evolved from the cell, but such a mechanism has little other evidence in its favor. The chlorination and Ca reduction mechanisms appear the most likely possibilities at present.

When the salt bath is exhausted of Ti, a voltage rise and current drop occur. A red flame is then detected at the cell vent indicating heavy calcium production. The cathode is withdrawn from the bath and the power shut down. The cathode is allowed to cool in the argon atmosphere and subsequently removed from the cell.

TABLE III. *Electrolysis of TiO in CaCl$_2$*

Run No.	TiO %	Pre-electrolysis		Electrolysis					Yield %	BHN arc-melted ingot	Remarks
		Volts	Amp hr	Temp, °C	Volts	Current density amp/dm^2	Amp hr	Current efficiency %			
61–23	8	1–2	9	880	4–6	200–450	288	51	88	—	
74–151	3.2	1.4–2	10	900	5.2–6.3	150–450	95	33	51	362	Run to end of fuming
75–182	4.2	1.3–1.8	1	885	7.3–6.4	250–300	166	40	79	382	
93–125	4.2	1.2–1.7	9	820	7.4–6.2	300	165	22	43	—	Low temperature

The cathode deposit is a cylindrical shaped mass of metal and salt particles. It is sponge-like in character and loosely adherent to the metal cathode rod. The deposit is gray in color and contains many metal agglomerates, but no well-defined large crystals. Such deposits are from 40–60 % metal.

The deposits are mechanically broken off the rod, crushed to −40 mesh, and washed in warm water to remove excess salts. An acid treatment in dilute HCl or HCOOH removes CaO. Final water washing removes the acid.

Typical data for the electrolysis of TiO—CaCl$_2$ baths are shown in Table III including power and efficiency figures. Fig. 2 illustrates the type of cathode deposit obtained.

As-recovered metal powder is largely +150 mesh.
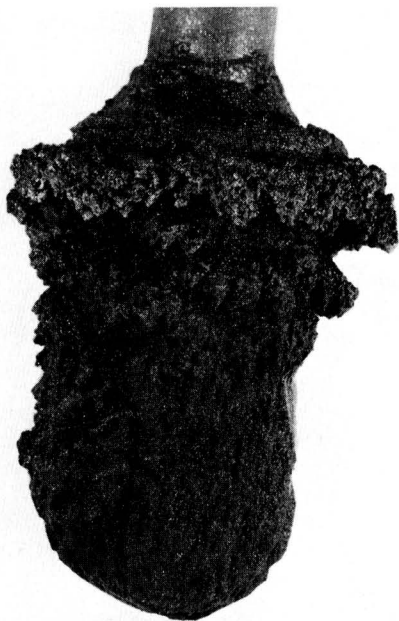
FIG. 2. Typical cathode deposit. Titanium produced by electrolysis of TiO in CaCl$_2$.

The material analyzes up to 99 % titanium, the balance being principally oxygen and carbon.

Consolidated arc melted pellets have shown a hardness range of 200–900 Vickers. They have averaged 300–400 Vickers which is outside the range of commercial titanium. The high hardness values are due principally to carbon and residual oxygen.

Decomposition Potentials of Titanium Oxides

As a supplement to this program, decomposition potentials of TiO and TiO$_2$ were determined in CaCl$_2$. This entailed a series of current-voltage curves using standard salt baths of TiO and TiO$_2$ in CaCl$_2$ as employed in the electrolytic TiO and metal preparations.

A small, 100 g inert atmosphere graphite resistance furnace was used as the cell. A selenium rectifier was coupled with a current voltage control for use as a d-c source. This unit can be set for a given current or voltage and will maintain such a setting on the cell regardless of resistance changes. A recorder is included in the circuit to plot temperature, current, or voltage. Measurements were made with AGR graphite electrodes. The regulator was set at voltages from 1–5 progressively. Currents corresponding to these settings are then recorded. On plotting such data as current density vs. voltage

FIG. 3. Decomposition potential measurements; 15% TiO in CaCl$_2$.

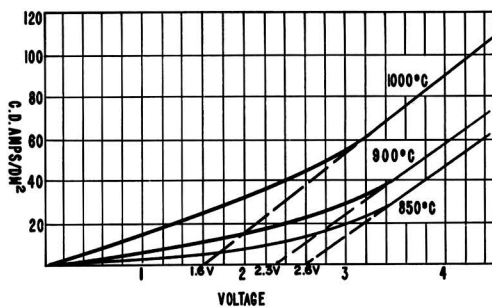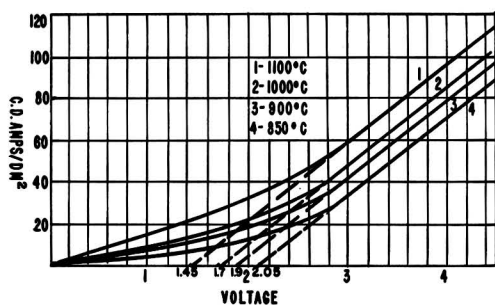FIG. 4. Decomposition potential measurement; 20% TiO₂ in CaCl₂.

and extrapolation to zero current, an approximate value of the decomposition voltage is obtained. Measurements were made using baths of 15% TiO and 20% TiO₂ at 850°, 900°, 1000°, and 1100°C. Results are shown in Fig. 3 and 4.

DISCUSSION

The effects of various factors on operation of and results from the process have been largely ascertained and are discussed below.

Reagents.—It has been demonstrated that high purity chemical reagents lead to better over-all results. It is not difficult to obtain high purity TiO, but the CaCl₂ is difficult to obtain in a pure dry state. Thus this material is thoroughly air-dried at 110°C for long periods prior to charging to the cell. Water is deleterious to the process since oxygen is anodically liberated on electrolysis, causing oxidation of the TiO. Small amounts of CaO are not harmful, since this is normally produced as a by-product in the electrolysis.

Despite oven drying of the CaCl₂, a low voltage pre-electrolysis of the molten salt gives off large amounts of H₂ and CO. This has been carried out routinely through all the work to obtain as anhydrous a bath as possible. In general, this pre-electrolytic cycle is run at 1–2 v for approximately 10 amp-hr. Gas evolution is noted at both electrodes; the effluent gases are primarily CO and H₂.

The use of the CaCl₂ electrolyte is reasonably specific for the process. A series of runs with varying bath compositions are reported in Table IV. In no case has an alkali metal halide resulted in a satisfactory run. The CaCl₂ bath may be mixed with LiCl up to 50 wt % and be run with reasonable success [74–16]. Similarly, KCl may be used up to 20–25% [74–20]. Presumably, other alkaline earth chlorides may be used if they are sufficiently anhydrous. Successful runs have been made with a good grade of BaCl₂ in 30–35% concentration with CaCl₂, but even BaCl₂ seems to have a deleterious

TABLE IV. *Electrolyte composition*

Run No.	Electrolyte composition %	Current efficiency	Yield %	Remarks
74–16	55% CaCl 45% LiCl	22	50	Bath vacuum melted
75–44	28% CaCl₂ 72% LiCl	—	—	No deposit
93–131	80% CaCl₂ 20% LiCl	10	16	
74–20	80% CaCl₂ 20% KCl	20	45	Bath vacuum melted
93–140	80% CaCl₂ 20% KCl	7	9	Bath vacuum melted
74–36	80% CaCl₂ 20% MgCl₂	—	—	No deposit
74–40	50% NaF 50% KF	—	—	Only Na produced
74–44	40% MgF₂ 60% CaF₂	—	—	Small deposit—not recovered
75–16	100% NaCl	—	—	No deposit—TiO not soluble
75–37	84% NaCl 16% CaCl₂		—	No deposit—many polarizations
75–40	65% CaCl₂ 35% NaCl	—	—	No deposit
75–199	90% CaCl₂ 10% CaF₂	7	14	Very poor deposit
93–17	55% CaCl₂ 45% BaCl₂	2	4	
93–128	68% CaCl₂ 32% BaCl₂	35	67	
93–27	60% CaCl₂ 40% Na₂CO₃	—	—	Na₂TiO₃ produced 131 g

effect if this concentration is exceeded (runs 93–17, 93–128). It is thought that MgCl₂ could be used if it were sufficiently pure; the grade used [74–36] was high in oxide and moisture content.

In no case has a successful run been obtained with fluoride present. Even the addition of 10% CaF₂ resulted in a gross reduction in efficiency and metal quality [75–199].

When alkali halides (NaCl, KCl) are substituted for CaCl₂ as an electrolyte, only the alkali metal is
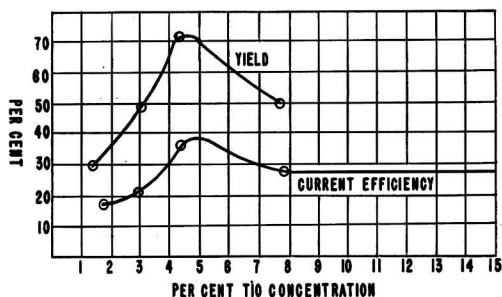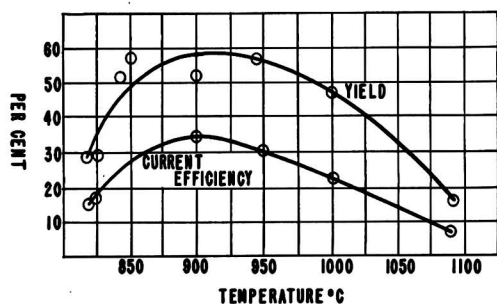
FIG. 5. Effect of TiO concentration

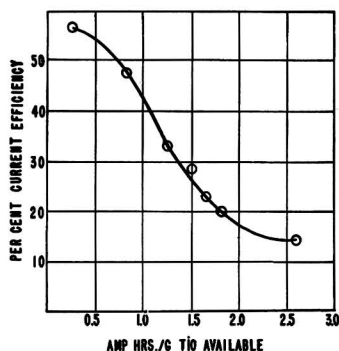FIG. 6. Effect of temperature on current efficiency and yield.

FIG. 7. Change in current efficiency with time of electrolysis.

TABLE V. *Variation of cathode current density*
$900° \pm 25°C$; 3.2% TiO bath

Run No.	Current density amp/dm²	Volts E	Current efficiency	Yield %	Remarks
74–14	600	10	—	—	Poor results
75–182	260–300	7.3–6.4	40	79	BHN 382
74–130	200	6.8–5.9	18	45	BHN 509
74–109	200	7.9–7	21	51	
74–104	120–130	5.4	8	18	

The rate of reaction is apparently governed largely by solubility of TiO in the melt and/or its interaction with the melt rather than initial concentration. The concentration effect is illustrated by Fig. 5.

Temperature.—The optimum salt bath temperature has been found to be about 900°C for the $CaCl_2$–TiO melt. At this point efficiency and metal recovery are at a maximum. The process is not operable at less than 800°C or above 1100°C. Runs of varying temperature are plotted as Fig. 6.

Time of electrolysis.—Reduction efficiency is at a maximum in the initial stages of a run. It falls off quite rapidly after about one-half the TiO has been utilized (5–6% bath). Thus, it is preferable to charge more TiO after a run is about half done rather than to attempt to exhaust the bath. The effect of time is demonstrated in Fig. 7 where current efficiency is plotted as a function of ampere hours/gram TiO input current. It is noted that this curve falls off rapidly after about 1 amp-hr/g.

Current density.—Current density and voltage may be varied to some extent and still yield satisfactory results. However, maximum efficiencies are obtained at about 300 amp/dm². Runs made at less than 150 or more than 500 amp/dm² are generally poor with respect to current efficiency. Voltages of 4–8 yield satisfactory results. Typical runs showing this variation are listed in Table V.

Metal Evaluation

As previously stated, titanium metal produced by electrolysis of TiO in $CaCl_2$ has not generally been acceptable by present purity standards. Its oxygen content is somewhat high and the carbon content is excessive. This is evidenced by the typical structures in Fig. 8 and 9. These are arc melted 10 g ingots electrolytically polished. The lattice-like structure is typical of high oxygen titanium and a large amount of carbide precipitation is evident at the grain boundaries. Carbon is a more serious contaminant than oxygen despite the nature of the source material.

The hardness of metal produced was generally in the range BHN 250–400. Arc melted ingots have been successfully hot rolled, but the sheet produced is

produced. The TiO remains inert and has been recovered in its original form after such runs.

Concentration of TiO.—TiO concentration has a profound effect on operation or efficiency of the electrolytic cell. Low concentrations of the order of 1–2 wt% are undesirable and result in lower efficiencies. There is apparently an optimum concentration of 4–5% TiO where maximum efficiency and recovery are obtained. At higher concentrations the total yield is reduced, possibly due to a cyclic reaction whereby metal produced reacts with available TiO or a halide intermediate.
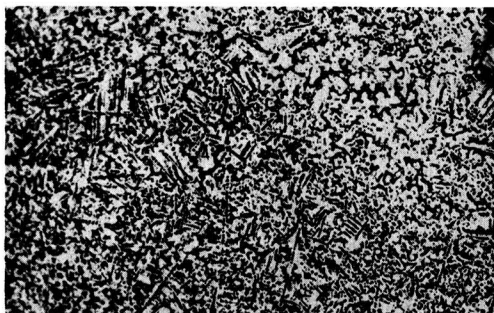
FIG. 8. As-cast titanium, showing dendritic structure of carbide phase. Lattice-like typical high oxygen titanium structure. Unetched. 100× before reduction for publication.
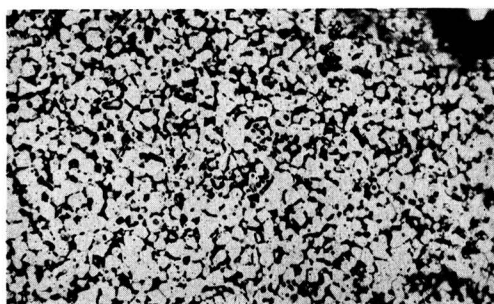

FIG. 9. Same as Fig. 8, but at 250X before reduction for publication, showing carbide precipitation at grain boundaries in detail.

TABLE VI. *Spectrographic analyses*

	Ti Metal 75-178	TiO 83-44
ZrO_2	0.07	0.20
TiO_2	Major	Major
SiO_2	0.50	0.35
Fe_2O_3	0.20	0.10
MgO	0.05	0.002
MnO	0.05	0.001
HfO_2	—	—
Al_2O_3	0.15	0.20
Cb_2O_5	0.05	0.05
MoO_3	0.001	0.003
V_2O_5	0.60	0.60
CaO	1.5	0.05
CuO	0.003	0.005
NiO	0.001	0.001
PbO	0.001*	0.001*
K_2O	0.001*	0.001*
Cr_2O_3	0.07	0.03
Na_2O	0.001*	0.001*
Li_2O	0.001*	0.001*
P_2O_5	0.02	0.02

* Less than.

Not detected: Co, B, Sb, As, Cd, Sn.

brittle. The metal in general runs from 96–98% titanium, 0.1–0.3% oxygen, and 1.5–3% carbon. Nitrogen and hydrogen contents are quite low, both <0.05%. Other impurities of some significance are Si, Fe, Al, V, and Ca. Of these, all but Ca presumably have their major source in the TiO and could be reduced by improvement in the purity of the TiO. Table VI shows spectrographic analyses of a lot of TiO and metal prepared from it. The relationship and carry-over of impurities is quite evident.

CONCLUSIONS

A process has been developed whereby titanium metal of moderate purity may be electrolytically produced from its monoxide. The process at present is not suitable for preparation of commercially pure titanium, but suitable modifications in cell design and operational procedures may enable further improvement in the process.

The exact mechanism by which the reduction proceeds is not known. It is known that TiO is soluble in $CaCl_2$ to a small extent, whereas it is not soluble in NaCl which likewise will not function as an electrolyte. Thus, the process apparently depends on this factor at least to some extent.

The loosely packed sponge-like cathode deposits suggest that the titanium may be the result of a secondary reaction, i.e., reduction of a titanium ion by calcium metal. Calcium metal has been found in deposits and salt baths on occasion. The production of CaC_2 as a side reaction is also suggestive of this type of mechanism. The fact that process efficiency is essentially nil above 1100°C is further evidence, since calcium boils at about 1200°C.

Alternatively, the process may be electrolytic in nature whereby Ti^{2+} ions are cathodically reduced. The fact that titanium is found in a cathode mass and not dispersed throughout the bath seems to indicate this. Calcium metal is liquid at the operating temperature and is found in areas of the cell other than the cathode. The fact that very little Cl_2 is produced at higher temperatures is also support for this mechanism. Gas evolution is primarily CO under these conditions.

The most complete phase of this work is in the methods developed for producing TiO. Any of the four methods described, with the possible exception of the electrolytic procedure, are well defined and could be commercially adapted to production of TiO in pure form. The reaction mechanism and operating characteristics of the thermal reactions are well worked out.

Even though pure titanium has not been produced from TiO, it has been shown that minimum oxygen products can be produced. A revised cell type to overcome the carbon contamination prob-

lem conceivably could enable the successful validation of this process.

ACKNOWLEDGMENT

Any discussion of this paper will appear in a Discussion Section to be published in the December 1955 JOURNAL.

REFERENCES

1. N. N. GRATSIANSKII AND A. P. VOVKOGON, *Zapiski Inst. Khem. Akad. Nauk U.R.S.R.*, **7**, 173 (1940).
2. M. HAISSINSKY AND H. EMMANUEL-ZAVIZZIANO, *Compt. rend.*, **204**, 759 (1937).
3. M. HAISSINSKY AND H. EMMANUEL-ZAVIZZIANO, *J. chim phys.*, **34**, 641 (1937).
4. E. POKORNY AND K. SCHNEIDER (I. G. Farbenind, A.-G.), German Pat. 582,528, April 22, 1934; 605,551, Nov. 13, 1934.
5. R. H. LEUTZ, German Pat. 741,670, Sept. 30, 1943.
6. G. J. MOUNDRITCH, "Contribution to the Study of the Coating of Iron with Titanium," Part II, ScD. Thesis, University of Nancy, France (1931).
7. B. DIETHELM AND F. FORSTER, *Z. physik. Chem.*, **62**, 129 (1908).
8. A. S. RUSSELL, *Nature*, **127**, 273 (1931).
9. H. BOZON AND A. BOZON, *Bull. Soc. Chim.*, **18**, 917 (1951).
10. D. B. KEYES AND S. SWANN, *Univ. Illinois Bull. Eng. Exp. Station Bull. Ser.*, No. 206, **23**, 13 (1930).
11. A. TRAVERS, *Chimie & industrie*, Special No. 347 (1932).
12. R. GROVES AND A. S. RUSSELL, *J. Chem. Soc.*, **1931**, 2805.
13. J. L. ANDRIEUX, *J. four elec.*, **57**, 26 (1948).
14. J. L. ANDRIEUX, *Rev. met.*, **45**, 49 (1948).
15. R. KEENEY, *Elec. J.*, **17**, 206 (1920).
16. N. S. SPENCE, *Canadian Mining Met. Bull.*, **44**, 21 (1951).
17. G. GIN, *Trans. Am. Electrochem. Soc.*, **11**, 291 (1907).
18. Y. HAYAKAWA, *J. Electrochem. Assoc. Japan*, **15**, 64 (1947).
19. H. FISCHER AND K. DORSCH (Siemens and Halske, A.-G.), German Pat. 615,951, July 16, 1935.
20. W. HUPPERTZ, *Electrochem. and Met. Ind.*, **3**, 35 (1905).
21. J. KONIGSBERG AND J. SHILLER, *Physik. Z.*, **9**, 347 (1908).
22. M. DODERO, *Compt. rend.*, **208**, 799 (1939).
23. S. I. SKLYARENKO, Y. M. LIPKES, et al., *Zhur. Priklad. Khim.*, **13**, 51 (1940).
24. Shawinigan Water and Power Co., British Pat. 678,807, May 11, 1951.
25. G. D. P. CORDNER AND H. W. WORNER, *Australian J. Appl. Sci.*, **2**, 358 (1951).
26. A. BRENNER AND S. SENDEROFF, *This Journal*, **99**, 223C (1952).
27. Electrolytic Titanium, *Chem. Eng.*, **59**, 103 (1952).
28. M. A. STEINBERG, M. E. SIBERT, S. S. CARLTON, AND E. WAINER, to be published in this Journal.
29. P. BERTHIER, *Ann. chim. et phys.*, **7**, 84 (1843).
30. A. LAUGIER, *ibid.*, **89**, 306, 317 (1814).
31. H. MOISSAN, *Compt. rend.*, **120**, 290 (1895); **115**, 1034 (1892); *Ann. chim. et phys.*, **9**, 229 (1896); **4**, 136 (1895); *Bull. Soc. Chim.*, **9**, 957 (1892).
32. C. M. KERSTEN, *Pogg. Ann.*, **50**, 313 (1840); *J. Prakt. Chem.*, **20**, 373 (1840).
33. H. ROSE, *Pogg. Ann.*, **61**, 513 (1844).
34. C. WINKLER, *Ber.*, **23**, 2642 (1890).
35. T. KOENIG AND O. VON DER PFORDTEN, *ibid.*, **22**, 1485 (1889).
36. C. W. CARSTENS, *Z. Krist.*, **67**, 260 (1928); Kongelige Norske Videnskabers Selskabs, Det, Forhandlinger, 1926–28, No. 20, 56 (1929).
37. E. NEWBERRY AND J. N. PRING, *Proc. Roy. Soc.*, **A92**, 276 (1916).
38. M. BILLY, *Ann. chim. Paris*, **16**, 5 (1921).
39. H. BRÄKKEN, *Z. Krist.*, **67**, 547 (1928).
40. L. R. BRANTLEY AND A. O. BECKMANN, *J. Am. Chem. Soc.*, **52**, 3956 (1930).
41. E. JUNKER, *Z. anorg. u. allgem. Chem.*, **228**, 97 (1936).
42. W. DAWIHL AND K. SCHROETER, *ibid.*, **233**, 178 (1937).
43. Gmelin's Handbuch der Anorganischen Chemie, Vol. 8, p. 220, Verlag. Chemie, GMBH, Weinheim/Bergstrasse (1951).
44. W. G. GULDNER AND A. L. BEACH, *Ind. Eng. Chem., Anal. Ed.*, **22**, 366 (1950).
45. M. A. STEINBERG, M. E. SIBERT, AND E. WAINER, *This Journal*, **101**, 63 (1954).

The Electrochemistry of Some Nonaqueous Solutions of Alkali Metal Salts[1]

Harry C. Mandell, Jr.,[2] Wallace M. McNabb, and J. Fred Hazel

Department of Chemistry, University of Pennsylvania, Philadelphia, Pennsylvania

ABSTRACT

Conductivities of lithium chloride and bromide and potassium iodide and thiocyanate in pyridine have been redetermined and results are in good agreement with literature values. Previously unreported conductivities of lithium iodide dihydrate in pyridine, lithium chloride, bromide, and iodide dihydrate in quinoline, and lithium iodide dihydrate and potassium iodide and bromide in nitrobenzene have been determined.

The decomposition potential of lithium chloride in pyridine has been redetermined in agreement with an earlier worker. Original determinations were made of decomposition potentials of lithium bromide and iodide dihydrate in pyridine and in quinoline, and of potassium iodide and lithium iodide dihydrate in nitrobenzene. The decomposition potential of potassium thiocyanate in pyridine was found to be different than that recorded in the literature. The decomposition potential of potassium iodide in pyridine was not reproducible.

Using a platinum cathode, it was shown that it is possible to electrodeposit lithium from its bromide and iodide dihydrate in pyridine and quinoline and from its iodide dihydrate in nitrobenzene. In contradiction to results published by others, deposition of potassium from its iodide and thiocyanate in pyridine was accomplished. Metal deposits were all amorphous in gross appearance and were probably impure. These methods hold little promise of value as commercial means for alkali metal production.

INTRODUCTION

As early as 1897 conductances of lithium chloride, potassium iodide, and potassium thiocyanate in pyridine were studied. Laszczynski and Gorski (1) deposited lithium in a black crust from this solvent. A gray deposit from the potassium thiocyanate solution seemed to be potassium mixed with potassium sulfide. No decomposition potentials were given for this work. Kahlenberg (2) reported the plating out of lithium from its chloride in pyridine. Patten and Mott (3) gave the decomposition potential for this system as 4.0 v. Lithium has also been deposited from its iodide in pyridine (4).

Muller and coworkers (5) plated lithium from lithium chloride in pyridine above 4.05 v and from the nitrate above 5.0 v. Solutions of sodium iodide, nitrate, and potassium thiocyanate in pyridine were said to deposit the metals only when a mercury cathode was used. Potassium thiocyanate had decomposition potentials of 1.8 and 2.6 v on platinum. With regard to the electrolysis of potassium thiocyanate in pyridine, there is disagreement between the results of Laszczynski and Muller.

Lithium, sodium, and potassium have been deposited from solutions of their halides plus aluminum halides in nitrobenzene (6–8). There is no report of the electrolysis of alkali halides alone in nitrobenzene. The only recorded deposition of a metal from quinoline solution is silver from silver nitrate (9).

EXPERIMENTAL

Apparatus

The cell (Fig. 1) was $1\frac{1}{4}$ in. in diameter and 3 in. high. A loose fitting Plexiglass cover carried removable electrodes used for electrolyses and fixed electrodes for conductance measurements. All electrodes and connecting wires were of bright platinum. The area of the electrodes was 1 cm² each.

A glass encased stirring bar was used in the cell. The magnetic stirring motor was enclosed in a water-tight can, and the entire assembly was immersed in a constant temperature bath held at $25° \pm 0.05°C$.

The cell constant was determined using 0.001, 0.010, and 0.100N potassium chloride solutions. It was found to be 0.400 ± 0.001. There was no appreciable polarization effect on the bright platinum electrodes up to specific conductance values of 1.6 millimhos.

The power sources were 6 v wet storage batteries and a 125 v d-c line. Potentiometers were used to
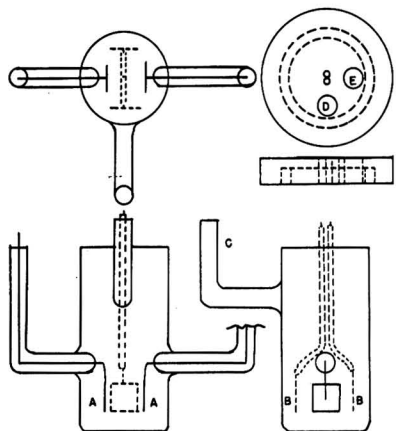
FIG. 1. Electrolysis cell and cover. (A) Fixed conductance electrodes; (B) removable electrolysis electrodes; (C) gas admission side arm; (D) burette tip admission hole; (E) thermometer admission hole.

obtain intermediate values of voltage. The current was measured with the 1.2 and 12 μa ranges of a Triplett multimeter. Voltages were determined with a 0–15 v Simpson meter which had three extended ranges made by placing empirically cut resistances in series with it.

Conductances were determined with a Serfass RCM 15 model bridge. By placing a one megohm precision resistor in parallel with the test leads of the bridge, its range was extended from 10^6 to 10^8 ohms.

Reagents

Nitrobenzene.—Eastman Kodak White label nitrobenzene was stored over anhydrous potassium carbonate for one week. It was decanted and distilled under dry nitrogen, a 1.5° fraction being collected. This was redistilled in vacuo, the fraction boiling 55°–57°C at 0.5 mm of mercury being collected. The specific conductivity was 4×10^{-8} mho.

Other portions of nitrobenzene were stored over phosphorus pentoxide for two weeks. These were distilled twice under dry nitrogen at atmospheric pressure. Fractions collected boiled over 0.5° to 1.0°C ranges. The specific conductivity was also 4×10^{-8} mho.

Pyridine.—Baker and Adamson reagent pyridine was stored over pellet potassium hydroxide for ten weeks. This was decanted and distilled under dry nitrogen. A central fraction boiling over 1.5°C was collected and redistilled under nitrogen. A portion boiling 114.5°–115.5°C was kept and found to have a specific conductivity of 4×10^{-7} mho.

Quinoline.—Paragon Division (Matheson Company) quinoline was dried and distilled in the same manner as was pyridine. From the second distillation a 2°C fraction was collected and found to have a specific conductivity of 2×10^{-8} mho.

Potassium bromide, potassium iodide, lithium chloride.—These Baker analytical reagents were pulverized and stored at 140°C.

Lithium bromide monohydrate.—Merck N.F. salt was recrystallized from water then heated to 175°C. The salt melted and then solidified. The solid was pulverized and stored at 175°C. According to Mellor (10) this salt is anhydrous above 159°C.

Lithium iodide trihydrate.—Merck. The salt was recrystallized from water. Attempted dehydration by simple heating led to obvious decomposition. The salt was stored over phosphorus pentoxide in a vacuum desiccator for two months. A sample of the resulting material was weighed out and treated with excess sulfuric acid. Evaporation and ignition converted it to the sulfate. Calculation from the weight of sulfate produced indicated that the salt resulting after desiccation was lithium iodide dihydrate.

Potassium thiocyanate.—Baker reagent salt was recrystallized from absolute alcohol and dried 18 hr at 95°C. It was stored over phosphorus pentoxide in a vacuum desiccator.

Procedure

The thoroughly dried cell and cover were placed in the constant temperature bath. Nitrogen was dried by passing it through saturated potassium hydroxide solution, anhydrous magnesium perchlorate, and phosphorus pentoxide. A brisk stream of the dry gas was passed through the side arm of the cell for at least 15 min. The salt to be studied was added swiftly from a weighed vial while the cover of the cell was raised. A measured volume (about 30 ml) of solvent was added from a buret through a hole in the cover.

The electrolysis electrodes were raised from the solution and the conductance was determined with the fixed conductance electrodes. The electrolysis electrodes were returned to their normal position and connected to the power supply. Five minutes after the voltage was applied, the current passing was noted, and a new, higher voltage was applied. In most cases, 0.5 v steps were taken. After a sufficiently complete polarization curve had been obtained, prolonged electrolysis was carried out to obtain a characteristic cathode deposit.

RESULTS

Results are presented in Tables I to III. The straight portion of the current vs. voltage curve for each system was extrapolated to zero current and

TABLE I. *Electrochemical studies in pyridine at 25°C*

Run	Solute	Conc. m/l	Spec. cond. $\times 10^6$ mho	Molar cond.	Dec. pot. v	Cathode current density amp/dm^2	Cathode product
1	LiBr	0.178	372.0	2.09	4.00	0.33	Lithium
2	LiCl	0.284	99.6	0.351	4.00	0.17	Yellow slime
3	LiI·2H$_2$O	0.534	6520.0	12.2	3.90	0.50	Lithium
4	KI	Sat.	181.0	—	5.40	0.50	Pot. and sludge
5	KI	Sat.	186.0	—	1.95	0.93	Pot. and sludge
6	KI	Sat.	210.0	—	1.90	0.44	Pot. and sludge
					5.40	—	
7	KI	Sat.	206.0	—	1.50	0.43	Brown sludge
8	KI	Sat.	208.0	—	1.50	0.29	Brown sludge
9	KCNS	0.2185	1440.0	6.59	3.70	0.32	Potassium
10	KCNS	0.205	1344.0	6.56	3.65	0.84	Potassium
11a	KCNS	0.1132	840.0	7.42	3.70	0.58	Potassium
11b	KCNS	0.1132	876.0	7.73	3.70	0.59	Potassium
12	KCNS	0.1327	944.0	7.12	3.65	0.54	Potassium

TABLE II. *Electrochemical studies in quinoline at 25°C*

Run	Solute	Conc. m/l	Spec. cond. $\times 10^6$ mho	Molar cond.	Dec. pot. v	Cathode current density amp/dm^2	Cathode product
13	LiBr	Sat.	5.20	—	3.4	0.038	Lithium
14	LiI·2H$_2$O	Sat.	588.0	—	3.45	0.10	Lithium
15	LiCl	Sat.	0.40	—	—	—	—
15a	LiCl	Sat.					
	LiI·2H$_2$O	ca 0.1	184.0	—	3.40	0.22	Lithium

TABLE III. *Electrochemical studies in nitrobenzene at 25°C*

Run	Solute	Conc. m/l	Spec. cond. $\times 10^6$ mho	Molar cond.	Dec. pot., v	Cathode current density amp/dm^2	Cathode product
16	KBr	Sat.	0.36	—	—	—	—
17	KI	Sat.	6.80	—	1.80	0.11	Brown sludge
18	LiI·2H$_2$O	Sat.	88.0	—	2.50	0.34	Lithium

the corresponding voltage was taken as the decomposition potential.

Concentrations are expressed in moles of solute per liter of solvent. For dilute solutions this is almost identical to molarity, and these concentration values were used in computing molar conductances.

The current density at which prolonged electrolysis was carried out was calculated using the apparent cathode area of 2 cm^2 (both sides of the electrode). The voltages necessary to obtain these currents were, of course, mostly a function of the resistance of the solution. For systems of low conductivity, up to 115 v were applied.

Lithium deposits were all smooth and dull and ranged from dark gray to black in color. The potassium deposits were light gray in color and were characterized by extensive treeing and nugget formation on the edges of the cathode. All deposits appeared amorphous and were probably impure. There was never any discernible crystalline nature.

Deposits of both metals were completely adherent and did not peel or flake off the cathode.

Lithium and potassium deposited from pyridine were quickly and completely converted to metal oxide (or hydroxide) upon exposure to the air. In a few cases, the potassium reacted rapidly enough as the solvent (pyridine) evaporated to produce a small burst of flame.

Lithium and potassium produced by electrolysis were identified by the fact that the deposits dissolved vigorously in water with gas evolution. In some cases, an explosive flash of flame was observed. Characteristic flame tests were obtained with a platinum wire dipped in the water solution of the deposit. These tests were negative when no cathode product was observed.

The specific conductivity of lithium bromide was in good agreemene with the value 375 micromhos which is obtained for that concentration by the authors' interpolation in Anderson's work (11).

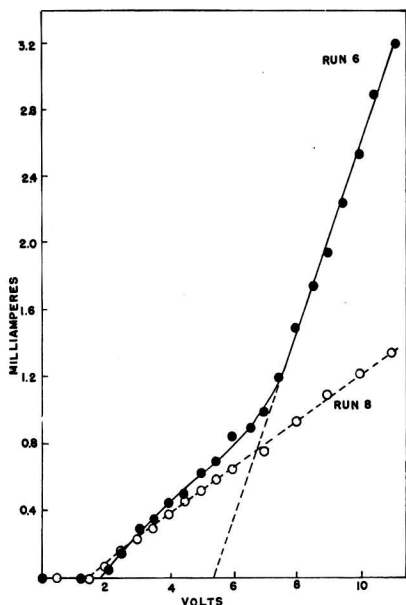The specific conudctivity of lithium chloride

FIG. 2. Decomposition curve for KI in pyridine. Curve A, Run 6, Table I; Curve B, Run 8, Table I.

compared only fairly well with the value 88×10^{-6} mhos obtained by interpolation in the literature values of Anderson (11). The decomposition potential found was identical to that reported by others. Since only small currents were passed, it is reasonable to assume that the failure to deposit lithium was due to its reacting with the solvent as it deposited slowly. Emmert (12) has described the reaction of lithium with pyridine.

The iodide dihydrate of lithium was employed since it was the lowest hydrate of the iodide readily obtainable. The deposition of the metal from this system containing, molewise, twice as much water as lithium ion, was an unexpected result. The implication is that the extreme precautions taken to insure anhydrous conditions may not be necessary for the deposition of lithium. Others who have worked with lithium iodide in pyridine do not give the details of solute preparation. Anderson dried lithium iodide trihydrate by "constant heating." Since the hydrate he used is unknown, comparison of conductivities is not very meaningful. Von Hevesy (4) reported depositing lithium from its "iodide" in pyridine, but gave no decomposition potential or details concerning the solute.

The literature value for the conductivity of a saturated solution of potassium iodide in pyridine is 210×10^{-6} mhos (13). In runs 4 and 5 where the observed values were significantly lower, the fault was undoubtedly in allowing insufficient time for

solubility equilibrium. The solubility of potassium iodide in pyridine is 0.25 g/100 ml of solution at 10°C (17).

As is seen from Table I there was difficulty in reproducing the electrolysis of potassium iodide in pyridine. In runs 4, 5, and 6 the cathode products were gray nuggets mixed with brown sludge. These deposits dissolved explosively in water with a burst of flame and certainly seemed to contain metallic potassium. The polarization curves for runs 4–6 varied in shape for the region 2–6 v giving breaks at 1.9 and/or 5.4 v. Fig. 2 compares polarization curves for runs 6 (typical of runs 4–6) and 8 (typical of 7 and 8). Note that they were essentially the same up to 7 applied volts, whereupon run 6 displayed a rise in potential and potassium nuggets began to appear on the cathode. The cathodic product in runs 7 and 8 was only a brown sludge appearing after prolonged electrolysis. The same results were obtained by Patten and Mott (3). Part of the difficulty here was probably due to the relatively low conductivity of the system. Such a solution would be expected to be proportionately more sensitive to the effects of traces of impurities. This may not be the full reason for the lack of reproducibility.

The values of conductances for potassium thiocyanate in pyridine in runs 9 and 10 were in agreement with a smooth extrapolation of the data of Anderson (11). The values for runs 11 and 12 agreed
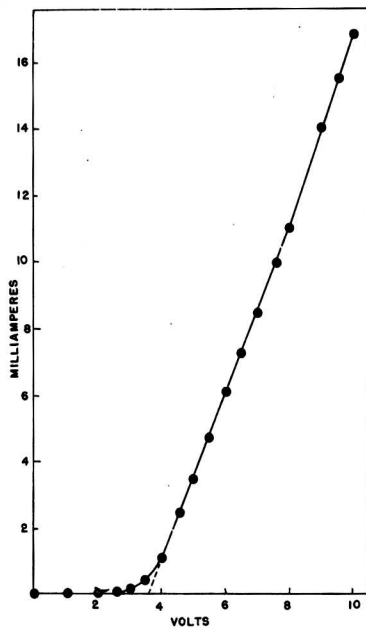

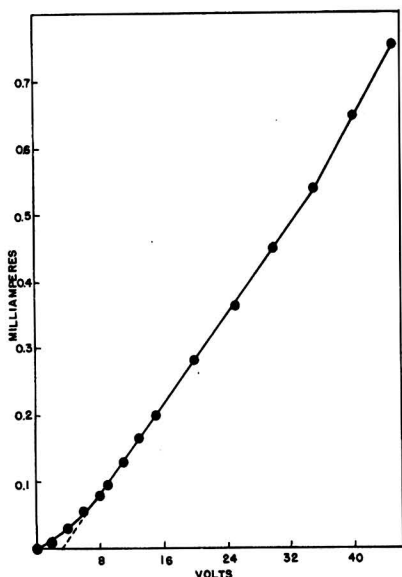FIG. 3. Decomposition curve for KCNS in pyridine
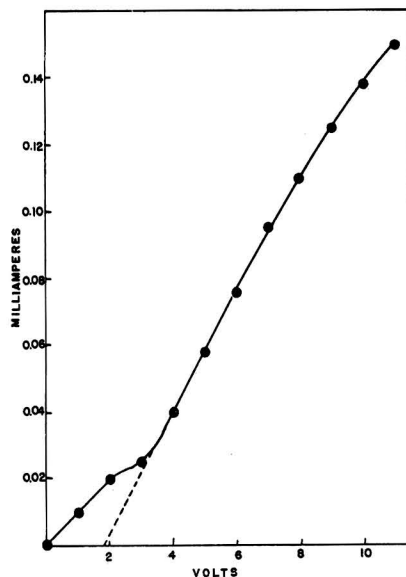
FIG. 4. Decomposition curve for LiBr in quinoline

FIG. 5. Decomposition curve for KI in nitrobenzene

well with the values 840 and 950 $\times$ 10^{-6} mhos obtained by interpolation in Anderson's work.

The deposition of potassium on a platinum cathode confirms the observation of early workers (4, 15). The decomposition potential (Fig. 3) and the deposition of potassium observed are contradictory to the results presented by Muller (5).

The conductivity of lithium bromide in quinoline (Table II and Fig. 4) was so low that it was necessary to carry out electrolysis at 115 v for an hour to obtain an appreciable deposit. The concentration of saturated lithium iodide dihydrate in quinoline was about 0.26M.

Although the solubility of lithium chloride in quinoline is reported to be appreciable [0.3538 g/ 100 g quinoline (16)], the conductivity was too low to carry out electrolysis.

The conductivity of potassium bromide in nitrobenzene was too low to carry out electrolysis.

In run 17 (Fig. 5) a trace only of brown deposit appeared on the cathode. It dissolved in water, but the amount was too small to permit identification. Walden (14) reported the solubility of potassium iodide in nitrobenzene as 0.0019 g/100 ml solvent at 25°C.

Dawson and Jackson (18) report forming polyiodides of potassium in nitrobenzene by simple mixing of potassium iodide and iodine. These were more soluble and much more highly dissociated than the simple iodide. Therefore, as the electrolysis of potassium iodide proceeded and free iodine (presumably) was liberated at the anode, a great increase

in conductivity was anticipated. This was observed. After one hour of electrolysis at 120 v, the specific conductivity rose from 6.8 to 41.2 micromhos.

The solution in run 18 was pale yellow immediately upon mixing, suggesting a chemical reaction. It has been reported (19) that the compound lithium iodide:nitrobenzene exists as yellow crystals, and this may have been the source of the color. The deposit on the cathode above 2.5 v was black in color. Above 11 v it became lighter gray.

DISCUSSION

The salts employed in all runs were weighed to the nearest 0.2 mg, liquids measured to the nearest 0.02 ml. Thus, concentrations were known with better than 1% accuracy. The error inherent in the conductance measuring system was 1%. Conductivity values, then, were known to ±1%.

The voltmeter used in finding decomposition potentials was accurate to 2%. It was read to the nearest 0.05 v. The ammeter also was accurate to 2%. For most cases, the 0–12 ma scale was used and readings were to the nearest 0.05 ma. In poorly conducting systems the 0–1.2 ma scale was used, and it was read to 0.005 ma.

Since the accuracy and precision of the ammeter and voltmeter used were constant, there was greater precision of decomposition potential determination in systems of higher conductivity. When the conductivity was high, the break in the polarization curve at the decomposition potential was a sharper one.

Another factor may have decreased the accuracy and precision of conductance and polarization measurements in solutions of low conductivity. Traces of impurity in the solute and solvent would have greater effect on the observed results when the initial conductivity was low.

As an estimate of precision, the standard deviation of the decomposition potential was calculated for a typical well conducting system. Results of 5 separate determinations of decomposition potential were used. It must be remembered that for cases of lower conductivity the standard deviation was undoubtedly greater.

For potassium thiocyanate in pyridine $\sigma = 0.024$ v.

Standard Deviation

$$\sigma = \sqrt{\frac{\sum d_a^2}{n}}$$

Where $d_a = x - a$ and $a = \frac{\sum x}{n}$ (20).

Any discussion of this paper will appear in a Discussion Section to be published in the December 1955 JOURNAL.

REFERENCES

1. St. v. Laszczynski and St. v. Gorski, *Z. Elektrochem.*, **4**, 290 (1897).
2. L. Kahlenberg, *J. Phys. Chem.*, **3**, 602 (1899).
3. H. E. Patten and W. R. Mott, *J. Phys. Chem.*, **12**, 49 (1908).
4. G. von Hevesy, *Z. Elektrochem.*, **16**, 672 (1910).
5. R. Muller, F. Holzl, A. Pontoni, and O. Wintersteiner, *Monatsh.*, **43**, 419 (1922).
6. V. A. Plotnikov and E. Ya. Gorenbein, *J. Gen. Chem. (U.S.S.R.)*, **7**, 372 (1937).
7. S. I. Yakubson, *J. Phys. Chem. (U.S.S.R.)*, **21**, 343 (1947).
8. S. I. Yakubson and M. A. Abramova, *C.A.*, **47**, 7348 (1953); *Ukrain. Khim. Zhur.*, **15**, 362 (1949).
9. R. Muller, E. Pinter, and K. Prett, *Monatsh.*, **45**, 525 (1925).
10. J. W. Mellor, "Comprehensive Treatise on Inorganic and Theoretical Chemistry," Vol. II, p. 582, Longmans, Green and Co., London (1922).
11. E. X. Anderson, *J. Phys. Chem.*, **19**, 753 (1915).
12. B. Emmert, *Ber.*, **49**, 1060 (1916).
13. L. F. Audrieth and J. Kleinberg, "Non-Aqueous Solvents," p. 125, J. Wiley & Sons, Inc., New York (1953).
14. P. Walden, *Z. phys. Chem.*, **55**, 709 (1906).
15. M. G. Levi and M. Voghera, *Gazz. Chim. Ital.*, **35**, 277 (1905).
16. J. H. Walton and C. R. Wise, *J. Am. Chem. Soc.*, **44**, 103 (1922).
17. P. Walden, "Electrochemie Nichtwasseriger Losungunen," p. 470, J. A. Barth (1924).
18. H. M. Dawson and C. G. Jackson, *J. Chem. Soc.*, **93**, 2063 (1908).
19. H. M. Dawson and E. E. Goodson, *ibid.*, **85**, 796 (1904).
20. T. B. Crumpler and J. H. Yoe, "Chemical Computations and Errors," p. 132, J. Wiley & Sons, Inc., New York (1940).

Conductance of Lithium Bromide at Low Concentrations in Methanol within the Temperature Range 20° to −50°C[1]

Paul G. Sears, Robert L. McNeer,[2] and Lyle R. Dawson

Department of Chemistry, University of Kentucky, Lexington, Kentucky

ABSTRACT

The conductance of lithium bromide in methanol has been determined over the temperature range 20° to −50°C for several concentrations ranging from 4×10^{-4} to $1 \times 10^{-1}N$. Limiting equivalent conductances were obtained by extrapolation of Λ_0' vs. C plots. Fair agreement was found to exist between the experimental and the theoretical conductance behavior of lithium bromide in dilute methanol solutions. A plot of the logarithm of the limiting equivalent conductance in methanol as a function of the reciprocal of the absolute temperature over the range 20° to −50°C was found to be linear and to have the same slope as several corresponding plots constructed from experimental data for low concentrations.

INTRODUCTION

This investigation represents a part of a broad program, being carried out in this laboratory, concerned with the conductance of nonaqueous solutions at low temperatures. The objective of the investigation reported here has been to determine the conductance behavior of lithium bromide in dilute methanol solutions and to compare the observed behavior with that theoretically predicted by the Onsager equation (1). Methanol is a low-freezing hydroxylic solvent for which dielectric constant data are available at low temperatures. Lithium bromide was selected primarily because of its pronounced solubility in this solvent.

EXPERIMENTAL

Absolute methanol ("Baker Analyzed" reagent) was refluxed several hours over calcium oxide prior to fractionation through an efficient column. The middle fractions, which were retained, had conductivities of approximately 1×10^{-6} ohm^{-1} cm^{-1}. Anhydrous lithium bromide was obtained from A. D. Mackay, Inc. Triplicate potentiometric titrations performed on a Fisher titrimeter using a standardized silver nitrate solution showed the lithium bromide to be 99.3% pure. Because of a trace of material (assumed to be lithium oxide) in the lithium bromide which was insoluble in methanol, the weight of the salt used was multiplied by 0.993 to determine the actual quantity of lithium bromide. Solutions were prepared by the weight dilution of concentrated stock solutions. Appro-priate buoyancy corrections were applied. All transfers were made in a dry box and other precautions were observed throughout the experimental procedure in an attempt to ensure that the solutions remained anhydrous.

The resistances of the solutions contained in the conductance cells were measured with a Jones bridge (2) manufactured by the Leeds and Northrup Company. Resistances greater than 30,000 ohms were measured in parallel with 30,000 ohms of shunted bridge resistance, and the series cell resistance was computed from the measured parallel resistance. Confirmatory determinations by independent workers using the Jones and Bradshaw method (3) showed the two Washburn conductance cells employed to have constants of 2.075 and 2.206 cm^{-1} at 25°C. It was assumed that the change in a cell constant is negligible over the temperature range studied. This assumption is supported by calculations of changes in cell measurements expected to result from temperature changes.

The temperature of solutions in the conductance cells was maintained constant to within 0.3 degree during determinations by a manually controlled thermostat consisting of a clear 1 gal Dewar flask filled with denatured alcohol. The bath liquid was cooled by the addition of powdered Dry Ice and agitated effectively by a motor-driven stirrer. Temperatures in all cases were measured with total-immersion thermometers which are periodically compared with thermometers calibrated by the National Bureau of Standards. The estimated uncertainties of the conductance data range from 0.5% at 20° to 1.0% at −50°C. The conductivity of the lithium bromide was obtained by subtracting the conductivity of the solvent from that of the solution.

[2] Present address: Carbide and Carbon Chemical Company, Charleston, West Virginia.

TABLE I. *Equivalent conductance of lithium bromide in methanol*

(a) 20°C		(b) 10°C		(c) 0°C		(d) −10°C		(e) −20°C		(f) −30°C		(g) −40°C		(h) −50°C	
$C \times 10^4$	Λ	$C \times 10^4$	Λ	$C \times 10^4$	Λ	$C \times 10^4$	Λ	$C \times 10^4$	Λ	$C \times 10^4$	Λ	$C \times 10^4$	Λ	$C \times 10^4$	Λ
918	50.3	929	43.8	940	37.8	951	32.2	962	26.9	973	22.1	984	17.8	995	14.0
382	60.2	387	51.9	391	44.6	396	38.1	401	31.9	405	26.3	410	21.3	414	16.8
197	65.2	199	56.7	202	48.7	204	41.6	207	34.8	209	28.7	211	23.2	214	18.3
91.8	70.8	92.9	61.5	94.0	52.8	95.1	44.9	96.2	37.7	97.3	31.1	98.4	25.1	99.5	20.1
57.5	73.8	58.2	63.9	58.8	54.8	59.5	46.6	60.2	39.1	60.9	32.2	61.6	26.0	62.3	20.4
37.0	75.5	37.4	65.3	37.9	56.1	38.3	47.7	38.7	39.8	39.2	32.8	39.6	26.5	40.1	21.0
8.98	82.1	9.09	70.8	9.20	60.6	9.31	51.6	9.42	43.0	9.52	35.7	9.63	28.5	9.74	22.5
6.39	83.1	6.46	71.7	6.54	61.6	6.62	52.5	6.69	43.7	6.77	36.2	6.85	29.0	6.92	22.9
4.09	84.7	4.14	73.2	4.19	62.6	4.24	53.2	4.29	44.4	4.34	36.4	4.39	29.3	4.44	23.2

RESULTS

Values of the equivalent conductance, Λ, and the concentration in gram equivalents of lithium bromide per liter of methanol solution, C, are presented in Table I.

DISCUSSION

Plots of the equivalent conductance of lithium bromide in methanol vs. the square root of the concentration may be found in Fig. 1. Owing to the curvature of these plots at low concentrations, accurate extrapolations to infinite dilution were unobtainable. Hence, recourse to another method for determining Λ_0 was necessary.

The Onsager equation, which may be written in the following form for a uni-univalent electrolyte,

$$\Lambda = \Lambda_0 - [A + B\Lambda_0]\sqrt{C}$$

where

$$A = \frac{82.42}{(DT)^{1/2}\eta}$$

$$B = \frac{8.203 \times 10^5}{(DT)^{3/2}}$$

in which D and η are the dielectric constant and viscosity of the solvent, can be rearranged into the form suggested by Shedlovsky (4)

$$\Lambda_0 = \frac{\Lambda + A\sqrt{C}}{1 - B\sqrt{C}}$$

which permits the computation of Λ_0 directly from the Λ values and the Onsager constants, A and B. Λ_0 values calculated by this method are usually designated as Λ_0' to differentiate them from the true limiting conductance. In the concentration range in which Onsager's equation holds, Λ_0' is equal to Λ_0; under other conditions Λ_0' varies with concentration. Shedlovsky found that for many salts Λ_0' varied linearly with concentration, or

$$\Lambda_0' = \Lambda_0 + aC$$

where a is a constant. This equation describes the conductance of many strong uni-univalent electrolytes in water to 0.1N. Fig. 2 shows plots of

Λ_0' vs. C for lithium bromide in methanol at various temperatures. It may be observed that all of the graphs are very similar and appear to be merely displaced at various magnitudes along the ordinate. While these plots are not exactly linear and cannot be analytically extrapolated, smooth-curve extrapolations across a short distance should yield fairly accurate values for the limiting equivalent conductance. According to Baker and Kraus (5), $\Lambda_0' - C$ plots which show a slight minimum are rather common and the conductance of such systems can be expressed by an equation of the form proposed by Onsager and Fuoss (6),

$$\Lambda_0 = \Lambda_0' + aC + bC \log C$$

where a and b are constants. The concentration at which the minimum occurs may be designated as C_{min} and another concentration, C^*, which is equal to 2.7 C_{min}, represents the concentration at which the terms aC and $bC \log C$ are of equal magnitude
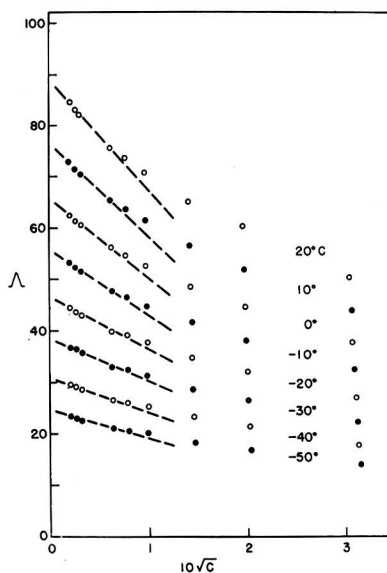

FIG. 1. Kohlrausch plots for lithium bromide in methanol. Dashed lines represent theoretical slopes.
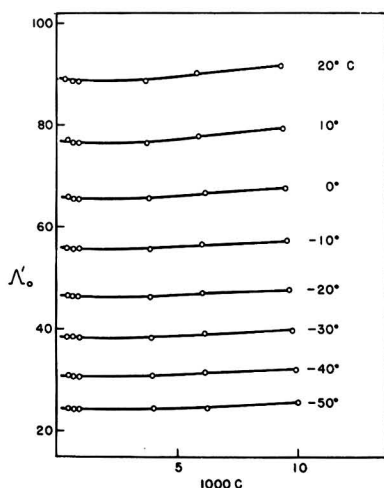
FIG. 2. Plots of Λ_0' as a function of concentration of lithium bromide.
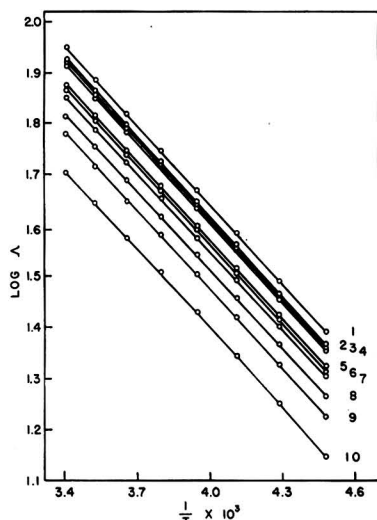

FIG. 3. Temperature dependence of the logarithm of the equivalent conductance of lithium bromide at concentrations expressed as molality $\times 10^4$. (1) 0.00; (2) 5.17; (3) 8.07; (4) 11.3; (5) 46.7; (6) 72.6; (7) 116; (8) 249; (9) 483; (10) 1160.

TABLE II. *Dielectric constant (7; 8) and viscosity (9) data for methanol and the limiting equivalent conductance and Walden product for lithium bromide in methanol at temperatures with the range 20° to −50°C*

°C	D	$\eta \times 10^3$ (poise)	Λ_0 (ohm^{-1} cm^2)	$\Lambda_0\eta_0$
20	33.7	5.81	89.1	0.518
10	35.6	6.76	76.9	0.520
0	37.5	7.94	65.9	0.523
−10	39.6	9.41	56.0	0.527
−20	41.8	11.31	46.7	0.528
−30	44.0	13.81	38.6	0.533
−40	46.2	17.17	30.9	0.531
−50	48.5	21.89	24.6	0.538

viscosity are probably very closely related in this system; however, the general trend of the product which decreases with increasing temperature is evidence that the temperature coefficient of viscosity is decreasing more rapidly than the temperature coefficient of conductance is increasing.

Utilizing the Λ_0 values in Table II, theoretical slopes at the various temperatures were calculated and drawn in Fig. 1. It may be observed from this figure that in dilute solutions the experimental points coincide very well with the theoretical slope.

Fig. 3 shows plots of the logarithm of the equivalent conductance vs. the reciprocal of the absolute temperature for various molal concentrations of lithium bromide in methanol. Examination of this figure reveals that all of the plots have identical slopes within experimental error. Points on plot 1 represent the Λ_0 values which are listed in Table II. An extrapolation of plot 1 in Fig. 3 to the $1/T$ value for 25°C permits the estimation of a Λ_0 value for lithium bromide in methanol which may be compared with existing data in the literature for that temperature. The authors' value of 96.0 ohm^{-1} cm^2 obtained in this manner compares favorably with 96.4 ohm^{-1} cm^2 which is the sum of the ionic conductances of the lithium and the bromide ions at 25°C reported by Gordon (10).

Any discussion of this paper will appear in a Discussion Section to be published in the December 1955 JOURNAL.

REFERENCES

1. L. ONSAGER, *Physik. Z.*, **27**, 388 (1926); **28**, 277 (1927).
2. P. H. DIKE, *Rev. Sci. Instruments*, **2**, 379 (1931).
3. G. JONES AND B. C. BRADSHAW, *J. Am. Chem. Soc.*, **55**, 1780 (1933).
4. T. SHEDLOVSKY, *ibid.*, **54**, 1405 (1932).
5. E. G. BAKER AND C. A. KRAUS, *Proc. Nat. Acad. Sci.*, **37**, 726 (1951).
6. L. ONSAGER AND R. M. FUOSS, *J. Phys. Chem.*, **36**, 2689 (1932).
7. A. A. MARYOTT AND E. R. SMITH, National Bureau of Standards Circular 514, August 10, 1951.
8. "International Critical Tables," Vol. VI, p. 83.
9. P. G. SEARS, F. J. SHELL, AND L. W. DAWSON, Unpublished data.
10. R. E. JERVIS, D. R. MUIR, J. P. BUTLER, AND A. R. GORDON, *J. Am. Chem. Soc.*, **75**, 2855 (1953).

but of opposite sign, making Λ_0' equal to Λ_0. In Fig. 2, C_{min} appears between 0.0015 and 0.0020N, and the Λ_0' values at approximately 0.005N are very nearly equal to the corresponding extrapolated Λ_0 values. Limiting equivalent conductances obtained from these graphs are listed in Table II. Listed also in Table II are dielectric constant and viscosity data used in the calculation of the Onsager constants and the Walden products, that is, the products of the limiting equivalent conductance and the viscosity of the solvent. The approximate constancy of the Walden products indicates that conductance and

Technical Note

Potentiometric Study of Bimetallic Electrodes in Corrosive Solutions[1]

M. G. FOUAD

Department of Chemical Technology, Faculty of Engineering, Alexandria University, Alexandria, Egypt

Potentials of zinc, zinc-copper composite electrodes and amalgamated zinc electrodes dissolving in hydrochloric acid solutions of zinc chloride were measured. Zinc-copper composite electrodes were made by plating copper on a portion of the zinc surface. The results shown below can be explained on the basis of the electrochemical theory of corrosion (1).

The reducing potential (e) of each system was calculated by subtracting the observed emf, E', of the cell $H_2/HCl(M)$, Hg_2Cl_2/Hg. Values of E' were obtained by interpolation of the results of various authors (2). The rate of dissolution of amalgamated zinc in acids is extremely small (3) and as the emf of systems of the type Zn-Hg $ZnCl_2$, HCl were found to be reproducible within 1 mv and independent of stirring, it is reasonable to suppose that emf values measured in such systems are reversible values (4).

RESULTS

Zinc-Copper Composite Electrodes

I. [ZnCl$_2$] constant

Ratio of areas Zn:Cu 10:1

(a) N-HCl-0.2M-ZnCl$_2$

	E.v.	E'v.	(e)v.
Zinc	1.055	0.278	−0.777
Copper	1.053	0.278	−0.775

(b) 0.3N-HCl-0.2M-ZnCl$_2$

Zinc	1.086	0.342	−0.744
Copper	1.085	0.342	−0.743

(c) 0.1N-HCl-0.2M-ZnCl$_2$

Zinc	1.109	0.396	−0.713
Copper	1.108	0.396	−0.712

II. *Change of* [ZnCl$_2$]

0.3N-HCl-0.02M-ZnCl$_2$

Zinc	1.086	0.342	−0.744
Copper	1.085	0.342	−0.743

III. *Change of areas of copper*

0.3 N-HCl-0.2M-ZnCl$_2$

	E.v.	E'v.	(e)v.
(a) Zn:Cu 2:3			
Zinc	1.078	0.342	−0.736
Copper	1.067	0.342	−0.725
(b) Zn:Cu 2:1			
Zinc	1.078	0.342	−0.736
Copper	1.067	0.342	−0.729
(c) Zn:Cu ∞:1			
Zinc	1.082	0.342	−0.740
Copper	1.081	0.342	−0.739

Pure and Amalgamated Zinc

(a) N-HCl-0.2M-ZnCl$_2$

(Zinc in the composite electrode)	1.055	0.278	−0.777
Pure zinc	1.062	0.278	−0.784
Amalgamated zinc	1.075	0.278	−0.797

(b) 0.3 N-HCl-0.2M-ZnCl$_2$

(Zinc in the composite electrode)	1.086	0.342	−0.744
Pure zinc	1.086	0.342	−0.744
Amalgamated zinc	1.096	0.342	−0.754

All emf values recorded were independent of rate of stirring.

Any discussion of this paper will appear in a Discussion Section to be published in the December 1955 JOURNAL.

REFERENCES

1. cf. U. R. EVANS, "Metallic Corrosion, Passivity and Protection", p. 5, 8, 256, etc., Edward Arnold Co., London (1946).
2. J. H. ELLIS, *J. Am. Chem. Soc.*, **33**, 737 (1916); G. A. LINHART, *ibid.*, **39**, 2601 (1917); M. RANDALL AND G. F. BRECKENRIDGE, *ibid.*, **49**, 1435 (1927).
3. R. VONDRACEK AND J. ISAK-KRIZKO, *Rec. trav. Chim.*, **44**, 376 (1925).
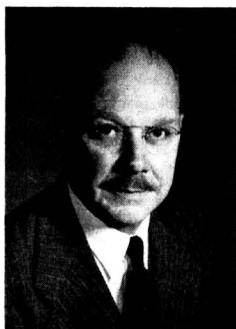4. R. LUTHER, quoted in *Chem. Rev.*, **1**, 394 (1925).

News Notes in the Electrochemical Field

Lighton Heads New Research Division

C. F. Norberg, president, The Electric Storage Battery Company, has announced the creation of a new research division on the corporate level and expansion of the company's research activities under direction of Dr. L. E. Lighton, vice-president.

L. E. LIGHTON

Research for all company divisions will be separated from development engineering and will be carried on in a new center located at the site of the battery manufacturer's Crescentville Plant, Rising Sun and Adams Aves., in Northeast Philadelphia.

Dr. Lighton's division has been assigned to work toward improvement of present lines and methods and to do basic research on future requirements for storage battery power.

Simultaneously, Dr. Lighton was appointed chairman of a research committee to review, determine action, and assign priorities to research projects coming from any of the company's divisions and subsidiaries. Members of the committee are the directors of engineering of the automotive and industrial divisions. Mr. Norberg is a member of the committee, *ex officio.*

Dr. Lighton has been vice-president in charge of engineering of The Electric Storage Battery Company since 1945. He joined the company in 1920 as a sales engineer in the Detroit (Mich.)

branch and was transferred to Philadelphia in 1925 as manager of automotive manufacturers sales. In 1935 he was moved to the engineering department and in 1940 became assistant manager, advancing to engineering manager later that year.

"Chemical Who's Who"

The beginning of the compilation of the 4th edition of "Chemical Who's Who" is announced by the editors, Dr. W. S. Downs and Williams Haynes, Lewis Historical Publishing Co., 265 W. 14th St., New York 11, N. Y. Qualifications for representation under three groups have been established in consultation with an advisory committee chosen from these three divisions of the chemical field, and are as follows:

Scientific. Graduates of colleges or schools of recognized standing, with at least ten years of activity in their specialties.

Educational. Graduates of colleges or schools of recognized standing, with the rank of full professor in colleges or schools of like standing, who have taught chemical subjects for at least ten years, at least five of which have been spent in responsible charge of a major chemical course in such colleges or schools.

Industrial and Business. Ten years of service, with present rank as officer, or head of department, branch office, or plant, of an organization of the chemical industry.

(Military assignments will have proper consideration in the above groups. Upon recommendation by competent authority covering special accomplishment by an individual, the above may apply only in part.)

The editors plan a coverage of the chemical field in this edition that will place this reference volume on the level of its sister publication, "Who's Who in Engineering," and request the prompt cooperation of those receiving invitations to supply personal data. There is no obligation, actual or implied; space

or listing in this volume cannot be purchased.

Crane Co. Celebrates Centennial Year

A chronology of product development by Crane Co., Chicago, now celebrating its centennial year, is much more than an impressive record of business expansion, a list of achievement, or a story of financial success. It is an industrial backdrop for the history of the United States . . . a panoramic view of productive progress . . . a study in sociology and standards of living . . . a long list of ideas, theories, and dreams that have become reality.

Today, Crane is the largest producer of valves and fittings in the world. The company is also engaged in the manufacture and distribution of fabricated piping and piping accessories, plumbing fixtures, plumbing brass trim, heating equipment, kitchen cabinets, and accessory equipment for aircraft.

But on July 4, 1855, when Richard Teller Crane first opened his foundry, a one-room frame building that he put up himself, his only product was brass couplings and copper tips for lightning rods, articles then in great demand. By 1856, Mr. Crane was turning out engine trimmings and finished brass goods, having been put into that business by an order from P. W. Gates & Co., builders of freight cars, stationary and portable engines, saw mills, and similar equipment. He must have filled their orders well and promptly because Gates & Co. gave him all their brass casting business. Crane Co. had a substantial start.

With what had grown quickly into one of Chicago's best plants, Richard Teller Crane and his brother Charles, who had joined the firm, decided in 1857 to take up the jobbing of wrought iron pipe and to enter the steam heating field. Years later Mr. Crane recalled that this decision was made because the company was feeling the first rumblings of the expansion that were to reoccur so

frequently in the years ahead. As he phrased it in his autobiography: "The decision was probably made because the firm felt it had the ability to conduct a larger business than was afforded by the limited demand in the west for the articles the company was manufacturing." It was an important step. In 1858 the company was awarded its first big job, the steam heating contract for the Cook County courthouse in Chicago. This job accomplished several things: It catapulted Crane into its future main business of making valves; it boosted the company over the financial panic of 1857–1861; it enhanced the company's public reputation, and it lifted Crane into a leading position in the steam heating business.

In 1861, after the outbreak of the war between the States, the government placed large contracts for infantry and cavalry equipment with Chicago saddlery makers—and Crane began to do a great deal of the work, making brass fittings, spurs, and stirrups. Later, as Crane's general business improved, the line was dropped. Charles Crane, who had been an iron foundryman and machinist before joining his brother, was still interested in that type of business, and in 1862, when the company's consumption of iron castings had become a large item, an iron foundry was built. Now the company began producing steam pumps, jobbing machine work, and increasing the variety of iron pipe products.

In 1863, Crane began the manufacture of machinery, primarily for the company's own use. Production was on a larger scale in 1864 and 1865 with sales to other firms. After that, sales were discontinued. Expansion accelerated by 1865 and decisions to branch out came rapidly. A new plant was built and the company began producing cast iron and malleable fittings, engines, steam pumps, shafting, pulleys, and wrought iron radiators. Fire hydrants and ventilating fans were added to the Crane lines in 1866; in 1867 came factory freight elevators; in 1870, blast furnace hoists. In 1872, the elevator business had grown and Crane Co. added a line of steam passenger elevators.

The company retired from the steam warming business in 1874—to avoid competition with its own customers—for sales of supplies to the steam-fitting trade had become large. In 1887, Mr. Crane obtained a patent for a non-heat hand wheel, the first of its type to be used on valves, and began producing the product. In 1889 came cast-iron

sectional radiators. Until 1890, the demand for fittings had continued along practically the same lines. The chief change was in the gradual increase in sizes and varieties.

But the period from 1890 until 1910 was one of extraordinary growth, one of the most important phases in Crane Co. history. It was the opening of the age of electricity and for the resultant bigger engines and turbines, with their intense heat and higher pressures, special valves and fittings were needed. To fill the need, Crane added to its already impressive product list: pop safety valves, drainage fittings, ammonia fittings, steam and oil separators, and a great variety of special valves.

The company began manufacturing air brake repair parts in 1891 and by 1893 supplied a full line of railroad air brakes. The line was abandoned in the United States in 1893, and Crane joined Westinghouse in manufacturing this and other lines in Russia.

With demand for Crane products high, the elevator business was sold in 1895. It was a choice of specializing in the valve and fitting business, rather than branching out too far afield.

Crane added the products for which it is probably best known to the consumer—plumbing fixtures, jobbed to exact specifications—in 1895. From 1913 to 1916 came new Crane Co. valves: the Y pattern stop check valve, the plug-type disk valve, and the union bonnet brass glove valve with composition disk. Crane began the manufacture of its own plumbing fixtures in 1921, and in 1923 it pioneered colored bathroom fixtures. The company entered the residential heating field in 1928 and brought out radiant baseboard heating in 1942.

During the years of World War II, Crane produced heavily for the armed services, with products ranging from gun barrel liners to valves for submarines, and earned an enviable production record while doing so. Crane, through it subsidiary, Hydro-Aire, began manufacturing aircraft accessories in 1951. In 1952, Crane entered the air conditioning field.

Next to be added to the list is titanium, both mining and manufacturing, with a new plant operated by Cramet, Inc., another Crane Co. subsidiary, due for dedication in 1955. After that will come new products for a new kind of industry and only the future can determine what Crane Co. will produce in its second hundred years. But a look at the past list indicates that

the products will be important, integral parts of American progress and America's way of living, for such production and contribution is the continuous story of Crane during the first hundred years.

C.I.T.C.E.

The seventh annual meeting of the International Committee of Electrochemical Thermodynamics and Kinetics (C.I.T.C.E.) will take place at Lindau (Lake Constance, West Germany) on July 29 to 31, 1955, immediately after the Zurich meeting of the International Union of Pure and Applied Chemistry. This year's meeting of the C.I.T.C.E. will be restricted to the work of the Commissions and Study Groups, with a small number of contributed papers pertaining to the work of these Commissions and Study Groups. These are: commission 1—electrochemical equilibria and potential-pH diagrams; commission 2—electrochemical nomenclature and definitions; commission 3—electrochemical experimental methods; study group 1—corrosion and its prevention; study group 2—cells and storage batteries; study group 3 (in process of formation)—semiconductors.

Information concerning the meeting can be obtained from Professor E. Lange, national secretary of C.I.T.C.E. for West Germany, University of Erlangen, Erlangen, or from Professor P. Van Rysselberghe, past president of C.I.T.C.E. and national secretary for the U. S., University of Oregon, Eugene, Oreg. Other officers are: T. P. Hoar, Cambridge University, president; and R. Piontelli, Politecnico of Milan; M. Pourbaix, University of Brussels; and G. Valensi, University of Poitiers—vice-presidents. M. Pourbaix is also secretary general-treasurer and E. Lange is also vice-president, these six persons constituting the C.I.T.C.E. Board.

A total of 22 countries are now represented in a membership of about 120.

C.I.T.C.E. Study Group No. 2

There has been created within the International Committee of Electrochemical Thermodynamics and Kinetics a study group dealing with current research work on the interpretation of the fundamental physical chemical phenomena occurring at electrodes in cells and storage batteries. Membership in this group is open to all C.I.T.C.E. members whose research activities are directed toward these areas of electrochemistry.

Each member consents to bring to the group the experimental and theoretical results of his own research work and of that of his collaborators. In no case will the group be concerned with problems pertaining to technical fabrication processes or methods. Each member of the group agrees to contribute actively and effectively to the program of study; no one will be accepted as a mere observer.

The results of the group's work on any particular problem will be the object of a report which will be communicated only to the members of the study group. However, the group may decide to proceed with the publication of such reports, either through the C.I.T.C.E. or through specialized journals of various countries. This publication will take place under the joint authorship of all members of the group, appropriate mention being made of the results brought about by individual members on the basis of their own work.

The present members of this study group are: F. Bäcklin, Uppsala, Sweden; E. Blomgren, Uppsala, Sweden; J. P. Brenet, Chairman, Paris, France; B. Forsén, Uppsala, Sweden; K. Nagel, Erlangen, Germany; M. Pourbaix, Brussels, Belgium; R. Thirsk, Newcastle, England; and A. U. Trägårdh, Stockholm, Sweden.

Information on C.I.T.C.E. activities can be obtained from the following: the Secretary General-Treasurer, Dr. M. Pourbaix, 50 avenue F. D. Roosevelt, Brussels, Belgium; the National Secretaries (for the U. S., Dr. P. Van Rysselberghe, University of Oregon, Eugene, Oreg.); the Chairman of Study Group No. 2, Dr. J. P. Brenet, 9 rue d'Artois, Paris 8, France.

Pennsalt Subsidiary to Develop Fluorspar Resources

The Pennsylvania Salt Manufacturing Company, Philadelphia, has incorporated a new, wholly owned subsidiary for the development of extensive fluorspar resources in western Kentucky. Chartered as the Calvert City Chemical Company, this organization will develop a new mine and expand existing milling and flotation facilities to meet growing requirements for acid grade spar used in the production of hydrofluoric acid and other fluorine chemicals at its Calvert City Works.

Construction, already begun under the direction of the company's central engineering staff, is scheduled for completion later this year. Operations of the

new mining-milling unit will be integrated with the activities of the Calvert City Works. Lamont West, presently in charge of the flotation plant, has been named superintendent.

Nuclear Research Reactor

The American Machine & Foundry Company has completed plans for the building of the first nuclear reactor to be owned and operated by private industry for research in industrial and humanitarian fields, it has been announced by General Walter Bedell Smith, vice chairman of AMF's Board of Directors.

A number of leading industrial concerns have been invited to participate in the program on a cooperative basis. Meetings to implement the program are now in progress. In addition to building the reactor, AMF will be one of the participants in the program, which, under the new Atomic Energy Act, will require licensing by the Atomic Energy Commission. Each company will be represented on a board of directors which will establish policy for the operation of the reactor facility. Participating companies will be from the electronics, petroleum, food, pharmaceutical, chemical, ceramics, rubber, metals, textile, agricultural, machinery, and other industries.

The first reactor and its supporting laboratory facilities will cost between 1 and 1½ million dollars and can be constructed and available for use within 18 months. It is planned that the facility will be built in the New York area on a site of approximately 250 acres.

Recently it was announced that AMF was awarded a contract by Battelle Memorial Institute, Columbus, Ohio, for the design, engineering, and construction of a nuclear research reactor. The reactor will be a key component in a research center Battelle is building 15 miles west of downtown Columbus.

The reactor proposed for the Industrial Research Facility will be of a design already proven by operating experience and will have the anticipated flexibility required to conduct a wide variety of work. It will be a solid-fuel type employing a core similar to that in the Materials Testing Reactor at the National Reactor Testing Station in Idaho. This type research system is the only one which has successfully operated at the high flux levels required for industrial development work. The design concept of the AMF-built reactor would be one of "unitization." This concept permits the standardization of certain

components resulting in ease of construction and prevents early obsolescence.

The Industrial Reactor Research Facility will make possible research investigations in materials, sterilization and pasteurization of foods, radiation, chemistry, biochemistry and biology, radioisotope production, medicine, physics, and reactor technology. The outstanding advantage of nuclear reactors as a research device is their capacity to handle relatively large volumes of experimental work, their ease of operation, and over-all flexibility.

Actively engaged in atomic energy development since the earliest days of the U. S. Atomic Energy program, AMF has designed and developed a variety of special atomic energy equipment. The company has been especially engaged in reactor design, and in the development and manufacture of reactor control and remote handling systems. AMF was one of the first companies to join, on an individual basis, the AEC Industrial Participation Program for the development of competitive nuclear power.

Colombia Laboratory Center

The first laboratory center in Colombia devoted specifically to technological research will be established in Bogota with the technical assistance of Armour Research Foundation of Illinois Institute of Technology, Chicago. The announcement was made by Dr. Haldon A. Leedy, director of the Foundation. Known as the Departamento de Investigaciones Tecnologicas, the new center will undertake research leading to developments in agriculture, industry, and mining in Colombia. Benefits of the research are to be turned over to the general public.

The center is sponsored by the quasi-official Colombian bank, the Caja de Credito Agrario, Industrial, y Minero de Colombia, which supplies a general banking and low-rate credit service throughout the country.

Paul B. W. Gollong, manager of Armour Research Foundation's international department, said the contract is for three years initially. The contract was signed by Dr. Pedro Navas Pardo, general manager of the Caja Agraria, and Dr. Leedy for the Foundation. Dr. Misael Pastrana, the Caja's agent in New York City, Dr. Joaquin Gutierrez, Colombian consul general, Chicago, and Mr. Gollong witnessed the signing at the Foundation.

The agreement calls for a field staff

consisting of a resident research advisor for three years, a resident engineer for two years, and several industrial research and development engineering specialists for one year. Dr. Paul J. Kolachov, who has been special advisor to the Foundation's biochemistry section since 1951, has been named resident advisor.

The first of three phases in the program will be an investigation of existing research installations to determine the direction of Colombian economic development. This will include technical personnel, equipment, and facilities that might be available to the new laboratories. Phase two will be concerned with organizing the structure of the laboratories and commencing the initial research and engineering work. Training of the staff in the fundamentals of practical technological research will comprise phase three of the program.

The Colombian laboratories will be the fourth technological installation to be established under Armour Research Foundation's overseas program. The others are the State Industrial Research Institute in Rangoon, Burma; the Foundrymen's Training Center at the Indian Institute of Technology in Kharagur, India; and the Instituto Mexicano de Investigaciones Tecnologicas in Mexico City.

The new center will assist in creating in Colombia a greater awareness of the value of technological research and engineering and of the part that laboratories can play in assisting economic development.

Monsanto Forms Product Sales Group

Establishment of a new product sales group to handle all surfactants, and the creation of a new section to coordinate sales of phosphate and surfactant products with the production effort in Monsanto Chemical Company's Inorganic Chemicals Division has been announced by Tom K. Smith, Jr., division director of marketing.

At the same time, Dr. Louis Fernandez, St. Louis, was named manager of surfactant sales, and Herbert W. Yeagley, St. Louis, was named manager, sales-production liaison.

The new coordinating section is being established to aid in the continuing improvement of service to customers for the division's various phosphate and surfactant products.

The new product group will handle such products as alkyl benzene, the various forms of Sterox and Santomerse, and other surface active agents manufactured by the division. Sales of sodium phosphates will remain in a product group under Thomas F. Gogan as product manager.

EJC Nuclear Congress

Engineers Joint Council has announced that 24 organizations, with a total membership of 250,000, will participate in the Nuclear Engineering and Science Congress in Cleveland, December 12–17, 1955. To date, 183 titles have been submitted covering the entire present range of developments in the peace-time applications of atomic energy.

The organizations thus far accepting invitations to participate are: American Society of Civil Engineers, American Institute of Mining and Metallurgical Engineers, The American Society of Mechanical Engineers, American Water Works Association, American Institute of Electrical Engineers, The Society of Naval Architects and Marine Engineers, American Society for Engineering Education, American Institute of Chemical Engineers, American Chemical Society, American Institute of Physics, American Nuclear Society, Atomic Industrial Forum, Institute of Radio Engineers. Also, the American Society for Metals, American Rocket Society, Institute of Aeronautical Sciences, Society of Automotive Engineers, American Society for Testing Materials, and the American Geological Institute, which will be represented by the Mineralogical Society of America, Society of Exploration Geophysicists, Society of Economic Geologists, Geological Society of America, American Association of Petroleum Geologists, and Society of Economic Paleontologists and Mineralogists.

Emphasis will be on the industrial possibilities of atomic energy. In addition to scientific and engineering phases, attention also will be centered on management problems. In many instances the papers will be the first public discussions of important nuclear field developments.

Dr. Thorndike Saville, Dean of Engineering, New York University, is President of Engineers Joint Council. EJC is composed of eight major national engineering organizations with a total membership of 170,000. Dr. John R. Dunning, Dean of Engineering at Columbia University, is Chairman of the General Committee on Nuclear Engineering and Science. Dr. Donald L. Katz, Chairman of the Chemical and Metallurgical Engineering departments at the University of Michigan, is Chairman of the Program Committee of the Congress. Professor Barnett F. Dodge, of Yale University, is President of the American Institute of Chemical Engineers, sponsor of the Atomic Exposition to be held in connection with the Congress.

M-H Features Transistors, Controls at I.R.E. Show

New electronic controls, components, and instruments—some of which use transistors instead of vacuum tubes—were shown by the Minneapolis-Honeywell Regulator Company at the Institute of Radio Engineers Show in New York, March 21–24. Six of the firm's divisions participated.

Featured were five new instruments unveiled by the Doelcam Division (formerly the Doelcam Manufacturing Company of Boston). These included a new magnet null indicator for laboratory and industrial use as a d-c null balance detector to make fast, accurate low-level measurements; a new tubeless data transmission system for testing and monitoring operations and remote indication up to 25 miles away; and a two-stage 400 cps magnetic servo amplifier used in high performance servo systems. Also exhibited were a selected range amplifier and a d-c indicating amplifier, both of which use Doelcam's Second-Harmonic Magnetic Converter as the input stage.

Heiland Division (formerly the Heiland Research Corporation of Denver) displayed its Model 700-C Recording Oscillograph—an improved dynamic testing instrument. It features record speeds from 0.03 in./sec to 144 in./sec in overlapping ranges using 12 quick-change gear speeds and four selectable recording speeds.

Use of transistors in fuel measurement systems were among the aircraft applications shown. The company's Aeronautical Division, Minneapolis, displayed a new thermistor level switch, a jet engine temperature indicating system, E-10 electronic autopilot designed for supersonic jet planes and jet engine controls and system components.

The company also displayed new power-type transistors used in amplifiers to drive motors and for use in switching circuits.

A new line of illuminated push-button, snap-action switches which can be mounted on one-in. centers, either

horizontally or vertically for a wide variety of automatic control, computer, and other electronic equipment applications, were also displayed by M-H's Micro Switch division.

The division also introduced a number of new multicircuit assemblies incorporating the use of subminiature snap-action switches. These include precision rotary selector switches, three-position slide actuators, toggle switches, "memory" switches, and sealed and protected subminiature switches for use in severe service exposure conditions.

Lithium Carbonate Price Reduction

American Potash & Chemical Corporation, a major producer of lithium chemicals and the largest producer of lithium carbonate, has announced a reduction in the price of lithium carbonate from its main plant at Trona, Calif., from $1.00 per lb to 90 cents per lb, delivered, in carload lots.

Announcement of the price drop, effective January 25 on shipments from Trona, was made by William J. Murphy, vice-president in charge of sales, who said, "The reduction was made possible by increased production facilities at the company's Trona plant."

American Potash & Chemical Corporation recently announced plans for an increase in its production of lithium chemicals with the formation of a new company, American Lithium Chemicals, Inc., which will build a $6,600,000 manufacturing plant near San Antonio, Texas, to produce lithium hydroxide and other lithium chemicals. Production is scheduled to begin at the new plant by the end of the year.

Pittsburgh Meeting Abstract Deadline

Triplicate copies of abstracts of papers to be scheduled for presentation at the Pittsburgh Meeting of the Society, October 9 to 13, 1955, must reach the Secretary's office, 216 West 102nd Street, New York 25, N. Y., not later than *June 15, 1955* in order to be included in the program.

Sessions will be scheduled on: Batteries, Corrosion, Electrodeposition, Electro-Organics, and Electrothermics and Metallurgy.

Triplicate copies of abstracts of papers for the Spring Meeting of the Society in San Francisco, April 29 to May 3, 1956, must reach the Secretary's office not later than January 2, 1956.

Sessions probably will be scheduled on: Electric Insulation, Electronics, Electrothermics and Metallurgy, Industrial Electrolytics, and Theoretical Electrochemistry.

Triplicate copies of manuscripts are acceptable either before or after presentation of a paper at a meeting. There is no connection between presentation of papers and publication in the JOURNAL.

DIVISION NEWS

Theoretical Electrochemistry Division

At its business meeting to be held at the Spring Meeting in Cincinnati the Theoretical Division will elect officers to serve for a two-year term. The Nominating Committee, consisting of Walter J. Hamer, Chairman, Norman Hackerman, and Carl Wagner, has proposed the following nominations and has been assured of each nominee's willingness to serve:

Chairman—Ernest , Yeager, Morley Chemical Lab., Western Reserve University, Cleveland, Ohio

Vice-Chairman—Paul J. Delahay, Dept. of Chemistry, Louisiana State University, Baton Rouge, La.

Secretary-Treasurer—Ralph Roberts, Chemistry Branch, Office of Naval Research, Washington, D. C.

Executive Committee Members-at-Large (two to be elected):

Edgar L. Eckfeldt, Leeds and Northrup Co., Philadelphia, Pa.

Cecil V. King, Dept. of Chemistry, New York University, New York, N. Y.

Herbert A. Laitinen, William Albert Noyes Lab., University of Illinois, Urbana, Ill.

C. W. Tobias, Dept. of Chemistry and Chemical Engineering, University of California, Berkeley, Calif.

RALPH ROBERTS, *Secretary-Treasurer*

SECTION NEWS

Detroit Section

The Detroit Section held a meeting in the Wayne University Science Hall on November 12, 1954. Following the dinner, a talk on "Ultrasonics and Electrochemistry" was delivered by Dr. Ernest B. Yeager of Western Reserve University.

Dr. Yeager, a pioneer in this field of research, began his talk with a description of the type of instrumentation and accessories employed in ultrasonic measurements. The sound source for the vibrations are of two types, those making use of the piezoelectric effect (such as crystals of quartz or barium titanate), and those involving magnetostriction. RF generators with outputs of 200 to 400 watts are required as a source of alternating potential. Polarization measurements on the electrodeposition of copper indicated that ultrasonic waves produced a marked decrease in polarization, this effect being more pronounced with increase in intensity, until a limiting value was reached.

The possible application of ultrasonics to practical electrodeposition was discussed. It was pointed out that high frequency vibrations could destroy concentration gradients at areas inaccessible to mechanical agitation. Structural changes, such as production of smoother deposits, are similar to those obtained by mechanical agitation. Ultrasonics appeared to offer no advantages from the viewpoint of cathode efficiency. Although it was not tested, Dr. Yeager pointed out that the microflushing properties of ultrasonic vibrations might prevent occlusion of electrolyte in the pores of the deposit. The method has already proved itself in the preplating treatment of metals. Of great interest were the photographs of the diffusion layer at an electrode, obtained by use of the Schlieren technique, which demonstrated the effectiveness of ultrasonics in disrupting the concentration gradient.

M. SHAW, *Secretary-Treasurer*

Midland Section

The Midland Section held a dinner meeting at the Midland Country Club on February 21, 1955. After the dinner, members and guests were privileged to hear an address by Dr. R. B. Saltonstall, of the Udylite Corporation, Detroit, Mich., given in the Dow auditorium. His subject was "Plating in Industry."

Dr. Saltonstall traced the history of plating in industry for the past thirty years from a "black art," in which small operations used relatively small tanks, to a modern science with a single automotive company using 1½ million gallons of plating solutions.

It has been recently determined that the salt spray test is not reproducible

by different laboratories, and it is not used by many as a criterion of plate quality. In nickel plating the thickness of nickel is the important consideration, and copper undercoating is useful only to reduce buffing costs; it does not add to the plate's corrosion resistance.

Important applications of plating used during the war were chromate-treated zinc plating on steel for shell cases, copper plating on steel as a lubricant between drawing operations, electro tin plate for tin conservation, and silver plated steel bearings with indium or tin surface for aircraft bearings.

Electroforming provides a means for reproducing a form very accurately. It is used extensively in the phonograph record industry and recent improvements in cleaning methods have improved record quality.

Alloy plating is becoming more important. Two newer alloys are tin-nickel and tin-zinc. The former has a soft pink tinge, is hard, and is corrosion resistant. Tin-zinc is replacing cadmium in the electronics industry. Another new development is chemical nickel plating by the hypophosphite method. An advantage of this method is that the plating is of uniform thickness.

An interesting and extended discussion period followed Dr. Saltonstall's talk.

PAUL JUCKNIESS,
Secretary-Treasurer
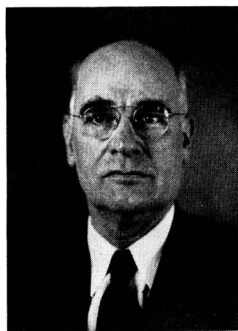
MARVIN J. UDY

Philadelphia Section

Marvin J. Udy, President of The Electrochemical Society, was the guest of honor and speaker at the March 2 meeting of the Philadelphia Section. Nearly 50 members and guests had the pleasure of meeting and dining with Mr. Udy before his talk. Mr. Udy spoke on "Electric Smelting Furnaces." He described the principal factors involved

in the design of such furnaces: voltage, electrode size, electrode spacing, depth of slag, and rate of feed. Using a specific problem as an example, Mr. Udy demonstrated the way in which these factors had to be considered in designing a large, full-scale furnace. Mr. Udy's answers to the numerous questions following his talk revealed many additional interesting facts about various electric smelting processes.

G. W. BODAMER, *Secretary*

PERSONALS

ROBERT C. FORD is now production superintendent at the Mississippi Works of the Oldbury Electro-Chemical Co. in Columbus. He was formerly technical supervisor at the company's plant in Niagara Falls, N. Y.

JOHN C. RUSSELL has been elected Vice-President of Sales by the Philadelphia Quartz Co., Philadelphia, Pa.

JAMES H. SCHULMAN and R. J. GINTHER, both with the Naval Research Laboratory in Washington, D. C., and L. W. EVANS, formerly of the Naval Research Laboratory and presently associated with Sylvania Electric Products Inc., Seneca Falls, N. Y., are among ten scientists who have received awards from the U. S. Department of Defense for their work in developing an inexpensive device for measuring radiation doses. The devices developed in the program, called dosimeters, are small plastic lockets containing a phosphate glass square. They are used to measure the radiation dose received by an individual exposed to an atomic blast. Measuring about $1\frac{1}{2}$ in. in diameter, they can be worn on dog tag chains. The work leading to the awards resulted from an Armed Services need for inexpensive, accurate, and reliable devices for field use in measuring nuclear radiation. The devices had to be capable of detecting at least 10 roentgens of gamma radiation, and of measuring doses up to 600 roentgens. No commercial dosimeters were available which fulfilled these requirements. The dosimeters purchased by the Bureau of Ships meet these specifications. They cost about 75 cents each.

JEAN SALAUZE

Dr. Jean Salauze, a member of The Electrochemical Society for many years, died at his home in Paris on February 24, 1955.

During recent years he was associated with the Societe des Accumulateurs Fixes et de Traction, at Romainville, near Paris, especially with their electroplating activities. He was the author of a valuable book on electroplating entitled "Traite Galvanoplastie," the second edition of which appeared in 1950.

He will be remembered and missed by his many American friends whom he entertained in Paris.

MEETINGS OF OTHER ORGANIZATIONS

MATHEMATICAL ASSOCIATION OF AMERICA, Illinois Section Meeting, Monmouth College, Monmouth, Ill., May 13–14; Upper New York State Section Meeting, University of Buffalo, Buffalo, N. Y., May 14. Further information from: Edith R. Schneckenburger, Associate Secretary, MAA, University of Buffalo.

DEUTSCHE GESELLSCHAFT FÜR CHEMISCHES APPARATEWESEN (DECHEMA), ACHEMA XI—Chemical Apparatus and Equipment Congress and Exhibition, Frankford am Main, Germany, May 14–22. The 1955 Congress of the European Federation for Chemical Engineering will be held in conjunction with the ACHEMA XI Congress, together with the active cooperation of the 19 technical and scientific societies, representing 11 different countries, that form the European Federation for Chemical Engineering. At the same time, special meetings of the Gesellschaft Deutscher Chemiker and other technical and scientific societies, as well as the Annual General Meeting of the DECHEMA, will also be held.

AMERICAN SOCIETY FOR TESTING MATERIALS (ASTM), Committee Meeting, E-11 on Quality Control of Materials, ASTM Headquarters, Philadelphia, Pa., May 17.

ASTM, Pittsburgh District Meeting—Joint with Purchasing Agents Association of Pittsburgh, Pittsburgh, Pa., May 17.

ASTM, Committee Meeting, C-20 on Acoustical Materials, ASTM Head-

Officers of Local Sections of the Society

Chicago

B. F. FREEBERG, Chairman
E. L. KOEHLER, Vice-Chairman
R. D. MISCH, Treasurer
  J. E. DRALEY, Secretary
  Argonne National Laboratory
  P. O. Box 299
  Lemont, Ill.
Representatives on Council of Local Sections:
  H. T. FRANCIS (1 year)
  C. A. HAMPEL (2 years)

Cleveland

E. B. YEAGER, Chairman
W. H. STOLL, Vice-Chairman
M. E. SIBERT, Treasurer
  K. S. WILLSON, Secretary
  General Dry Batteries, Inc.
  13000 Athens Ave.
  Cleveland 7, Ohio
Representatives on Council of Local Sections:
  L. E. PUCHER (1 year)
  N. C. CAHOON (2 years)

Detroit

WRIGHT WILSON, Chairman
ANDREW LIGER, 1st Vice-Chairman
G. V. KINGSLEY, 2nd Vice-Chairman
  MANNY SHAW, Sec.-Treas.
  19411 Winthrop Ave.
  Detroit, Mich.
Representatives on Council of Local Sections:
  L. O. CASE (1 year)
  FRANK PASSAL (2 years)

Midland

F. N. ALQUIST, Chairman
M. P. NEIPERT, Vice-Chairman
  P. R. JUCKNIESS, Sec.-Treas.
  The Dow Chemical Co.
  Midland, Mich.
Representatives on Council of Local Sections:
  F. W. KOERKER (1 year)
  H. A. ROBINSON (2 years)

New York Metropolitan

M. F. QUAELY, Chairman
M. B. DIGGIN, Vice-Chairman
  K. B. McCAIN, Sec.-Treas.
  Wilbur B. Driver Co.
  150 Riverside Ave.
  Newark, N. J.
Representatives on Council of Local Sections:
  F. A. LOWENHEIM (1 year)
  HERBERT BANDES (2 years)

Niagara Falls

G. M. BUTLER, Chairman
J. E. CURREY, Vice-Chairman
  L. A. STOYELL, Sec.-Treas.
  Electro Metallurgical Co.
  Niagara Works
  137-47th St.
  Niagara Falls, N. Y.
Representatives on Council of Local Sections:
  M. S. KIRCHER AND W. D. SHERROW

Pacific Northwest

J. B. HEITMAN, Chairman
G. H. KISSIN, Vice-Chairman
  K. L. SANBORN, Sec.-Treas.
  General Electric Co.
  2005 Pullen
  Richland, Wash.
Representatives on Council of Local Sections:
  G. H. KISSIN AND J. S. MURPHY

Philadelphia

J. F. HAZEL, Chairman
E. L. ECKFELDT, Vice-Chairman
G. F. TEMPLE, Treasurer
  G. W. BODAMER, Secretary
  Rohm & Haas Co.
  Philadelphia, Pa.
Representatives on Council of Local Sections:
  E. L. ECKFELDT (1 year)
  J. F. GALL (2 years)

Pittsburgh

R. A. WOOFTER, Chairman
R. B. HOXENG, Vice-Chairman
  A. J. CORNISH, Sec.-Treas.
  Rectifier Dev. 4N-N
  Westinghouse Electric Corp.
  East Pittsburgh, Pa.
Representatives on Council of Local Sections:
  L. E. LANCEY (1 year)
  R. A. WOOFTER (2 years)

San Francisco

C. W. TOBIAS, Chairman
MORRIS FEINLEIB, Vice-Chairman
  H. F. MYERS, Sec.-Treas.
  Columbia-Geneva Steel Div.
  Russ Bldg.
  San Francisco 6, Calif.
Representatives on Council of Local Sections:
  R. F. BECHTOLD AND S. H. DREISBACH

Washington-Baltimore

FIELDING OGBURN, Chairman
D. T. FERRELL, JR., Vice-Chairman
  JEANNE B. BURBANK, Sec.-Treas.
  3304 Cleveland Ave., N.W.
  Washington, D. C.
Representatives on Council of Local Sections:
  J. C. WHITE (1 year)
  D. T. FERRELL, JR. (2 years)

Ontario-Quebec

A. E. WESTMAN, Honorary Chairman
JOHN CONVEY, Chairman
P. J. ENZIO, Vice-Chairman
R. R. ROGERS, Vice-Chairman
  JOHN SUMNER, Sec.-Treas.
  637 Craig St. West
  Montreal 3, P.Q., Canada
Representatives on Council of Local Sections:
  P. J. ENZIO (1 year)
  R. R. ROGERS (2 years)

India

M. S. THACKER, Chairman
B. NARAYAN DAS, Vice-Chairman
S. RAMASWAMY, 2nd Vice-Chairman
  S. KRISHNAMURTHY, Sec.-Treas.
  543/1, 17th Cross Rd.
  Malleswaram P. O.
  Bangalore 3, India
Representatives on Council of Local Sections:
  L. CHARAT RAM AND K. RAJAGOPAL

Officers of
Divisions of the Society

Battery

N. C. CAHOON, Chairman
U. B. THOMAS, Vice-Chairman
E. J. RITCHIE, Sec.-Treas.
The Eagle-Picher Company
Joplin, Mo.

Corrosion

J. V. PETROCELLI, Chairman
T. P. MAY, Vice-Chairman
C. V. KING, Sec.-Treas.
Dept. of Chemistry
New York University
New York, N. Y.

Electric Insulation

C. F. MILLER, Chairman
L. L. DEER, Vice-Chairman
D. A. LUPFER, Sec.-Treas.
General Electric Co.
Syracuse, N. Y.

Electrodeposition

C. A. SNAVELY, Chairman
SIDNEY BARNARTT, Vice-Chairman
ABNER BRENNER, Sec.-Treas.
National Bureau of Standards
Washington, D. C.

Electronics

A. L. SMITH, Chairman
HERBERT BANDES, Vice-Chairman
(Luminescence)
A. E. MIDDLETON, Vice-Chairman
(General Electronics)
C. W. JEROME, Sec.-Treas.
Sylvania Electric Products Inc.
Salem, Mass.

Electro-Organic

H. M. SCHOLBERG, Chairman
STANLEY WAWZONEK, Vice-Chairman
G. W. THIESSEN, Sec.-Treas.
Dept. of Chemistry
Monmouth College
Monmouth, Ill.

Electrothermics and Metallurgy

I. E. CAMPBELL, Chairman
J. S. DEWAR, Vice-Chairman
A. C. HASKELL, JR., Sec.-Treas.
Titanium Alloy Mfg. Division
National Lead Co.
Box C, Bridge Station
Niagara Falls, N. Y.

Industrial Electrolytic

A. R. ORBAN, Chairman
MILTON JANES, Vice-Chairman
W. D. SHERROW, Sec.-Treas.
Great Lakes Carbon Corp.
Niagara Falls, N. Y.

Theoretical Electrochemistry

E. B. YEAGER, Chairman
PAUL DELAHAY, Vice-Chairman
RALPH ROBERTS, Sec.-Treas.
3308 Camalier Dr.
Washington 15, D. C.

Meetings of other Organizations

quarters, Philadelphia, Pa., May 18–19.

AMERICAN INSTITUTE OF ELECTRICAL ENGINEERS (AIEE), Telemetering Conference, Morrison Hotel, Chicago, Ill., May 18–20. Sponsored by AIEE, IRE, ISA, and IAS.

ILLUMINATING ENGINEERING SOCIETY, East Central Regional Conference, Abraham Lincoln Hotel, Reading, Pa., May 19–20. Further information from: Paul Kinsey, Metropolitan Edison Co., 412 Washington St., Reading, Pa.

ASTM, Committee Meeting, E-14 on Mass Spectrometry, Mark Hopkins Hotel, San Francisco, Calif., May 22–27.

CHEMICAL INSTITUTE OF CANADA, 38th Annual Conference, Quebec City, Canada, May 30–June 1. Featured events will include the award of the 1955 Chemical Institute of Canada Medal to an outstanding chemist, as well as two special lectures by prominent scientists. About 100 papers will be presented on such subjects as agricultural chemistry, analytical chemistry, biochemistry, chemical education, chemical engineering, organic and physical chemistry, and protective coatings. Many special events are being arranged, including plant tours through local industry and to the Saguenay area.

NATIONAL SOCIETY OF PROFESSIONAL Engineers, annual meeting, Bellevue-Stratford Hotel, Philadelphia, Pa., June 2–4.

ILLUMINATING ENGINEERING SOCIETY, Northeastern Regional Conference, Ft. William Henry Hotel, Lake George, N. Y., June 10–11. Further information from: C. E. Waldron, 45 Adams Place, Delmar, N. Y.

AIEE, Magnetics, Pittsburgh, Pa., June 13–15. Sponsored by the Subcommittee on Magnetics, of the Basic Sciences Committee.

AMERICAN SOCIETY FOR ENGINEERING EDUCATION, Annual Meeting, Pennsylvania State University, State

College, Pa., June 20–24. The meeting will feature over 75 conferences dealing with all areas of engineering education, physics, mathematics, international relations, research, and others bearing upon the broad subject of engineering education. All sessions will be open to foreign guests who wish to attend. For further information write to the Secretary of the ASEE, Northwestern University, Evanston, Ill. For information regarding housing accommodations write to Professor Kenneth Holderman, Pennsylvania State University, State College, Pa.

AMERICAN ELECTROPLATERS' SOCIETY, 42nd Annual AES Convention and 4th Industrial Finishing Exposition, Cleveland, Ohio, June 20–25.

AMERICAN PHYSICAL SOCIETY, Toronto, Canada, June 22–24. Further information from: Karl K. Darrow, Columbia University, New York 27, N. Y.

ASTM, 58th Annual Meeting, Chalfonte-Haddon Hall, Atlantic City, N. J., June 26–July 1.

AIEE, Committee on Technical Operations, Summer General Meeting, New Ocean House, Swampscott, Mass., June 27-July 1.

NEW MEMBERS

In March 1955 the following were approved for membership in The Electrochemical Society by the Membership Qualifications Committee:

Active Members

BENOIT BERNARD, Quebec Iron and Titanium Corp., Mail add: 411 Third Ave., St. Joseph de Sorel, P. Q., Canada (Electrothermics & Metallurgy)

D. JOSEPH DONAHUE, Radio Corp. of America, Mail add: 1716 Lititz Pike, Lancaster, Pa. (Electronics)

JOHN V. FESTA, Sylvania Electric Products Inc., 500 Evelyn Ave., Mountain View, Calif. (Electronics)

CHARLES A. GIERACH, International Graphite & Electrode Div., Mail add: 730 Maple Ave., Niagara Falls, N. Y. (Electrothermics & Metallurgy)

THOMAS E. HARR, General Electric Co., General Engineering Lab., Mail add:

240 Pinewood Dr., Schenectady 3, N. Y. (Corrosion, Electrodeposition)

ROBERTO PIRANI, Montecatini, Soc. Gen. per l'Industria Mineraria e Chimica An., via F; Turati 18, Milan, Italy (Industrial Electrolytic)

EMILE PRUVOT, Cie Pechiney, 23 rue de Balzac, Paris 8, France (Industrial Electrolytic)

DAVID R. SIVERTSEN, Bendix Aviation Corp., Mail add: 14 Edstan Dr., Moonachie, N. J. (Corrosion, Electrodeposition, Theoretical Electrochemistry)

ROBERT A. WEBBER, Electro Refractories & Abrasives Canada Ltd., 60 Notre Dame St., Cap de la Madeleine, Quebec, Canada (Electrothermics & Metallurgy)

ANNOUNCEMENTS FROM PUBLISHERS

CHEMICAL PROCESS PRINCIPLES, Part I, second edition, by Olaf A. Hougen, Kenneth M. Watson, and Roland A. Ragatz. Published by John Wiley & Sons, Inc., 440 Fourth Ave., New York 16, N. Y., 1954. 539 pages, $8.50.

Part I of this three-volume work, which concentrates on material and energy balances, brings together the important principles of physical chemistry and stresses their practical application. With this objective again in mind, the authors have completely revised their material on physical and chemical constants and provide a new correlation of critical constants. Up-to-date information is supplied on material balances in stagewise extraction, and new discussions appear on equilibria in ternary systems, material balances in stepwise countercurrent processing, and thermochemistry of nuclear reactions. Illustrations and examples keep pace with this late information. Part II of their work, dealing with thermodynamics, and Part III, covering kinetics and catalysis, were both published by Wiley in 1947 and are priced at $6.00 and $5.25, respectively.

ORGANIC REACTIONS, Volume III, Roger Adams, editor-in-chief. Published by John Wiley & Sons, Inc., 440 Fourth Ave., New York 16, N. Y., 1954. 437 pages, $12.00.

In accordance with the established procedure of the series, the new volume goes exhaustively into a select set of reactions or a definite phase of a reaction, each examined from the preparative viewpoint, and with special attention given to limitations, interfering influences, effects of structure, and the selection of experimental techniques. The eight reactions that now join the growing group are studied by the authorities who work most closely with them and have been selected on the basis of their wide applicability and value to current research.

DIRECTORY OF COMMERCIAL AND COLLEGE TESTING LABORATORIES. Issued by the American Society for Testing Materials, 1916 Race St., Philadelphia 3, Pa. $1.00.

This is an up-to-date revision of National Bureau of Standards Miscellaneous Publication M187, *Directory of Commercial and College Laboratories*, which has been withdrawn from circulation. The two organizations have agreed that ASTM undertake the responsibility for compilation and publication of the Directory in the future. The Directory gives information regarding the location of testing laboratories, together with the types of commodities and the nature of the investigations the laboratories are pre-Pared to undertake.

TABLES OF FUNCTIONS AND OF ZEROS OF FUNCTIONS, National Bureau of Standards Applied Mathematics Series 37. Order from the Government Printing Office, Washington 25, D. C. 211 pages, $2.25.*

Prompted by a continuing demand for previously issued short tables of the National Bureau of Standards Computation Laboratory, NBS has decided to collect together groups of related short tables and issue them in convenient form. This volume is the first of certain projected numbers in the NBS Applied Mathematics Series to bear the subtitle *Collected Short Tables of the National Bureau of Standards Computation Laboratory.*

---

*Foreign remittances must be in U. S. exchange and should include an additional one-third of the publication price to cover mailing costs.

TABLES OF ERROR FUNCTION AND ITS DERIVATIVES, National Bureau of Standards Applied Mathematics Series 41. Order from Government Printing Office, Washington 25, D. C. 302 pages, $3.25.*

The present tables extend the range of all existing tables, and provide a smaller tabular interval. Provision has been made to facilitate interpolation, both direct and inverse, by the user of the tables. The tables are thus presented as the tabulation of a mathematical function, equally available for application to any one of numerous fields.

TABLE OF SALVO KILL PROBABILITIES FOR SQUARE TARGETS, National Bureau of Standards Applied Mathematics Series 44. Order from the Government Printing Office, Washington 25, D. C. ix, 33 pages; 30 cents.*

In modern planning, predicted performance of operations and devices is of basic importance. This is especially true of matters connected with the general problem of hitting a target. This table of kill probabilities should be useful to organizations concerned with such matters as operations analysis, strategic planning, engineering and field-test activities, and missile development programs. Although the terminology and notations used are directed to a particular defense problem for which the table was computed, the results are not limited to that field.

STANDARD SAMPLES AND REFERENCE STANDARDS ISSUED BY THE NATIONAL BUREAU OF STANDARDS, National Bureau of Standards Circular 552. Order from the Government Printing Office, Washington 25, D. C. 23 pages, 25 cents.*

This Circular contains a descriptive listing of the various Standard Samples issued by the NBS. A schedule of weights and fees, as well as directions for ordering, is included. Summarized tables of analyses are presented, to indicate the type of standards of composition presently available. The current status of the various standards will be indicated by a mimeographed insert.

PHOTOGRAPHIC DOSIMETRY OF X- AND GAMMA RAYS, by Margarete Ehrlich, National Bureau of Standards Handbook 57. Order from the Government Printing Office, Washington 25, D. C. 28 pages, 12 figures, 5 tables; 15 cents.*

This Handbook contains primary factual data and basic principles necessary for photographic dosimetry of x- and gamma rays. It was prepared in response to an urgent need for more complete information on this topic. The data presented in the Handbook are the results of an extensive program in this field conducted over a number of years by the Radiation Physics Laboratory of the NBS.

LETTERS TO THE EDITOR

Dear Sir:

In the new Cole Porter musical "Silk Stockings," which I have just had the pleasure of seeing, Ninotchka, the Soviet commissaress, remarks that sex is an electrochemical phenomenon. Considering its source this statement needs verification, but I can think of no project more worthwhile for the Society. Just imagine the increase in our membership and the JOURNAL's subscription list if it could be proved that this subject came within the purview of the Society's interest! Should a committee be set up immediately to investigate?

<div align="right">FREDERICK A. LOWENHEIM
Plainfield, N. J.</div>

Dear Sir:

I appreciated receiving two copies of your editorial, "The Crisis in Science Teaching," reprinted from the November 1954 issue of the JOURNAL of The Electrochemical Society. I thought this was well written and pointed to some of the very significant problems that must be faced if we are going to make progress in correcting many undesirable situations regarding high school science teaching.

I am wondering whether it might be appropriate for you to do a follow-up editorial and inform your readers of the positive efforts being made by the National Science Teachers Association and its Future Scientists of America Foundation. We feel considerable pride in the degree to which our program involves the coming together of science teachers, the trainers of science teachers, and representatives of professional and technical societies, science departments in the colleges, and representatives of science-based industries. It would be most helpful to us if you could

encourage your readers to throw their support behind our program both as individuals and through the companies which they represent.

I don't know how your own budget is fixed, but I can report that among the sponsors and participants in our 1955 program there are three technical societies, namely: the American Society for Metals, the American Ceramic Society, and the American Ceramic Institute. It would be encouraging and very much appreciated if The Electrochemical Society could also find it possible to provide some financial support for FSAF.

R. H. CARLETON
Executive Secretary
National Science Teachers Association
Washington, D. C.

Dear Sir:

Thank you very much for sending me the reprints of your recent editorial, "The Crisis in Science Teaching." And thanks even more for having *written* the editorial. It is encouraging to know that the crisis is being so aptly put before the public. I'm most pleased with your words about the Virginia Academy

and Junior Academy of Science. Such words make my work worthwhile.

Did you know that the AAAS has made it possible to use their research funds for scientific research grants at the secondary school level? They are to be administered by the Academies of Science Conference.

THELMA C. HEATWOLD
Chairman
Virginia Junior Academy of Science
Staunton, Va.

LITERATURE FROM INDUSTRY

SELENIUM RECTIFIER CARTRIDGES. Recently released bulletin contains the latest information on International Rectifier Corp.'s High Voltage Selenium Rectifier cartridges. The cartridges listed are typical of International's complete line. Due to the higher voltage rating of the selenium rectifier cells, a smaller number of cells is required for most standard applications. The result is a shorter over-all cartridge and a more economical rectifier unit. Particu-

lar attention is called to page 6, which illustrates valuable information for assistance in design work. International Rectifier Corp.   P-293

INSTRUMENT TRANSFORMER BUYER'S GUIDE. The 1955 edition of the G-E Instrument Transformer Buyer's Guide, containing basic, up-to-date information on the complete G-E line, has been announced. The fully illustrated, 100-page publication, contains ratings, ASA accuracy classifications, and prices of all Standard G-E indoor and outdoor potential and current transformers. Listings of ratio and phase-angle tests, tables of replacement types, and mechanical and thermal data are included. General Electric Co.   P-294

TITRATION BULLETIN. 16-page booklet, fully illustrated with in-use photographs, charts, and curves, shows reader why, in a generation, titration-by-instrumentation has made volumetric analysis just about the fastest, surest, and most convenient means of chemical control. Explained, in clear-cut terms, are the 3 main kinds of electrometric titration: potentiometric, conductomet-

ric, and amperometric. Instrumentation for each kind is shown and explained in detail. Of special value to those interested in quality control in industry, or in methods research. Fisher Scientific Co.   P-295

PRECISION ELECTRICAL INSTRUMENTS. New short-form catalogue has just been issued giving complete descriptions and specifications for the standard ESI products. The brochure has been divided into 3 major parts. The initial double-page spread features the ESI Impedance Bridges and Accessory Null Bridge Amplifiers. The middle section of the catalogue is devoted to laboratory instruments, namely Dekaviders® and Dekaboxes®. Listings of the ESI electronic components manufactured under the Dekastat and Dekapot registered tradenames are found in the final portion of the booklet. Circuit diagrams and sketches pertinent to all of the Deka instruments and components have been shown for clarity and understanding. Listings of current selling prices have also been included for all standard instrument and component models. Electro-Measurements, Inc.   P-296

COLLOIDAL GRAPHITE USES. A new publication containing information, photographs, and charts pertaining to colloidal graphite applications in the electronic and electrical industries is available. It describes how 'dag'® Colloidal Graphite, a high-purity electric-furnace graphite processed to colloidal size and dispersed in a wide variety of fluid carriers, is used for coating the insides of cathode-ray tubes in order to prevent stray electrons from reflecting back into the electron beam. Also mentioned is the utilization of graphite films for increasing thermal radiation and for decreasing secondary emission, "back" omission, and undesirable photoelectric effects in vaccum tubes. Methods for improving the efficiency of copper oxide rectifiers, improving connections between graphite coatings and ground wires, and attaching filaments to lead-in wires of various

types of carbon filament lamps by means of colloidal graphite dispersions, are presented. Acheson Colloids Co., Div. of Acheson Industries, Inc.   P-297

NEW PRODUCTS

CORROSION-RESISTANT LINING COMPOUND. The introduction of a new corrosion-resistant neoprene lining compound that flows on like paint to a variety of industrial surfaces—fan blades, fume ducts, process vessels, pump impellers, valves, and piping—has been announced. The product, called Pennsalt NeoLine, combines the corrosion inertness of neoprene with excellent strength and adhesion. NeoLine cures completely to a live, resilient vulcanized coating for full protection for metal, concrete, or wood where heavy duty coating or lining is required. It can be heat-cured or air-cured. Pennsylvania Salt Manufacturing Co.   N-164

PRECISION POTENTIOMETER. New, miniature 10-turn potentiometer features linearity of 0.05% standard and 0.025% as a special tolerance where required. Over-all length is $1\frac{3}{8}$ in. from front mounting surface. The red anodized aluminum housing is fully shielded. High resolution, low torque, long life, and stability under environmental conditions meeting military specifications are features. The synchro mounting provides precision positioning. Precision stainless steel ball bearings and high concentricity contribute to the low torque specifications. Technology Instrument Corp.   N-165

DIELECTRIC POTENTIOMETERS. A completely new and unique principle has been incorporated in the Type PD-2 Dielectric Potentiometer. This variable voltage divider is free of phase and frequency distortion over the wide range 20 cycles to 10 megacycles. The output voltage, therefore, has the identical waveform of the input voltage. Consequently, this device excels as a calibrated attenuator in wide-band oscilloscopes, transmission measuring sets, amplifiers, signal generators, network analysis systems, and waveform comparison or balancing schemes. The nature of the dielectric potentiometer principle permits wide design flexibility in input impedance, range of attenuation, adaptation to specific nonlinear

functions, and mechanical drive. Inquiries invited regarding specific applications. Technology Instrument Corp.   N-166

GERMANIUM RECTIFIERS. Recently developed germanium rectifiers offer 95% efficiency at full load. Available in several models from 300 to 50,000 amp d-c output, the rectifiers are designed to outlive all conventional types of d-c power supplies. Oil-immersed, fully motorized, continuously variable, inductor controls are furnished to vary the output from zero to full rated load at the touch of a button. The complete rectifier units are almost 100% completely sealed from adverse atmospheric conditions. The germanium junctions are hermetically sealed. Because the use of elaborate fans and cooling systems has been eliminated, the units are considerably smaller physically than conventional units. Rapid Electric Co.   N-167

EMPLOYMENT SITUATION

Please address replies to box shown, c/o The Electrochemical Society, Inc., 216 W. 102nd St., New York 25, N. Y.

Position Wanted

CHEMIST, 36, 11 years' experience, including batteries, electroplating, general physical and chemical commercial testing, seeks position in Middle Atlantic States locality. *Reply to Box 356.*

To receive further information on any New Product or Literature from Industry listed above, send inquiry, with key number, to JOURNAL of The Electrochemical Society, 216 West 102nd Street, New York 25, N. Y.
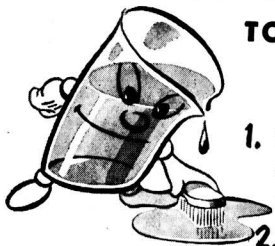
Please print your name and address plainly.

Sustaining Members of The Electrochemical Society

Air Reduction Company, Inc., New York, N. Y.

Ajax Electro Metallurgical Corporation, Philadelphia, Pa.

Alloy Steel Products Company, Inc., Linden, N. J.

Aluminum Company of America, New Kensington, Pa.

Aluminum Company of Canada, Ltd., Montreal, Canada

American Machine & Foundry Co., Raleigh, N. C.

American Platinum Works, Newark, N. J. (2 memberships)

American Potash & Chemical Corp., Los Angeles, Calif.

American Zinc, Lead and Smelting Company, St. Louis, Mo.

Armour Research Foundation, Chicago, Ill.

Auto City Plating Company Foundation, Detroit, Mich.

Bart Manufacturing Company, Bellville, N. J.

Becco Chemical Div., Food Machinery & Chemical Corp., Buffalo, N. Y.

Bell Telephone Laboratories, Inc., New York, N. Y.

Bethlehem Steel Company, Bethlehem, Pa. (2 memberships)

Burgess Battery Company, Freeport, Ill. (4 memberships)

Canadian Industries (1954) Limited, Montreal, Canada

Chrysler Corporation, Detroit, Mich.

Columbia-Southern Chemical Corporation, Pittsburgh, Pa.

Consolidated Mining and Smelting Company of Canada, Ltd., Trail, B. C. (2 memberships)

Corning Glass Works, Corning, N. Y.

Crane Company, Chicago, Ill.

Diamond Alkali Company, Pittsburgh, Pa. (2 memberships)

Dow Chemical Company, Midland, Mich.

Wilbur B. Driver Company, Newark, N. J.

E. I. du Pont de Nemours & Company, Inc., Wilmington, Del.

Eagle-Picher Company, Joplin, Mo.

Eaton Manufacturing Company, Stamping Div., Cleveland, Ohio

Electric Auto-Lite Company, Toledo, Ohio

Electric Storage Battery Company, Philadelphia, Pa.

The Eppley Laboratory, Newport, R. I.

Ford Motor Company, Dearborn, Mich.

General Chemical Division, Allied Chemical & Dye Corporation, New York, N. Y.

General Electric Company, Schenectady, N. Y.

General Motors Corporation, Research Laboratories Division, Detroit, Mich.

Gould-National Batteries, Inc., Depew, N. Y.

Graham, Crowley & Associates, Inc., Chicago, Ill.

Great Lakes Carbon Corporation, Niagara Falls, N. Y.

Hanson - Van Winkle - Munning Company, Matawan, N. J. (2 memberships)

Harshaw Chemical Company, Cleveland, Ohio (2 memberships)

Hooker Electrochemical Company, Niagara Falls, N. Y. (3 memberships)

Houdaille-Hershey Corporation, Detroit, Mich.

International Graphite & Electrode Div., Speer Carbon Company, St. Marys, Pa. (2 memberships)

International Nickel Company, Inc., New York, N. Y. (2 memberships)

Kaiser Aluminum & Chemical Corporation, Division of Metallurgical Research, Spokane, Wash.

Mathieson Chemical Corporation, Niagara Falls, N. Y. (4 memberships)

McGean Chemical Company, Cleveland, Ohio

Merck & Company, Inc., Rahway, N. J.

Metal & Thermit Corporation, New York, N. Y.

Monsanto Chemical Company, St. Louis, Mo.

National Carbon Division, Union Carbide and Carbon Corporation, New York, N. Y. (2 memberships)

National Cash Register Company, Dayton, Ohio

National Research Corporation, Cambridge, Mass.

Niagara Alkali Company, Niagara Falls, N. Y.

Norton Company, Worcester, Mass.

Pennsylvania Salt Manufacturing Co., Philadelphia, Pa.

Philco Corporation, Lansdale, Pa.

Philips Laboratories, Inc., Irvington-on-Hudson, N. Y.

Potash Company of America, Carlsbad, N. Mex.

Promat Division, Poor & Company, Waukegan, Ill.

Ray-O-Vac Company, Madison, Wis.

RCA Victor Division, Radio Corporation of America, Harrison, N. J.

Solvay Process Division, Allied Chemical & Dye Corporation, Syracuse, N. Y. (3 memberships)

Stackpole Carbon Company, St. Marys, Pa.

Standard Steel Spring Division of the Rockwell Spring and Axle Company, Coraopolis, Pa.

Stauffer Chemical Company, San Francisco, Calif.

Sylvania Electric Products Inc., Bayside, N. Y. (2 memberships)

Sarkes Tarzian, Inc., Bloomington, Ind.

Tennessee Products & Chemical Corporation, Nashville, Tenn.

Udylite Corporation, Detroit, Mich. (2 memberships)

Union Carbide Company, Electrometallurgical Division, New York, N. Y.

United Chromium, Inc., New York, N. Y.

Vanadium Corporation of America, New York, N. Y.

Victor Chemical Works, Mt. Pleasant, Tenn.

Wagner Brothers, Inc., Detroit, Mich.

Western Electric Company, Inc., Chicago, Ill.

Western Electrochemical Company, Henderson, Nev.

Westinghouse Electric Corporation, E. Pittsburgh, Pa.

Willard Storage Battery Company, Cleveland, Ohio.

Wyandotte Chemicals Corporation, Wyandotte, Mich.

Yardney Electric Corporation, New York, N. Y.